PHYSICS REPORTS (Review Section of Physics Letters) 95. No. 4 (1983) 201–282. North-Holland Publishing Company

MONTE CARLO COMPUTATIONS IN LATTICE GAUGE THEORIES*

Michael CREUTZ

Physics Department, Brookhaven National Laboratory, Upton, New York, 11973, U.S.A.

Laurence JACOBS‡

Institute for Theoretical Physics, University of California, Santa Barbara, CA 93106, U.S.A.

and

Claudio REBBI

Physics Department, Brookhaven National Laboratory, Upton, New York, 11973, U.S.A.

Received 10 January 1983

Contents:

Abstract:

The formulation of gauge theories on Euclidean space-time lattices and the application of the Monte Carlo computational technique to the ensuing systems are reviewed. A variety of numerical results obtained for lattice gauge theories are presented and discussed.

* This article has been authored under contract DE-AC02-76CH00016 with the U.S. Department of Energy. Accordingly, the U.S. Government retains a nonexclusive, royalty-free license to publish or reproduce the published form of this contribution, or allow others to do so, for U.S. Government purposes.

‡ Supported in part by the National Science Foundation under grant PHY77-27084.

0 370-1573/83/0000–0000/$24.60

MONTE CARLO COMPUTATIONS IN LATTICE GAUGE THEORIES

Michael CREUTZ

Physics Department, Brookhaven National Laboratory, Upton, New York, 11973, U.S.A.

Laurence JACOBS

Institute for Theoretical Physics, University of California, Santa Barbara, CA 93106, U.S.A.

and

Claudio REBBI

Physics Department, Brookhaven National Laboratory, Upton, New York, 11973, U.S.A.

NORTH-HOLLAND PUBLISHING COMPANY-AMSTERDAM

1. Introduction

Gauge theories play a fundamental role in our present understanding of particle physics. Originally invoked to describe electromagnetic interactions, the notion of a gauge field has been extended and used in successful models of weak interactions and strong interactions. Attempts to unify all these forces are also based on gauge theories and, if the connection in general relativity is recognized as a gauge potential, it appears that all particle interactions may be accountable in terms of gauge fields.

Many of the predictions of gauge theories have compared extremely well with experimental results. This has occurred whenever the presence of an effectively weak coupling constant allows for the use of the standard techniques of perturbation theory. Yet, there are classes of phenomena which are inextricably associated with a strong coupling. To reduce these problems to theoretical analysis, a very interesting alternative to the ordinary perturbative expansion has been proposed: it consists in defining the theory on a lattice rather than in continuous space-time. This provides, first, a regularization of the ultraviolet divergences and, second, the possibility of a simple strong coupling expansion.

Every field theory can be defined on a lattice; all that is required is the replacement of the partial derivatives occurring in the Lagrangian with finite difference operators. However, the lattice formulation of a gauge theory is particularly elegant and natural [1, 2]. Indeed, let us remember that the geometric role of the gauge potential is to specify the rotation of the frame of reference in some internal symmetry space as one moves between nearby points in space-time. If the continuum of points is replaced by the vertices of some lattice, the elementary displacements become those between neighboring vertices, i.e., along the links of the lattice itself. Thus, to specify the kinematical state of the system one must associate one definite element of the gauge group with each of the oriented links of the lattice (with the understanding that the inverse element is associated with the link in the opposite orientation). This collection of group elements, which we shall sometimes also call the "spins" of the system, takes the role of the gauge potentials of the continuum theory. Notice that finite group elements are associated with the links of the lattice, whereas infinitesimal generators (the gauge potentials) appear in the continuum theory. In particular, and this will be quite important, on a lattice one can define theories also with finite gauge groups, an option not allowed in the continuum.

As in the conventional theory, the dynamics of the lattice gauge system is formulated through the specification of the action. This function of the spins must be invariant, i.e., must not change under local gauge rotations at the individual vertices and under the transformation correspondingly induced on the spins. Although a variety of gauge invariant quantities exist, most commonly the action is defined as follows. One considers the product of the group elements along the closed oriented paths of smallest extension, or plaquettes (these would be the elementary squares of the lattice, if, as usual, a hypercubical lattice configuration is chosen), takes the trace to obtain a gauge invariant quantity, and sums over all plaquettes. It can be shown that in an appropriate definition of the continuum limit this lattice action reduces to the integral over space-time of the square of the field strength. If, proceeding further, the quantum mechanical averages are defined via a sum over all possible configurations weighted (after a Wick rotation to imaginary time) by the exponential of $-1/\hbar$ times the action, a striking analogy between the lattice gauge theory and a statistical spin system emerges, $\exp(-(1/\hbar)S)$ playing the role of the Boltzmann factor. Considerations that will be expanded in the next section show that the square of the gauge coupling constant (times $\hbar$, to be exact, but we shall henceforth set $\hbar = 1$) plays the role of the temperature in the statistical theory; thus, strong coupling and high temperature or, respectively, weak coupling and low temperature become identified. Of course, the fact that the system is four-dimensional remains as a reminder that we are considering a quantum field rather than an ordinary thermodynamical system.

When one speaks of coupling constant, one should remember that the parameter which governs the strength of the interaction on the lattice is a bare coupling constant, rather than the physical one. However interesting the lattice model may be per se, the ultimate goal of the field theorist is to understand the properties of the continuum system. Thus, one must proceed to a limit in which the lattice spacing vanishes. This demands a careful readjustment of the coupling constant (renormalization) lest the whole physics collapse together with the lattice itself. Indeed, to keep the physical correlation lengths (and other observables) finite as the lattice spacing is set to zero, one must make them extend over larger and larger numbers of lattice points through a judicious change of the bare coupling constant. In the limit the correlations will extend over an infinite number of lattice points, but this is the very definition of a continuous critical point of the system. We see then, that the continuum limit can be recovered from the lattice only if the coupling constant is renormalized to one of its critical values (zero included). It is, therefore, of paramount importance to understand the structure of the lattice gauge system, its critical points, and their nature.

For many years, physicists studying analogous problems in ordinary statistical mechanical systems have been able to obtain invaluable information by means of Monte Carlo simulations [3]. The basic idea of these numerical computations is to represent in the memory of a high speed computer a definite state of the statistical variables of the system under consideration and to set up a Markovian process in which the state is iteratively replaced by new configurations. The algorithm is defined in such a way that the process approaches statistical equilibrium in the sense that the probability of encountering any definite state becomes proportional to the Boltzmann factor. When this regime of equilibrium is reached, statistical averages may be approximated by averages over a number of the configurations encountered in the process.

Application of this method, which has been extremely successful in the study of two- and three-dimensional models, to the four-dimensional systems met in lattice field theories may seem highly problematic because of the large number of statistical variables which must be considered for any but the minimal size of the lattice. During the past few years, however, it has become apparent that these systems are also amenable to Monte Carlo simulations. Even if the extent of the lattice is necessarily small (the largest lattices so far considered measure 16 sites in each of the four dimensions), a remarkable amount of information can be derived on the dynamical structure of the underlying models. Thus, Abelian and non-Abelian pure gauge systems and systems with matter fields of bosonic and fermionic nature all have been studied, with a degree of detail dependent on the techniques and computer resources available.

In this way, Abelian lattice systems, based on the U(1) gauge group, have been shown to possess two phases: a strong coupling phase where the charges of the group are confined and a spin-wave Coulombic phase, which contains the quantized photon field in the continuum limit. This two-phase structure is in welcome agreement with theoretical expectations and indeed essential if lattice theory is to be relevant to particle physics. At strong coupling, all quantized gauge systems exhibit confining properties; consequently a critical point at some finite value of the bare coupling constant must intervene if a non-confining continuum limit representing electrodynamics is to exist. The Abelian models constructed with finite subgroups of U(1) also exhibit interesting properties. There, beyond the two phases described above, a further weak coupling phase, arising from the discrete nature of the group, also occurs. Duality arguments have been used to relate this phase to the strong coupling one.

The situation with non-Abelian pure gauge systems is quite different. Monte Carlo computations have produced substantial evidence that the strong coupling phase persists to the limit of vanishing bare coupling constant. Moreover, the behavior of the observables as the coupling constant becomes smaller

is in agreement with a perturbative analysis via the renormalization group. Thus for the first time one has a demonstration, albeit of numerical nature, that non-Abelian gauge theories do indeed confine isolated charges at large separation while behaving in an asymptotically free fashion at short distances. Beyond giving evidence for confinement, Monte Carlo simulations permit the computation of the actual value of several observables beyond the reach of perturbative analysis. By now a variety of relevant physical parameters, including the string tension, the deconfining temperature, and the masses of low lying hadrons have been estimated.

Matter fields can also be incorporated in the simulation. With scalar fields the generalization is straightforward. The simulation of systems with fermionic degrees of freedom is more difficult. Various computational schemes have been devised to deal with this situation and it appears that fermions can also be subject to the analyzing power of the Monte Carlo procedure.

The goal of this article is to describe the Monte Carlo method in the context of lattice gauge theories and to review the major results which have been obtained. We address our work both to the readers who themselves intend to apply this powerful technique to specific investigations as well as to those who only wish to be sufficiently informed about the method so as to appraise the reliability of the computations. The plan of the review is as follows. In section 2 we present a brief general review of the lattice formulation of gauge theories. In section 3 we describe the basic ideas behind the Monte Carlo technique. Sections 4, 5 and 6 illustrate various results which have been achieved, respectively, on the phase structure of pure gauge theories, on the determination observables, and on combined Higgs–gauge systems. Section 7 is devoted to an analysis of the various techniques to extend Monte Carlo simulations to systems with fermions together with the consequent results. The exposition in section 7 will be rather brief because substantial research is still in progress on Monte Carlo computations for fermionic systems and this topic may well soon be the subject of a separate review. Finally, very short concluding remarks are offered in section 8.

2. Gauge theories on a lattice

2.1. Basic definitions

To formulate a gauge theory on a lattice it is useful to recall the geometrical role of the potentials $A^{\alpha}{}_{\mu}(x)$ in the continuum theory. These specify the rotation U of the frame in some intrinsic internal symmetry space upon transport between neighboring space-time points x^{μ} and $x^{\mu} + \mathrm{d}x^{\mu}$:

$$U = \exp\{\mathrm{i}gA^{\alpha}{}_{\mu}(x)\lambda_{\alpha}\mathrm{d}x^{\mu}\}, \tag{2.1}$$

where g is the coupling constant and λ_{α} are the infinitesimal generators of the gauge group.

Let us denote by indices $i, j, \ldots$ the sites of the lattice and assume that every site has a well-defined set of neighboring sites. Then, in analogy with the continuum case, the dynamical state of the system will be specified upon assigning an element U_{ji} of the gauge group G to every link between neighboring sites i and j. U_{ji} should satisfy

$$U_{ij} = U_{ji}^{-1}. \tag{2.2}$$

The rotation of the frame in the transport along a path γ proceeding through the neighboring sites i_1, i_2,

$i_3, \ldots i_n$ is given by

$$U_\gamma = U_{i_n i_{n-1}} \cdots U_{i_3 i_2} U_{i_2 i_1} , \tag{2.3}$$

which plays the role of the path ordered operator

$$U_\gamma = P \exp\left\{ \mathrm{i}g \int_\gamma A^\alpha{}_\mu(x) \lambda_\alpha \, \mathrm{d}x^\mu \right\} \tag{2.4}$$

of the continuum theory.

Gauge transformations are defined assigning to each site a group element $g_i \in \mathrm{G}$. The dynamical variables U_{ji} transform as follows

$$U_{ji} \to U_{ji}' = g_j U_{ji} g_i^{-1} . \tag{2.5}$$

This induces the transformation

$$U_\gamma \to U_\gamma' = g_{i_n} U_\gamma g_{i_1}^{-1} . \tag{2.6}$$

A priori there is no restriction on the geometry of the lattice. Most frequently, however, this is taken to be hypercubical and, unless otherwise specified, this is the discretization of space-time we shall assume. We shall denote the lattice spacing by a. In some applications it is convenient to introduce different lattice spacings a_s and a_t in the space-like and time-like dimensions.

An interesting possibility consists in not taking a regular lattice, but rather considering a random distribution of points in space-time. By appropriately defining the measure of the distribution one can maintain Poincaré covariance in spite of the discrete structure of space-time. This approach has recently been pursued in ref. [4].

As a final remark, we would like to stress that in lattice gauge theories the dynamical variables U_{ij} always represent finite (not infinitesimal) group transformations, because they correspond to the transport along a path of finite length. Thus in the lattice formulation there is no restriction that the gauge group should be a Lie group and indeed it is sometimes convenient to consider models where the gauge group is some discrete, finite group.

2.2. The action

In analogy with the continuum theory the dynamical properties of the lattice gauge system are formulated by introducing an action S. In the continuum case S is the functional

$$S = \frac{1}{4} \int \mathrm{d}^4 x \, F_{\mu\nu}{}^\alpha F_\alpha{}^{\mu\nu} , \tag{2.7}$$

where

$$F_{\mu\nu}{}^\alpha = \partial_\mu A_\nu{}^\alpha - \partial_\nu A_\mu{}^\alpha + \mathrm{i}g f^{\alpha\beta\gamma} A_\mu{}^\beta A_\nu{}^\gamma$$

is the field strength associated with the potential $A_\mu{}^\alpha$ and $f^{\alpha\beta\gamma}$ are the structure constants for the group. The action is originally defined in Minkowski space-time. As we shall see in the next subsection, to formulate the quantum theory it is useful to perform a Wick rotation to imaginary time, which renders space-time Euclidean. There is then no distinction between upper and lower indices and the integrand in eq. (2.7) is positive definite. The following formulae are presented for Euclidean space-time; they may be immediately extended to Minkowski space-time upon the introduction of suitable negative signs.

The field strength $F_{\mu\nu}{}^\alpha$ specifies the rotation of a frame in the transport around an infinitesimal rectangular closed path of sides $\mathrm{d}x^\mu$ and $\mathrm{d}x^\nu$. This rotation is represented by the operator

$$U_P = \exp\{\mathrm{i}gF_{\mu\nu}{}^\alpha \lambda_\alpha \, \mathrm{d}x^\mu \, \mathrm{d}x^\nu\} \tag{2.8}$$

(no sum over μ and ν).

In a lattice there will be some elementary closed paths which play the role of the infinitesimal rectangles $(\mathrm{d}x^\mu, \mathrm{d}x^\nu)$. If the hypercubical form is assumed, these paths are naturally taken along the sides of the smallest squares of the lattice, commonly referred to as "plaquettes". The transporter around a plaquette of vertices $i_1 i_2 i_3 i_4$ according to eq. (2.3) will be

$$U_P = U_{i_1 i_4} U_{i_4 i_3} U_{i_3 i_2} U_{i_2 i_1} . \tag{2.9}$$

In the continuum theory $F^\alpha{}_{\mu\nu} F_\alpha{}^{\mu\nu}$ (sum over α only) vanishes when the transport around the infinitesimal rectangle $(\mathrm{d}x^\mu, \mathrm{d}x^\nu)$ gives the identity. The same quantity then takes increasing positive values the more the transport deviates from I. In analogy, we shall associate an action with the plaquette

$$S_P = \beta f(U_P) , \tag{2.10}$$

where $f(U_P)$ is a function with the following properties:

(i) it is a class function

$$f(gU_P g^{-1}) = f(U_P) \tag{2.11}$$

(which guarantees invariance of S under gauge transformations, see eq. (2.6));

(ii) it vanishes when $U_P = I$ and takes positive values otherwise;

(iii) S behaves as $(a^4/2)F^\alpha{}_{\mu\nu} F_\alpha{}^{\mu\nu}$ (sum over index α only) if the link variables U_{ji} take the infinitesimal form of eq. (2.1) and the displacements $\mathrm{d}x^\mu$, $\mathrm{d}x^\nu$ are identified with the lattice spacing a. (This last requirement is imposed so that one may, at least formally, recover the continuum form of the action in a suitable limit.)

The total action S will be obtained summing S over all plaquettes.

The parameter β in eq. (2.10) is a constant which is convenient to factor out of the function f. It will be useful to call $f(U_P)$ the (internal) energy of the plaquette. β is a coupling parameter, which governs the strength of the dynamical gauge field self-interaction. To illustrate this point let us assume that for definiteness the gauge group G is SU(2). We shall then represent the group elements in the form

$$U = \cos\theta + \mathrm{i}\boldsymbol{\sigma} \cdot \boldsymbol{n} \sin\theta , \tag{2.12}$$

where $\boldsymbol{\sigma}$ represents the Pauli matrices and $\boldsymbol{n}$ is a unit vector. Following the standard convention, $\lambda_\alpha = \sigma_\alpha/2$. If we introduce the obvious notation

$$U_{ji} = \cos\theta_{ji} + \mathrm{i}\boldsymbol{\sigma}\cdot\boldsymbol{n}_{ji}\sin\theta_{ji} \tag{2.13}$$

and

$$U_{\mathrm{P}} = \cos\theta_{\mathrm{P}} + \mathrm{i}\boldsymbol{\sigma}\cdot\boldsymbol{n}_{\mathrm{P}}\sin\theta_{\mathrm{P}}\,, \tag{2.14}$$

simple algebra shows that in the limit where U_{ji} assumes the infinitesimal form of eq. (2.1) and up to terms of higher order

$$\theta_{ji} = \tfrac{1}{2}g|A_\mu{}^\alpha|a\,, \qquad n_{ji}{}^\alpha = A_\mu{}^\alpha/|A_\mu{}^\alpha| \tag{2.15}$$

and

$$\theta_{\mathrm{P}} = a^2 g^{-2}|F_{\mu\nu}{}^\alpha|\,, \qquad n_{\mathrm{P}}{}^\alpha = F_{\mu\nu}{}^\alpha/|F_{\mu\nu}{}^\alpha| \tag{2.16}$$

(the modulus refers to vectors in the space of SU(2) generators, the components of which are labelled by the index α). The choice

$$f(U_{\mathrm{P}}) = 1 - \tfrac{1}{2}\,\mathrm{Tr}\,U_{\mathrm{P}} = 1 - \cos\theta_{\mathrm{P}}\,, \tag{2.17}$$

together with the identification

$$\beta = 4/g^2\,, \tag{2.18}$$

will guarantee

$$S_{\mathrm{P}} = \frac{4}{g^2}(1-\cos\theta_{\mathrm{P}}) \approx \frac{a^4}{2}F_{\mu\nu}{}^\alpha F_\alpha{}^{\mu\nu} \qquad \text{(sum over } \alpha \text{ only)} \tag{2.19}$$

for $\theta_{\mathrm{P}} \to 0$. If we now construct the full action as a sum over all plaquettes, we find that in the formal limit $a \to 0$

$$S = \sum_{\mathrm{P}} S_{\mathrm{P}} \xrightarrow[\theta_{\mathrm{P}}\to 0]{} \sum_{\mu\nu}\frac{a^4}{4}F_{\mu\nu}{}^\alpha F_\alpha{}^{\mu\nu} \xrightarrow[a\to 0]{} \int \mathrm{d}^4x\,\tfrac{1}{4}F_{\mu\nu}{}^\alpha F_\alpha{}^{\mu\nu}\,, \tag{2.20}$$

i.e. S reduces to the form of the continuum action. (In deriving eq. (2.20) remember that the sum over indices μ, ν counts every plaquette twice.)

The specific choice for the plaquette energy given by eq. (2.17) (with its obvious generalization $f(U_{\mathrm{P}}) = 1 - N^{-1}\,\mathrm{Re}\,\mathrm{Tr}\,U_{\mathrm{P}}$ for an SU(N) gauge group) corresponds to what is commonly called Wilson's form of the lattice action. But the formal passage to the continuum limit requires only $f(\theta) \approx \theta^2/2$ for $\theta \to 0$. We will later discuss some other forms of the lattice action which have been studied in the literature.

2.3. The observables and the continuum limit

A convenient way to define a quantum field theory consists in the following. A Wick rotation to imaginary time is performed first, to allow for a more rigorous definition of functional averages [5]. The observables, which will thus be defined in a Euclidean four-dimensional space, can be later continued, if necessary, back to Minkowski space-time. The quantum expectation value of an observable functional of the fields $O(A)$ is then obtained by averaging its value over all field configurations with a measure proportional to $\exp\{-S(A)\}$:

$$\langle O\rangle = Z^{-1}\int \mathrm{d}A\, O(A)\, \mathrm{e}^{-S(A)} \tag{2.21}$$

where the vacuum to vacuum persistence amplitude or partition function Z is given by

$$Z = \int \mathrm{d}A\, \mathrm{e}^{-S(A)}. \tag{2.22}$$

Of course one must give a meaning to the functional integrals introduced in eqs. (2.21), (2.22) by a suitable regularization procedure, but this need not worry us because it is precisely what we shall achieve by replacing the continuum of points of space-time with a discrete lattice.

In analogy with the continuum formulation, the expectation values for the observables of the lattice quantum theory are defined by averages

$$\langle O\rangle = \sum_{\{U_{ji}\}} O(U_{ji}) \exp\{-S(U_{ji})\}/Z, \tag{2.23}$$

$$Z = \sum_{\{U_{ji}\}} \exp\{-S(U_{ji})\} \tag{2.24}$$

where the sums are ordinary sums if the dynamical variables U_{ji} belong to a discrete gauge group or multiple invariant integrals over the group manifold if we have a Lie gauge group. It is useful to initially consider a lattice of finite extent, containing a definite number N of sites. Then the averages in eqs. (2.23) and (2.24) are well defined definite sums or multiple integrals over a finite number of variables. After the finite volume averages are evaluated one proceeds to the thermodynamic limit $N\to\infty$.

Although in the lattice formulation of the quantum theory all quantities have precise mathematical meaning, one must not forget the goal is to define a quantum system in continuous space-time. For this one must proceed to a continuum limit, letting the lattice spacing a go to zero. A simple rescaling of a to zero, however, is not sufficient to define a continuum quantum theory. The divergences of quantum field theory force us to renormalize the couplings. Any observable with non-vanishing physical dimension, a correlation length l for instance, will be given by an expression of the form

$$l = a\,\lambda(g), \tag{2.25}$$

where the lattice spacing enters trivially. The non-trivial aspects of the theory are embodied in the dimensionless function λ of the coupling constant g (or, equivalently, of the coupling parameter β).

Clearly, it will be possible to define a non-trivial continuum limit only if as a approaches zero g can be readjusted so as to keep the product $l = a\lambda(g)$ constant. This demands that there exist a critical value g_{cr} such that

$$\lim_{g \to g_{cr}} \lambda(g) = \infty . \tag{2.26}$$

Requiring that l remains constant establishes then a functional relation

$$g = g(a): \qquad l = a\lambda(g(a)) = \text{const} . \tag{2.27}$$

Thus g appears as a non-renormalized or bare coupling constant, which must be readjusted as the cut-off is removed.

A further requirement must be satisfied for the lattice theory to define a continuum quantum field theory. The critical point $g = g_{cr}$ must have scaling properties; once the functional relation between g and a is determined by demanding constancy of a definite observable, the same relation must make all other observables also tend to well defined values as $a \to 0$.

In general, to establish the existence of a scaling critical point constitutes quite a non-trivial problem. In non-Abelian gauge theories, however, perturbative arguments tell us that $g = 0$ is such a point [6]. Precisely, it can be shown that perturbation theory is consistent with the bare coupling constant tending to zero as the cut-off is removed and for small g the relation between g and a must be governed by the equation

$$a \frac{dg(a)}{da} = \gamma(g) = \gamma_0 g^3 + \gamma_1 g^5 + O(g^7) . \tag{2.28}$$

The coefficients γ_0 and γ_1 assume the values [6, 7]

$$\gamma_0 = \frac{1}{16\pi^2}\left(\frac{11N}{3}\right), \qquad \gamma_1 = \left(\frac{1}{16\pi^2}\right)^2 \left(\frac{34N^2}{3}\right) \tag{2.29}$$

in a pure SU(N) theory. Eq. (2.28) is solved by

$$a = \frac{1}{\Lambda} f(g), \qquad f(g) = (g^2\gamma_0)^{-\gamma_1/2\gamma_0^2} e^{-1/2\gamma_0 g^2}(1 + O(g^2)), \tag{2.30}$$

where a dimensional integration constant Λ has been introduced to set the scale.

The observation that $g = 0$ is a possible scaling critical point in non-Abelian gauge theories does not solve the problem of defining a continuum quantum theory or even whether such can be defined. For this purpose one needs to show that as the cut-off is removed the coupling constant does indeed approach $g = 0$, without other intervening critical points, and moreover that the observables scale in a way consistent with eq. (2.30). Namely, if the mass dimension of the observable q is d, q will be given by a formula

$$q = a^{-d} K(g), \tag{2.31}$$

where the dimensionless function $K(g)$ expresses the value of q in lattice units. Then as $g \to 0$, $K(g)$ should behave as

$$K(g) \approx c[f(g)]^d \tag{2.32}$$

to make q approach its physical value. To establish that the non-Abelian lattice gauge theory defines a continuum quantum theory for $g \to 0$, the behavior of eq. (2.32) must be verified. If this is found to occur, the actual value of the observable (in the continuum theory) can be expressed in terms of Λ as

$$q = c\Lambda^d . \tag{2.33}$$

Although perturbative arguments can be used to establish the functional form of the scaling behavior where $g_{cr} = 0$, the determination of dimensional observables cannot be done perturbatively. Indeed the scaling relation itself, eq. (2.30), demonstrates that observables with non-trivial physical dimension must be given by expressions which are non-analytic at $g = 0$. Non-perturbative techniques are called for, and indeed this whole review is dedicated to an exposition of a particular non-perturbative method of computation. The observation that $g = 0$ is a possible scaling critical point in non-Abelian gauge theories has been, however, of fundamental importance. In particular, it has provided an explanation for the experimental observation that, although the constituents which form hadrons appear permanently bound, they exhibit almost free behavior when probed at very high energy and short distances. Indeed, the gauge theory of the strong interactions has led to several quantitative predictions for short distance phenomena.

2.4. *Inclusion of matter fields*

While the gauge dynamical variables are associated with the links of the lattice, matter fields are more naturally assigned to the sites. The matter field part of the action will in general contain terms coupling different sites. The gauge variables must then be used to transport the matter fields between neighboring sites and to construct gauge invariant quantities. For instance, if we denote by i and j neighboring sites, by ϕ_i and ϕ_j the values that some matter field takes there, and by a the lattice spacing, the covariant derivative of the continuum theory

$$\mathrm{D}_\mu \phi = \partial_\mu \phi + \mathrm{i} g A_\mu{}^\alpha \lambda_\alpha \phi \tag{2.34}$$

will find its transcription in the covariant finite difference (no sum over j)

$$(\Delta\phi)_i = \frac{U_{ij}\phi_j - \phi_i}{a} . \tag{2.35}$$

It is assumed here that ϕ transforms under a definite representation of the gauge group: λ_α and U_{ij} are then matrices which express the infinitesimal generators and, respectively, a finite transformation within that representation. U_{ij} serves the purpose of transporting the matter field from site j to site i. In a gauge transformation represented by matrices g_i, ϕ_i and ϕ_j transform as follows:

$$\phi_i \to \phi_i' = g_i \phi_i , \qquad \phi_j \to \phi_j' = g_j \phi_j . \tag{2.36}$$

Then $(\Delta\phi)_i$ transforms as ϕ_i itself:

$$(\Delta\phi)_i \to (\Delta\phi)'_i = g_i(\Delta\phi)_i \tag{2.37}$$

(remember $U_{ij} \to U'_{ij} = g_i U_{ij} g_j^{-1}$). If we denote by $\bar{\phi}\phi$ a scalar product, invariant under transformations of the group G, the quantity $(\Delta\phi)_i\,(\Delta\phi)_i$ would be invariant under gauge transformations and could serve to form the matter field action.

A variety of matter fields are possible in a lattice theory. They may be of bosonic or fermionic nature. It would serve little purpose here to try to classify the different possibilities. Specific models incorporating matter fields will be discussed in later sections of this review. Let us only mention that in a lattice theory the manifold of possible values for the matter field need not necessarily be continuous. In the same way as one can consider models where the gauge group is discrete, so the matter field can be restricted to a discrete set of values, provided this is consistent with the action of the gauge group.

The considerations about necessary requirements for the existence of a continuum limit apply also to models with matter fields. As we shall discuss in section 6, constraints on the matter fields of the σ-model variety, which for instance restrict the moduli to a definite value, do not necessarily prevent the definition of a continuum limit (whereas these constraints generally spoil renormalizability if imposed directly in the continuum quantum theory). The renormalized continuum field would emerge as averages over several lattice sites and would thus not necessarily be subject to the same constraints.

2.5. Analogy with statistical mechanics

The averages which are used to define expectation values of observables in the Euclidean quantum theory bear a noticeable resemblance to the expressions for thermal averages of observables in statistical systems. These are also given by sums over all possible configurations, as in eqs. (2.23) and (2.24), with a weight factor (the Boltzmann factor) equal to

$$\exp(-\beta E), \qquad \text{where } \beta = (kT)^{-1}$$

(T being the temperature, k the Boltzmann constant) where E is the internal energy of the system. If the action of the gauge theory is expressed, following eq. (2.10), as

$$S = \beta \sum_{\mathrm{P}} f(U_{\mathrm{P}}) \tag{2.38}$$

the analogy is complete, the coupling parameter of the quantum field theory playing the role of the inverse temperature, the sum over the "internal energies" of the plaquettes playing the role of internal energy of the system. We see that a regime of weak coupling (remember $\beta \propto 1/g^2$) corresponds to low temperature, whereas strong coupling becomes equivalent to high temperature.

Of course, one must not forget that the analogy is only formal. The fact that the lattice gauge system is four-dimensional is a reminder that one is dealing with a quantized field rather than with a real thermal medium. The true physical temperature of the quantized field is zero. It is actually possible to extend the formalism so as to incorporate finite temperature effects also in the quantized field system (the coupling parameter $\beta \propto 1/g^2$ then must not be confused with $1/kT$). This will be discussed in section 5.

In a statistical system the fact that the correlation length becomes infinite signals the onset of a phase transition (of order higher than first). The all important critical points of the lattice gauge theory which are needed to recover a continuum limit may thus also be seen as boundaries in the phase diagram of the system. Given a lattice gauge theory, then, one of the first questions we would like to answer is what is its phase structure.

For the study of statistical systems a variety of techniques have been developed. Some are of an analytical nature. They are based on expansions for either small or large values of the parameter β. Some studies use Hamiltonian formulations where the continuous nature of the time axis is kept and only space is in lattice form [8]. Other methods of investigation rely instead on numerical sums over configurations of the system. These sums can never be exhaustive, because even for the smallest systems of physical interest, the number of terms would be prohibitively large. Rather, they are based on importance sampling. Some algorithm is used to generate a stochastic sequence of configurations in such a way that the probability of encountering any definite configuration in the sequence is proportional to the weight factor $\exp(-\beta E)$. Then the averages over all configurations are approximated by averages over the configurations occurring in the sequence. The procedure is known as Monte Carlo simulation.

Monte Carlo simulations have produced invaluable results for the investigations of statistical systems. During the last few years they have been successfully applied to the analysis of quantum field theories as well, and the purpose of this article is to review work done on this subject. Other techniques available for the study of statistical systems can also be extended to lattice field theories. They will be very briefly discussed in the next subsections.

2.6. Weak coupling

Perturbation theory forms one of the mainstays in the development of modern theoretical particle physics. As our space-time lattice merely represents a regulator for ultraviolet divergences, in principle all perturbative results could be reproduced in this formalism. The basic expansion parameter g^2 represents the temperature in the analogue statistical system. At low temperatures the important degrees of freedom are low energy excitations involving gentle long wavelength variations of the fields. In magnetic systems the analogous excitations are referred to as spin waves and perturbation theory is a spin wave expansion.

Perturbative analysis did not motivate the original formulation of lattice gauge theory. Highly developed methods for calculation already exist for other cutoff schemes such as that of Pauli and Villars or dimensional regularization. Because of this, perturbation theory on a lattice has received rather little attention and remains quite awkward. It is somewhat ironic that this weak coupling regime has played such a minor role in lattice gauge theory and yet it is exactly this region to which we must go for a continuum limit, as discussed above.

As the inverse coupling β becomes large, the path integral is increasingly dominated by U_P near the identity. Perturbation theory begins with a saddle point approximation taken at this maximum of the exponentiated action. We parametrize the plaquette operators

$$U_P = \exp(i\lambda^\alpha \omega^\alpha{}_P) \tag{2.39}$$

where the matrices λ^α generate the group and are normalized such that to leading order we have

$$1 - \frac{1}{N} \operatorname{Re} \operatorname{Tr} U_P = \frac{1}{4N} \omega^\alpha{}_P \omega^\alpha{}_P + O(\omega_P{}^3) . \tag{2.40}$$

Thus we have

$$Z = \int \mathrm{d}U \exp\left(-\frac{\beta}{4N}\,\omega^{\alpha}{}_{\mathrm{P}}\omega^{\alpha}{}_{\mathrm{P}} + \mathrm{O}(\beta\omega_{\mathrm{P}}{}^{3})\right). \tag{2.41}$$

For large β the exponential is highly suppressed unless

$$\omega_{\mathrm{P}} = \mathrm{O}(\beta^{-1/2}) = \mathrm{O}(g_0). \tag{2.42}$$

The $\omega_{\mathrm{P}}{}^{3}$ terms in eq. (2.41) are then of order the coupling constant.

To proceed we would like to evaluate the leading behavior of the integral in eq. (2.41) in the Gaussian approximation. Here we encounter a technical difficulty in that the integrand is not damped in all directions when considered as a function of the link variables U_{ji}. Indeed, a gauge transformation can arbitrarily alter any given link and yet leave the action unchanged. Gauge fixing is an essential first step in the perturbative analysis. Our integrand receives a Gaussian damping only for those directions which do not represent gauge degrees of freedom.

The details of the gauge choice will be unimportant to the discussion here. We merely note that after the gauge fixing, one quarter of the degrees of freedom are no longer variables [9]. The remaining dynamical variables are driven to the identity, about which we can expand

$$U_{ji} = 1 + \mathrm{i}\lambda^{\alpha}\omega^{\alpha}{}_{ji} + \mathrm{O}(\omega_{ji}^{2}) \tag{2.43}$$

$$\omega^{\alpha}{}_{\mathrm{P}} = \sum_{ji\in\mathrm{P}} \omega^{\alpha}{}_{ji} + \mathrm{O}(\omega^{2}). \tag{2.44}$$

The integration measure in the vicinity of the identity takes the simple form

$$\mathrm{d}U_{ji} = (J + \mathrm{O}(\omega_{ji}^{2}))\,\mathrm{d}\omega \tag{2.45}$$

where the weight J will ultimately be absorbed as an irrelevant constant. Now the partition function assumes the form

$$Z = K\int \mathrm{d}\omega \exp(-\tfrac{1}{2}\beta\omega D^{-1}\omega) \tag{2.46}$$

where K is an overall constant factor and D^{-1} is a matrix operating in the space of the variables ω_{ji}. The operator D is the propagator for the gauge gluons and enters into the Feynman diagrams of the theory.

For actual calculations these lattice propagators are quite cumbersome. However we can obtain some information on the average plaquette with very little effort. As our integral is now Gaussian, its value is a determinant

$$Z = K'|D/\beta|(1 + \mathrm{O}(\beta^{-1})). \tag{2.47}$$

The matrix D has the dimensionality of the parameter space after gauge fixing; consequently, it is a square matrix of $3n_{\mathrm{g}}N$ rows. Here n_{g} is the number of generators of the group, 3 is the number of

non-fixed links per site, and N is the number of lattice sites. Removing a factor of β from each row of the matrix, we find

$$Z = K'|D|\beta^{-3n_g N}(1 + O(\beta^{-1})) . \tag{2.48}$$

For the average plaquette or internal energy this implies

$$E = -\frac{1}{6N}\frac{\partial}{\partial\beta}\log Z = \frac{n_g}{4\beta} + O(\beta^{-2}) . \tag{2.49}$$

This result has a simple interpretation in statistical mechanics. We have $3n_g N$ physical variables distributed over $6N$ plaquettes. If we give each degree of freedom $\frac{1}{2}kT = 1/(2\beta)$ average energy, then we obtain exactly eq. (2.49). This simple counting of variables receives corrections at higher temperatures where nonlinear interactions come into play.

2.7. Strong coupling

In the statistical analogue, the strong coupling regime is the high temperature limit. High temperature expansions are an old subject in solid state physics, but before Wilson's work they were relatively unknown to particle theorists. Indeed, in the continuum theory the strong coupling limit is rather unnatural and difficult to treat. In contrast, on the lattice strong coupling is by far the simplest limit. One merely expands the Boltzmann factor in powers of the inverse temperature and evaluates the terms in the resulting series. In the gauge theory each power of β is associated with a plaquette somewhere in the lattice. This gives a simple diagrammatic intepretation in terms of graphs built up from such plaquettes [1, 10].

Consider the internal energy for the SU(N) theory

$$E = \left\langle 1 - \frac{1}{N}\mathrm{Tr}\, U_P \right\rangle = \frac{1}{Z}\int \mathrm{d}U\, \mathrm{e}^{-\beta S(U)}\left(1 - \frac{1}{N}\mathrm{Tr}\, U_P\right), \tag{2.50}$$

where we have explicitly extracted the factor of β from the action. We now observe that because

$$\int \mathrm{d}U\, U_{ji} = 0 \tag{2.51}$$

E must go to unity as β goes to zero. Indeed, for each link in U_P we must bring down at least one corresponding link from an expansion of the exponential of the action to avoid the zeros from eq. (2.51). Correspondingly, every link from the action must have a partner, either from the action itself or the inserted loop. The first non-trivial contribution in the strong coupling series comes from covering our plaquette with another from the exponential. The simple integral needed to evaluate this contribution is [11]

$$\int \mathrm{d}U\, U_{ji}\, U^{-1}_{kl} = N^{-1}\,\delta_{jl}\,\delta_{ik} . \tag{2.52}$$

Combining the δ functions and multiplying with $\beta/(2N)$ for the plaquette brought down from the exponential of the action, we obtain the result

$$E=\begin{cases}1-\dfrac{\beta}{2N^2}+\mathrm{O}(\beta^2), & N>2\\[2ex] 1-\dfrac{\beta}{4}+\mathrm{O}(\beta^3), & \mathrm{SU}(2).\end{cases} \tag{2.53}$$

Strong coupling expansions have been carried out for SU(3) to order β^{12} for the coefficient of the linear interquark potential and to order β^8 for the mass gap [12]. Various attempts to match these expansions onto the weak coupling behavior in eq. (2.32) have provided interesting predictions on the numerical values of these parameters in the continuum limit.

3. Monte Carlo simulations

3.1. General discussion

The sums over configurations which define quantum averages (eqs. (2.23) and (2.24)) contain so many terms that even if the system has been restricted to a limited volume and the dynamical variables to finite set, a straightforward numerical computation is impossible. On the other hand, it is well known, especially in the context of the analogous formulation of statistical mechanics, that effectively only a small subset of all possible configurations contributes to the averages. The basic idea of Monte Carlo (MC) simulations [3] is to sample this set with a stochastic sequence of configurations C_i such that the probability of encountering any definite configuration C is proportional to the measure factor $\exp\{-S(\mathrm{C})\}$. The average of an observable O can then be approximated by the mean value taken by the observable over several states in this sequence

$$\langle O\rangle \approx \frac{1}{N}\sum_i O(\mathrm{C}_i)\,. \tag{3.1}$$

The passage from one configuration C_i to the next one C_{i+1} is determined by a transition matrix $P(\mathrm{C}\to\mathrm{C}')$, satisfying the constraints of stochastic matrices:

$$P(\mathrm{C}\to\mathrm{C}')\geq 0 \tag{3.2}$$

and

$$\sum_{\mathrm{C}'} P(\mathrm{C}\to\mathrm{C}')=1\,. \tag{3.3}$$

In the customary implementation of the MC algorithm, the transition involves the change of just one of the dynamical variables at a time: $U_{ji}\to U_{ji}'$. The variable undergoing the change could be picked up at random, but it is computationally more convenient to proceed through the lattice in an orderly fashion, modifying one of the dynamical variables (which constitutes a Monte Carlo step), then another one and

so on, until all the variables have been sampled and thus one Monte Carlo iteration or sweep of the lattice is completed. Properly speaking, therefore, one does not define a single transition matrix $P(C \to C')$, but a whole collection $P_{ji}(C \to C')$, P_{ji} coinciding with the transition probability $P(U_{ji} \to U'_{ji})$ for the variable U_{ji}, the other dynamical variables being kept fixed. A Markovian chain is still defined by the matrix $P_{tot} = \ldots P_{j''i''}(C'' \to C''')P_{j'i'}(C' \to C'')P_{ji}(C \to C')$, where the product extends over all individual transition probabilities in the order in which the variables are sampled. $P_{tot}(C \to C')$ determines the change at the end of one full Monte Carlo iteration. In the following we shall leave the index ji in $P_{ji}(C \to C')$ implicit. Also let us mention that one can define, and in some applications this may be necessary, Monte Carlo steps where two or more variables are modified simultaneously.

The goal is to define a stochastic sequence with the property that, after statistical equilibrium is reached, the probability of finding any configuration C in the sequence becomes proportional to $\exp\{-S(C)\}$. In other words $\exp\{-S(C)\}$ must be an eigenvector of the stochastic process and the probability vector state of the system must converge to it. A sufficient condition is that each step of the transition matrix obeys a requirement of detailed balance:

$$e^{-S(C)} P(C \to C') = e^{-S(C')} P(C' \to C) . \tag{3.4}$$

(In the case where P_{tot} is a product it is sufficient that each piece satisfy this condition and not necessarily the entire transition probability.) If eq. (3.4) is satisfied it is immediate to show that $\exp\{-S(C)\}$ is an eigenvector. Indeed one has

$$\begin{aligned} \sum_C e^{-S(C)} P(C \to C') &= \sum_C e^{-S(C')} P(C' \to C) \qquad \text{(by eq. (3.4))} \\ &= e^{-S(C')} \qquad \text{(by eq. (3.3))} . \end{aligned} \tag{3.5}$$

To study the convergence to this eigenvector we need a concept of distance between ensembles E and E′, each containing many configurations. Suppose that the probability density of configuration C in E or E′ is $P(C)$ or $P'(C)$, respectively. Then define the distance between E and E′ as

$$\|E - E'\| = \sum_C |P(C) - P(C')| . \tag{3.6}$$

Now it is possible to prove on general grounds that if E_{eq} represents an equilibrium distribution, associated with the eigenvector $P_{eq}(C)$ of $P(C \to C')$, the algorithm never increases the distance from equilibrium. Indeed if E′ is obtained from E by the Monte Carlo algorithm defined by $P(C \to C')$ then

$$P'(C) = \sum_{C'} P(C' \to C) P(C') . \tag{3.7}$$

We can now compare the distance of E′ from E_{eq} with the distance of E from equilibrium

$$\begin{aligned} \|E' - E_{eq}\| &= \sum_C \left| \sum_{C'} P(C' \to C)(P(C') - P_{eq}(C)) \right| \\ &\le \sum_{C \to C'} P(C' \to C) |P(C') - P_{eq}(C')| = \|E - E_{eq}\| , \end{aligned} \tag{3.8}$$

where the properties in eqs. (3.2) and (3.3) have been used. This shows that the distance from equilibrium never increases. Replacing the weak inequality in eq. (3.8) with a strict inequality is less straightforward and depends on the details of the algorithm (it is possible to define pathological cases where $\|E' - E_{eq}\| = \|E - E_{eq}\| \neq 0$). Moreover, one is not really interested in a theoretical convergence to equilibrium, but in a rate of convergence rapid enough to make application of the method practical. In most instances such convergence is indeed observed.

The detailed balance condition eq. (3.4) does not specify completely the transition probabilities $P(U_{ji} \to U_{ji}')$. There are variations of the MC algorithm which use different forms for $P(U_{ji} \to U_{ji}')$. We describe here the three implementations of the technique normally followed.

(i) The method of Metropolis et al. [13]. The transition from U_{ji} to U_{ji}' is a two step process. First a new candidate value $\hat{U}_{ji}$ is selected with an arbitrary probability distribution P_0 obeying:

$$P_0(U_{ji} \to \hat{U}_{ji}) = P_0(\hat{U}_{ji} \to U_{ji}) . \tag{3.9}$$

Then the change in action ΔS induced by the replacement $U_{ji} \to \hat{U}_{ji}$ is computed:

$$\Delta S = S(\hat{U}_{ji}) - S(U_{ji}) \text{ (all other variables kept fixed)} . \tag{3.10}$$

If $\Delta S \leq 0$ the change is accepted and $U_{ji}' = \hat{U}_{ji}$; otherwise a pseudorandom number r, selected in the interval between 0 and 1 with uniform probability distribution, is generated and:

– if

$r \leq e^{-\Delta S}$ the change is accepted $U_{ij}' = \hat{U}_{ji}$;

– if

$r > e^{-\Delta S}$ the change is rejected and $U_{ji}' = U_{ji}$.

Eq. (3.4) is clearly satisfied because, assuming for instance $S(\hat{U}_{ji}) \geq S(U_{ji})$,

$$\frac{P(U_{ji} \to \hat{U}_{ji})}{P(\hat{U}_{ji} \to U_{ji})} = \frac{P_0(U_{ji} \to \hat{U}_{ji})}{P_0(\hat{U}_{ji} \to U_{ji})} \cdot \frac{e^{-\Delta S}}{1} = \frac{\exp\{-S(\hat{U}_{ji})\}}{\exp\{-S(U_{ji})\}} . \tag{3.11}$$

The goal of the Metropolis method is to maximize the rate of change from one configuration to the next, which is achieved by making as large as possible (indeed unity) the probability of the transition in the direction which lowers the action. Its efficiency is however hampered by the fact that, especially in a regime of weak coupling where configurations of low action are favored, most of the proposed changes may lead to a drastic increase in action and thus to a rejection of the move.

(ii) The heat bath method [14]. The new value U_{ji}' is selected among all possible values for the dynamical variable with a probability distribution proportional to $\exp\{-S(U_{ji}')\}$ (the other U's being kept fixed), irrespective of the previous value U_{ji}. Eq. (3.4) is then satisfied in an obvious way. The advantage of this method is that, all new candidate values of U_{ij} being considered simultaneously, there is no possibility that the Monte Carlo step rejects a change only because a "poor" new candidate was

selected. On the other hand choosing a new value of the dynamical variable on the basis of a definite probability distribution is in general computationally rather demanding. For instance, if the U_{ji}' belong to a finite set, all possible values of $\exp\{-S(U_{ji}')\}$ must be calculated, up to a common factor. There are systems, though, where the selection of the new value can be done with a simple and elegant procedure for which the heat bath method becomes very convenient. These are discussed in subsection 3.3.

(iii) The modified Metropolis method.

The algorithm is basically the same as in the Metropolis method, except that after the move from U_{ji} to U_{ji}' has been completed, the whole procedure is repeated one or more times on the same link before proceeding to the next MC step (i.e., the next dynamical variable). We shall say that, rather than upgrading the value of U_{ji} once, one performs n ungradings per step. Of course, the net result is that the probability of considering an acceptable new candidate for U_{ji} is increased. The advantage of performing several upgradings per step, rather than simply doing more steps, is that a sizeable fraction of the computation leading to ΔS involves only the values of the neighboring dynamical variables, kept fixed in the move, and this does not have to be repeated. This is considerably more beneficial in gauge theories than spin models because of the complexity of the interaction. It will be noticed that as the number n of upgradings per step tends to infinity, the modified Metropolis method reduces to the heat bath. This algorithm, therefore, interpolates between the other two and usually a value of n which insures optimal efficiency can be found empirically.

We conclude this subsection with two considerations, which may appear straightforward now, but will be of relevance when we consider extensions to systems with fermions.

(i) The MC algorithm is possible because e^{-S} or, more precisely, $e^{-\Delta S}$ is a well-defined positive number. Of course, this looks like a trivial remark; but the measure would not be positive definite if, for instance, we were trying to calculate the quantum averages directly in Minkowski space. Then the expectation values would be the result of drastic cancellations between generally complex terms, and the summation based on importance sampling, as described in this section, could not be applied. Unfortunately, cancellations among positive and negative terms occur also when the sums over configurations are extended to include fermionic variables, and this makes the application of the MC method to fermions more problematic.

(ii) It is clear that a successful application of the technique requires averages over a very large number of configurations. Several MC steps for each dynamical variable must be performed. The number of times that the variation in action ΔS must be calculated is thus extremely high, and even with a powerful computer the simulation becomes possible only if the number of arithmetic operations required to determine the variation of the action is not too large. Luckily this is the case because of the locality properties of the action. Even in the lattice formulation the action is local, in the sense that it is built from terms which involve only couplings between a few neighboring dynamical variables. Performing an efficient MC simulation becomes much more difficult when, maybe as the result of partial summations over some of the variables, the dynamics is governed by a non-local effective action.

3.2. Practical considerations

While it is possible to formulate the general principles on which MC simulations are based, no fixed set of rules can be prescribed when it comes to doing an explicit computation. MC simulations are an art very much akin to experiments: the specifics of the execution will depend on the objectives, means and capabilities of the performer. There are, however, a few considerations which will enter into any MC simulation. They concern the choices of

(i) observables to measure,
(ii) lattice size,
(iii) boundary conditions,
(iv) initial configuration and length of the simulation.

We shall comment briefly on these points.

(i) Observables. There is of course a large variety of quantities whose averages can be measured by a MC simulation. The limitations are in the amount of computation which may be required and in the magnitude of the statistical fluctuations, which may make the measurement meaningless if the average value to be determined is too small relative to the background. In general, bulk quantities such as the expectation value of the internal energy (i.e., the average plaquette action) will be easier to evaluate than quantities which depend on correlations between dynamical variables at different points or on correlations among different MC iterations (such as the fluctuation in the average internal energy). On the other hand, bulk quantities are normally less directly related to the renormalized observables of the continuum limit. Although measurements may be easier to perform, they are of more relevance for the properties of the lattice theory per se. More refined analysis of correlation-dependent observables will be needed to extract information on the continuum limit.

(ii) The size of the lattice should of course be large enough to accommodate the physical dimensions involved in the measurement without marked finite size effects. Experience with four-dimensional lattice gauge theories has shown, however, that even lattices of rather small linear size can be useful to evaluate some quantities (especially of bulk nature). This is probably due to mean field effects from the large number of neighbors in high dimension. Fig. 1 illustrates measurements of the internal energies in the two phases which coexist at the first-order critical point in the Abelian Z_2-model [15]. One notices that lattices of 4^4 and even 3^4 sites are large enough to separate clearly the two phases and provide an estimate of the energies.

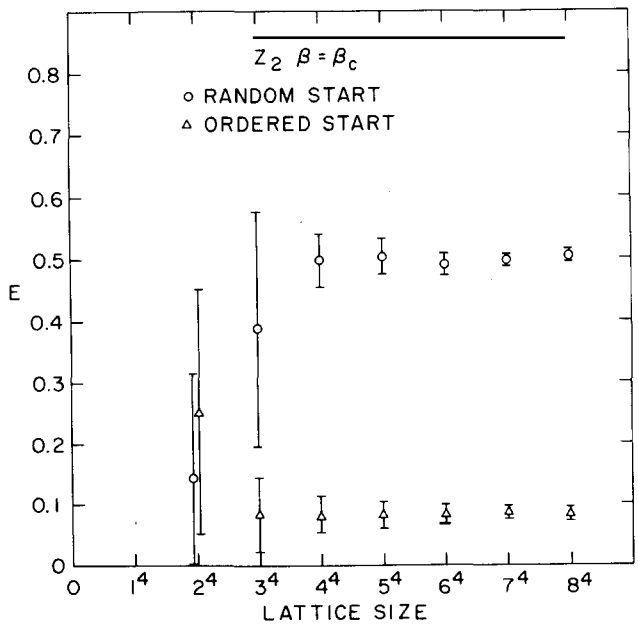

Fig. 1. Monte Carlo measurements of the internal energy on various size lattices with the gauge group Z_2. The runs were made at the temperature of the phase transition in the four-dimensional model. The error bars represent root mean square fluctuations. On each size lattice results from both random and ordered initial configurations are shown.

Beyond the advantage of reducing finite size effects, large lattices give better statistical accuracy if measurements are made over all positions that an observable can occupy in the lattice. This is a true advantage, however, only if for some technical reasons a sweep of a large lattice can be done at a faster rate (in terms of the time it takes to upgrade one dynamical variable) than the corresponding number of sweeps of a smaller lattice. Otherwise, one can make up for the loss of statistical accuracy in a smaller lattice by performing a larger number of Monte Carlo iterations. Finally, working with large lattices may require longer simulations to achieve statistical equilibrium in the proximity of a higher order critical point. This will be the case if the correlation length which governs approach to equilibrium becomes comparable to the lattice size.

(iii) The importance of choosing appropriate boundary conditions is clearly demonstrated by the fact that an 8^4 lattice has $8^4 - 6^4 = 2800$ points on its boundary and only 1296 points in its interior. Periodic boundary conditions are normally assumed in order to avoid finite size effects directly due to the boundary.

Periodicity may also be imposed modulo some transformation on the dynamical variables. Doing so, one can force excitations of topological nature into the system. One speaks then of twisted boundary conditions [16]. In a one-dimensional array of Ising spins, which can be oriented only up or down, twisted boundary conditions consist in assuming that the neighbor of the last spin in the array is the first spin with orientation reversed. Then the total number of spin reversals in the chain becomes necessarily odd and cannot be less than one.

Another variation of the periodic boundary conditions, of technical nature rather than bearing physical content (indeed, it should not affect the physics), consists in assuming periodicity up to a shift of one site in one of the orthogonal directions [17]. We use a two-dimensional system of N^2 sites to exemplify this choice of boundary conditions. The idea is that, proceeding columnwise, the neighbor of a spin $s_{i,N}$ will not be $s_{i,1}$ but rather $s_{i+1,1}$. Thus all the spins can be ordered into a single one-dimensional array $s_{11}s_{12}\ldots s_{1N}s_{22}\ldots s_{2N}s_{31}\ldots$, in such a way that neighbors in the array are also neighbors in the lattice. The procedure corresponds to assuming that the lattice winds in a helical fashion around the toroidal manifold induced by periodicity.

(iv) Initial configuration. With the possible exception of investigations focussing on the dynamical behavior of the Markovian chain itself, MC simulations effectively make use only of the configurations obtained after statistical equilibrium is reached. The specific choice of the initial configuration is therefore in principle irrelevant. One would like however to reduce the length of the transient needed to reach equilibrium; and, also, a simple test for equilibrium lies in the independence of results obtained from different initial configurations. Thus the selection of an appropriate set of initial values for the dynamical variables becomes of practical importance.

An obvious possibility for the initial data consists in setting all U_{ji} variables equal to the identity of the group. The action is then minimal and one speaks of a cold or ordered start. At the opposite extreme, one can let the U_{ji} take entirely random values within the group manifold. This is the infinite temperature configuration and one speaks of a hot, or disordered, start. Fig. 2 illustrates the behavior of the internal energy as function of the number of iterations in the simulation of a Z_6-model, very near the value of β where the system is known to undergo a second-order phase transition [15]. One notices that, in spite of the critical slowing down one may expect, both with ordered (upper line) and disordered starts (lower line) the simulation converges reasonably rapidly to statistical equilibrium. However, an analogous simulation for a system which undergoes a first-order phase transition, even slightly away from the critical point, may fail to converge to equilibrium because of metastability effects. Fig. 3 illustrates the results of ordered and disordered starts for the Z_2-model at the first-order critical point β_c

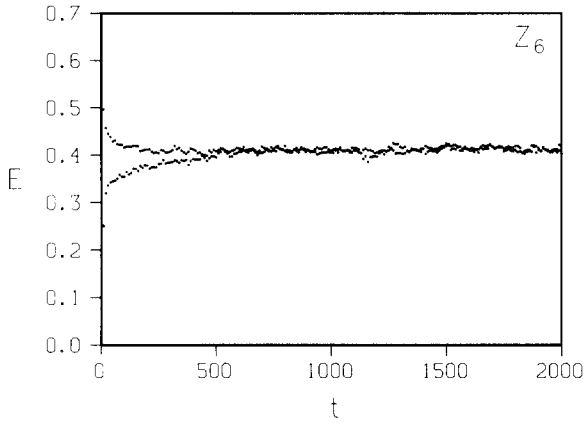

Fig. 2. The internal energy as a function of number of Monte Carlo iterations for the Z_6 system at $\beta = 1$, near the higher of its two critical temperatures. The upper and lower sets of points represent random and ordered configurations, respectively.

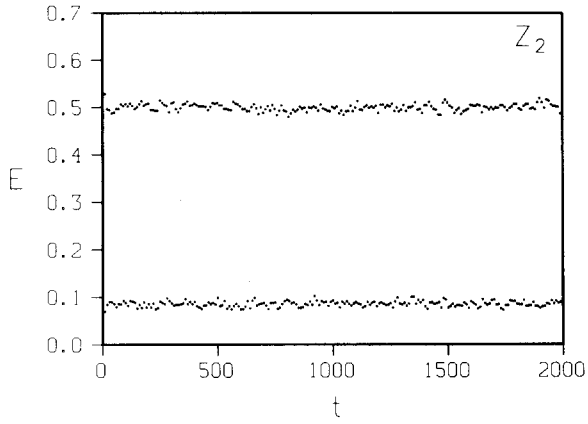

Fig. 3. The evolution of the internal energy from random and ordered configurations at the first-order transition of the Z_2 system.

[15]. The occurrence of two distinct, stable phases is what one indeed expects at $\beta = \beta_c$. The problem is that the computation produces similar results even if β is moved away from β_c by as much as ~5 to 10%, whereas only one of the phases should remain stable.

A useful procedure to overcome metastability effects consists in assuming an initial configuration which is half-ordered and half-disordered [15]. For example, we could take a random configuration and then set to the identity all links with time coordinate less than or equal to half the total time dimension in the periodic crystal. One speaks then of mixed-phase MC simulations. Fig. 4 illustrates the results of the procedure for the Z_2-model at several values of β in the neighborhood of β_c [15]. As soon as β is

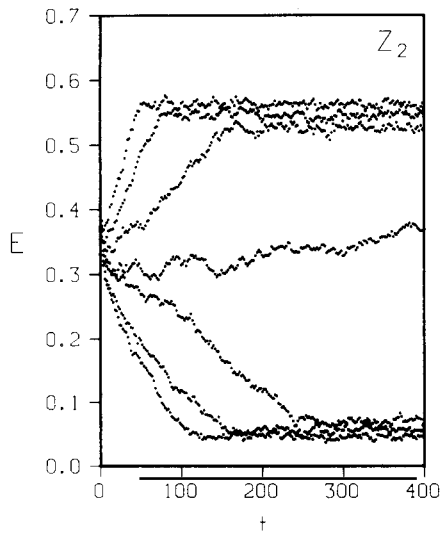

Fig. 4. The evolution of the Z_2 system from mixed phase initial conditions. From the top to the bottom sets of points, β runs from 0.41 to 0.47 in steps of 0.01.

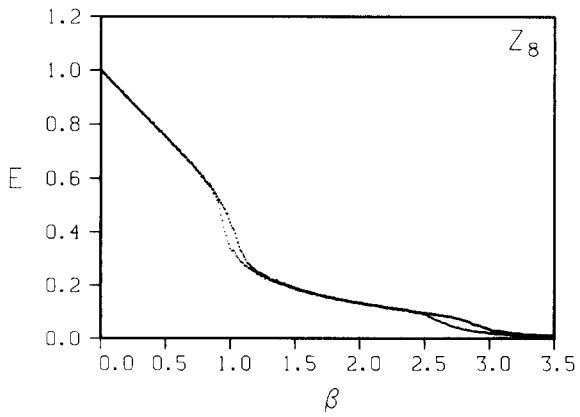

Fig. 5. A thermal cycle on the Z_8 system.

made different from β_c, the stable phase overtakes the metastable one. The almost linear drift of the internal energy to be final value, in the proximity of a first-order transition, is rather characteristic and can be related to the expansion of the boundary of the stable phase.

Finally, let us mention that it is often useful to perform simulations where the coupling parameter β is varied slightly after every iteration or every few iterations. One speaks then, especially if β is moved from some initial value β_0 to β_1 and then back to β_0, of a simulated thermal cycle. The gradual change of β induces a nearly adiabatic transformation on the system, which will never be strictly in statistical equilibrium, but in general will remain very close to it. In the vicinity of critical points, however, because of the increase in the relaxation time, the departure from equilibrium will become more marked and the simulation of the thermal cycle will exhibit characteristic hysteresis loops. Fig. 5 illustrates the results of such a simulation for the Z_8-model [15]. The two very marked hysteresis loops signal the occurrence of two phase transitions in the system.

3.3. Technical details

In this subsection we discuss a few points which may be of interest to the researcher planning to write an explicit MC program. Readers who are interested only in the general features of the method and in the results may want to skip this subsection.

The computation leading to the upgrade of one of the dynamical variables consists of three basic parts:

(i) A retrieval from memory of the required U_{ji} and its neighbors. The indices which specify the location in memory of these numbers must be determined taking into account the boundary conditions.

(ii) A computation, according to the algebra of the gauge group, of quantities which remain fixed during the upgrade. For instance, if the internal energy of a single plaquette is expressed as

$$-\mathrm{Tr}(U_{i_1 i_4} U_{i_4 i_3} U_{i_3 i_2} U_{i_2 i_1}) \tag{3.12}$$

and if $U_{i_2 i_1}$ is the variable to be upgraded, it will be convenient to evaluate the matrix product

$$V^{(i)} = U_{i_1 i_4} U_{i_4 i_3} U_{i_3 i_2} \tag{3.13}$$

first. If the total action is the sum of the individual plaquette energies multiplied by β, $U_{i_2 i_1}$ will intervene into six terms of the action. It will be useful to compute the products $V^{(i)}$, $i = 1, \ldots 6$, as in eq. (3.13), for these six plaquettes and add them up

$$V = \sum_{i=1}^{6} V^{(i)} . \tag{3.14}$$

The change in action induced when $U_{i_2 i_1}$ is varied will then be given by

$$\delta S = -\beta \, \mathrm{Tr}(V \, \delta U_{i_2 i_1}) \tag{3.15}$$

and only the relatively simple arithmetic operation of taking the trace will have to be repeated if $U_{i_2 i_1}$ is upgraded several times before proceeding to the next variable. This is particularly important for continuous gauge groups, in which case a major portion of the computer time is devoted to calculating V.

(iii) The decision, based on the extraction of a pseudorandom number, on whether to accept or reject the change.

A useful observation relative to point (i) is that periodic boundary conditions may be enforced in a very efficient way if the size of the lattice is a power of 2 and the compiler allows simple bit manipulations. One can take advantage of the binary structure of the representation of numbers inside the computer. For details see ref. [18]. Otherwise, it is covenient to impose periodicity by defining arrays of next and previous indices, following the obvious definitions (for periodicity modulo N)

$$\begin{aligned} &\text{next}\,(i) = i+1\,, \qquad i<N,\\ &\text{next}\,(N) = 1\,, \end{aligned} \tag{3.16}$$

$$\begin{aligned} &\text{previous}\,(i) = i-1\,, \qquad i>1\,,\\ &\text{previous}\,(1) = N. \end{aligned} \tag{3.17}$$

Use of modulus operations or conditional statements is more tedious.

About point (ii) – a general observation is that, if the gauge group is a finite group of reasonably low order, it is much more convenient to record the result of the group operation into a multiplication table, which will be stored in memory, and to combine U_{ji} variables according to this table, rather than performing the explicit matrix algebra. A general program for the simulation of a system with finite gauge groups is published in ref. [18]. Also, as long as the group elements may be labelled by an integer ranging over a limited set of values, it becomes possible to record several U_{ji} variables in the same memory word, allocating bits of different position to the different variables.

One can thus reduce the memory requirements and sometimes this procedure also allows a parallel processing of several U_{ji} by a single computer instruction. For details see [19]. This kind of parallel processing should not be confused with the capability of executing simultaneously several operations that some of the most modern and largest computers offer and which can be fruitfully applied to MC simulations, with no restriction on the group involved [20].

If the group is continuous, there is little that can be said of general nature, although variations in the way the program is written may imply substantial savings in computer time. For instance, with the algebra of the SU(3) group, it is more efficient to obtain the first two rows of the product of two matrices and determine the third one using orthogonality relations, than to proceed with the full matrix multiplication (a saving of about 10% in CP, central processor, time is achieved).

On the upgrading, a useful consideration is that if the gauge group is finite it is more efficient to store the possible values of $\exp\{-\Delta S\}$ in a memory array and retrieve them at the moment they are required, than calling the rather time consuming exponential function. If the group is continuous, again, not much of general nature can be said. The gauge groups U(1) and SU(2), however, are simple enough to allow efficient and elegant implementation of the heat bath algorithm, which we now briefly describe.

We first discuss the case of SU(2) [21]. When working on a particular link, we need to consider only the contribution to the action coming from the six plaquettes containing that link. Consider the matrix V from eq. (3.14), the sum of the six products of neighboring link variables that interact with the link in question. The heat bath method requires that we replace U_{ji} with a new group element selected randomly from SU(2) with probability distribution

$$\mathrm{d}P(U) \propto \mathrm{d}U \exp\{\tfrac{1}{2}\beta\,\mathrm{Tr}(UV)\}\,. \tag{3.18}$$

The manifold of the group SU(2) is the surface of a four-dimensional sphere. This follows from the parametrization

$$U = a_0 + \mathrm{i}\boldsymbol{a}\cdot\boldsymbol{\sigma}, \qquad a_0^2 + \boldsymbol{a}^2 = 1, \tag{3.19}$$

where $\boldsymbol{\sigma}$ represents the Pauli matrices. In terms of this parametrization, the invariant group measure takes the simple form

$$\mathrm{d}U = \frac{1}{2\pi^2}\,\delta(a^2 - 1)\,\mathrm{d}^4 a\,. \tag{3.20}$$

A useful property of SU(2) elements is that any sum of them is proportional to another SU(2) element. In particular, it follows from the representation in eq. (3.19) that

$$V = k\bar{U}, \tag{3.21}$$

where $\bar{U}$ is an SU(2) element and k is given by the determinant

$$k = |V|^{1/2}\,. \tag{3.22}$$

The utility of this observation appears when we use the invariance of the group measure to absorb $\bar{U}$,

$$\mathrm{d}P(U\bar{U}^{-1}) \propto \mathrm{d}U \exp\{\tfrac{1}{2}\beta k \operatorname{Tr} U\}\,. \tag{3.23}$$

Using eq. (3.20) gives

$$\mathrm{d}P(U\bar{U}^{-1}) \propto \mathrm{d}^4 a\,\delta(a^2 - 1)\exp(\beta k a_0)\,. \tag{3.24}$$

Thus the problem reduces to generating points on the surface of a four-dimensional hypersphere with exponential weighting along the a_0 direction. Generating an element U in this manner, the link in question is replaced with the product

$$U_{ji}' = U\bar{U}^{-1}\,. \tag{3.25}$$

To generate the appropriate weighting on the hypersphere, first do the $|\boldsymbol{a}|$ integral with the delta function to obtain

$$\delta(a^2 - 1)\,\mathrm{d}^4 a \exp(\beta k a_0) \to \tfrac{1}{2}\mathrm{d}a_0\,\mathrm{d}\Omega\,(1 - a_0^2)^{1/2}\exp(\beta k a_0)\,, \tag{3.26}$$

where $\mathrm{d}\Omega$ is the differential solid angle of $\boldsymbol{a}$. Thus we must generate a_0 in the inteval $[-1, +1]$ with weighting

$$\mathrm{d}P(a_0) \propto (1 - a_0^2)^{1/2}\exp(\beta k a_0)\,\mathrm{d}a_0\,. \tag{3.27}$$

Changing variables to $z = \mathrm{e}^{\beta k a_0}$ gives

$$dP(z) \propto dz\,(1-\beta^{-2}k^{-2}\log^2 z)^{1/2}, \qquad e^{-2\beta k} \le z \le e^{+2\beta k}. \tag{3.28}$$

This change removes the strong peaking for low temperatures from eq. (3.27). Now z can be generated by selecting a random number uniformly in the allowed interval and rejecting it with probability

$$(1-k^{-2}\beta^{-2}\log^2 z)^{1/2}. \tag{3.29}$$

This is repeated until a z is accepted. Then the direction for $\boldsymbol{a}$ is selected randomly and the group element can be reconstructed.

The group U(1) is isomorphic to SO(2), which in turn is just the set of SU(2) matrices which are real. Thus the above discussion through eq. (3.25) repeats itself except for eq. (3.24) which becomes

$$dP(U\bar{U}^{-1}) \propto d^2a\,\delta(a^2-1)\exp(\beta k a_0), \tag{3.30}$$

where the SO(2) elements are parametrized as

$$U = \begin{pmatrix} a_0 & a_1 \\ -a_1 & a_0 \end{pmatrix} = a_0 + i a_1 \sigma_2 . \tag{3.31}$$

The hypersphere is replaced now by the unit circle and we need to generate

$$\begin{aligned} &dP(a_0) \propto (1-a_0^2)^{-1/2}\exp(\beta k a_0)\,da_0, \\ &a_1 = \pm(1-a_0^2)^{1/2}. \end{aligned} \tag{3.32}$$

Here the sign of a_1 is chosen randomly.

The generation of a_0 is somewhat more complicated than for SU(2) because the weighting in eq. (3.32) is an unbounded (but integrable) function. The scheme we use is to change variables to

$$z = \exp\left\{-\frac{2\beta k}{\pi}\arccos a_0\right\}, \tag{3.33}$$

$$e^{-2\beta k} < z < 1, \tag{3.34}$$

$$dP(z) \propto \exp\left(\beta k \cos\left(\frac{\pi}{2\beta k}\log z\right) - \log z\right) dz. \tag{3.35}$$

This weighting is bounded and is reasonably smooth for moderate β. We select z uniformly in the range (3.34) and then reject it with probability proportional to the weighting in (3.35). As in the SU(2) case, this is repeated until a z is accepted, and the group element is reconstructed.

4. Phase structure of pure gauge systems

As we have discussed in section 2.3, the existence and nature of the critical points of a particular lattice model are issues of prime importance to the model's possible relevance to physics in the

continuum limit. Thus, one of the first things one would like to learn about a lattice gauge theory is its phase structure. The Monte Carlo methods described in section 3 are particularly well suited for the study of the non-perturbative effects responsible for the critical behavior of a statistical system.

4.1. Abelian models

The simplest lattice gauge theories are those in which the spin variables take on a finite set of N values uniformly distributed on the unit circle. They span the discrete Abelian group $Z(N)$ of planar rotations by integer multiples of $2\pi/N$. For $N=2$ the model corresponds to a gauge-invariant generalization of the Ising model, and as N approaches infinity, the $Z(N)$ models approach the U(1) theory. Therefore, although these theories do not necessarily lead to sensible gauge field theories in the continuum limit, they provide a tool for studying the U(1) theory indirectly. Furthermore, as we shall argue below, most of the relevant properties of the U(1) gauge theory can be analyzed using the discrete models, which, being amenable to treatment using the parallel processing techniques mentioned in section 3.3, allow a much more precise determination of these properties than is possible using the continuous group directly.

Since the work of Kramers and Wannier [22] on the two-dimensional Ising model, the concept of duality has played a crucial role in the study of spin systems. Generalization of the duality transformation to more complicated systems has been achieved and excellent reviews exist in the literature [23]. In broad terms, this transformation can be understood as a geometric map of a given model into another defined in the same number of dimensions, but with a (generally) different action, in such a way that the couplings of the transformed theory become monotonically decreasing functions of the original couplings. The dual theory is one in which the original "order" variables have been replaced by a new set of "disorder" variables, whose fluctuations are small at strong coupling, where the fluctuations in the original variables were large. In this way, the strong-coupling regime of the original theory is mapped into the weak coupling regime of the dual theory, and vice versa. Of particular interest is the situation where the action of the dual system coincides with that of the original system. When a model has this property it is said to be self-dual. In this case, a number of very important results follow. In particular, if a self-dual system undergoes a single phase transition, the critical coupling must be the point at which the original and dual couplings coincide. When more than one transition occurs, the critical points on one side of the self-dual point are related to those on the other. Furthermore, when a system is self-dual, expectation values of order and disorder operators are also related by duality. In many cases of interest, this fact leads to important conclusions concerning the nature of a given phase of the model.

With the Wilson form of the action, the $Z(N)$ models are self-dual for $N=2$, 3 and 4; the self-dual points being given by [10, 24]

$$\beta_2^{SD} = \tfrac{1}{2}\ln(1+\sqrt{2}) = 0.44\ldots \tag{4.1}$$

$$\beta_3^{SD} = \tfrac{2}{3}\ln(1+\sqrt{3}) = 0.67\ldots \tag{4.2}$$

$$\beta_4^{SD} = \ln(1+\sqrt{2}) = 0.88\ldots. \tag{4.3}$$

For $N>4$ these models are approximately self-dual in that the dual theory is again a four-dimensional $Z(N)$ gauge theory but with a somewhat different action.

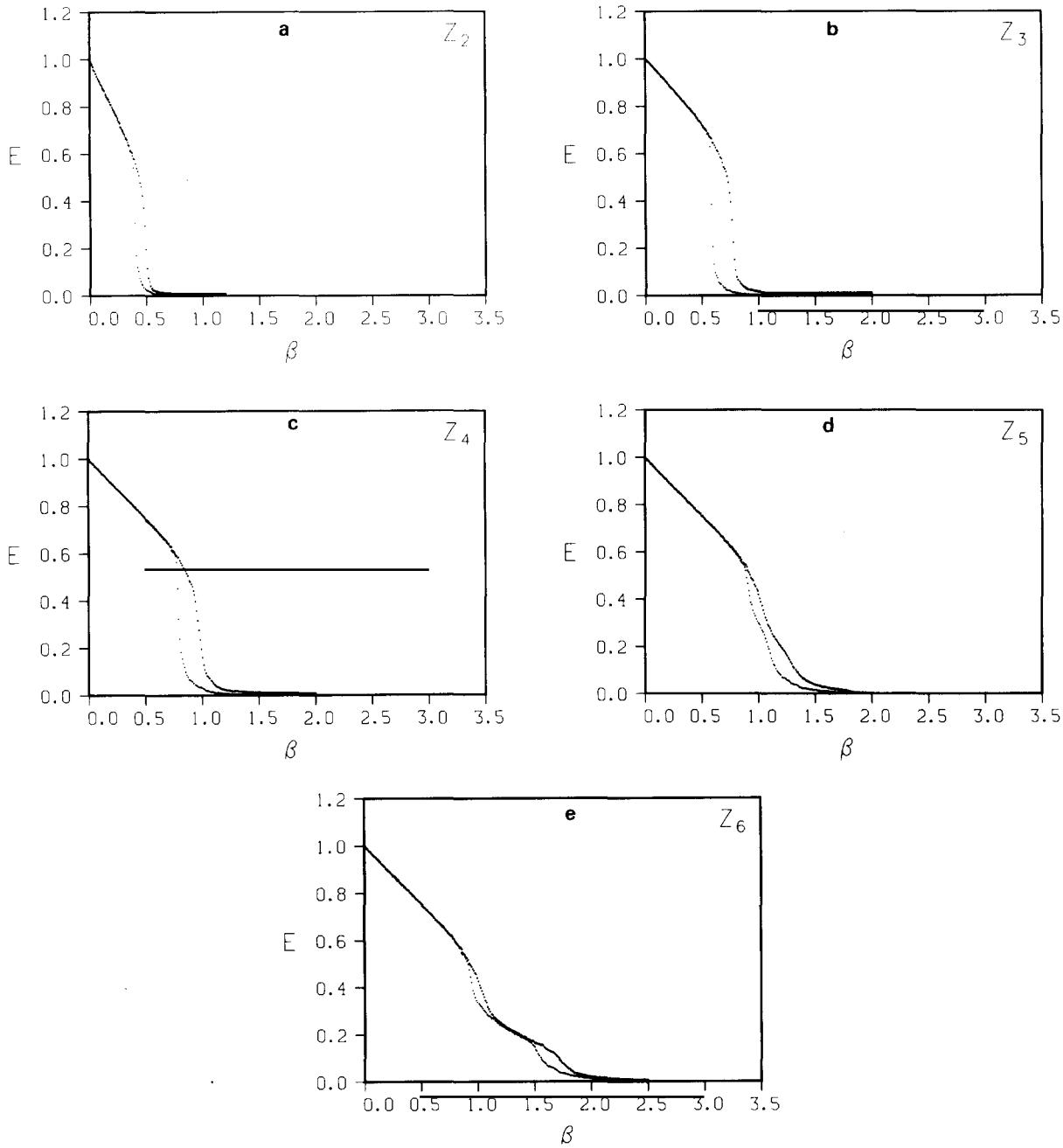

Fig. 6. Thermal cycles on the (a) Z_2, (b) Z_3, (c) Z_4, (d) Z_5 and (e) Z_6 models.

A rough overview of the phase structure of the Z(N) models can be obtained from the simulation of thermal cycles as discussed in section 3.2. One example of such a simulation was shown in fig. 5 and more are shown in fig. 6. In figs. 6a–c pronounced hysteresis-like loops are present in the region of the self-dual points for the Z(2), Z(3) and Z(4) models. Accordingly, we expect the existence of a single phase transition in those theories. Figures 6d–e are noticeably different. A hint of further

structure is apparent in the Z(5) model, and the probable existence of two separate transitions becomes more evident for the larger groups. That the $N > 4$ models undergo two transitions is confirmed through further analysis. Since these models are close to being self-dual, the two critical points are approximately related by duality. As discussed in section 3.2, the nature of the phase transitions can be elucidated by studying the evolution of special initial configurations in the vicinity of the critical points. Recall that systems undergoing first-order transitions possess two different stable states at the critical point which become metastable as the coupling is varied slightly away from this value. Higher-order transitions, on the other hand, do not have this property. In fig. 2 we plotted the evolution of the average plaquette in the Z(6) model at the strong-coupling critical point as function of the number of iterations. The two sets of points, corresponding to a hot start (upper set) and a cold start (lower set) are seen to converge to a common value after a relatively short time of about 700 iterations, indicating the existence of a single stable state at this value of the coupling and, hence, a continuous transition. Based on further analysis described later in this section, it has been found that this transition is indeed a second-order one. Because of duality, this implies that the weak-coupling transition is second-order as well. The same type of simulation, when carried out with the $N < 5$ models produces very different results as shown in figs. 3 and 7. In this case, the Z(4) model appears to have two stable states when simulated at its self-dual point and thus seems to undergo a first-order transition. However, because of the existence of metastable states, these simulations do not determine the value of the transition point with any precision. This difficulty is easily overcome with the use of mixed-phase configurations of the type discussed in section 3.2. The results of applying this technique in the case of the Z(2), Z(3) and Z(4) models are displayed in figs. 4 and 8. To within an accuracy of ± 0.005 in β, these simulations lend strong evidence supporting the existence of first-order phase transitions for the $N < 5$ models at their self-dual points. Several techniques exist for determining the critical coupling of continuous transitions. A simple but crude technique consists in simulating a configuration and repeatedly adjusting the inverse coupling after several iterations in such a way that the value of the average plaquette remains in the middle of the hysteresis cycle. Other methods, which are more accurate but require a considerably larger amount of computer time, rely on the measurement of average fluctuations as a means of finding the maximum value of the derivatives of the free energy with respect to the inverse coupling. The pattern which emerges from this analysis is shown in fig. 9. The Z(2), Z(3) and Z(4) models possess two phases separated by a first-order transition; the models for $N > 4$ have three phases which are separated by continuous, second-order transitions. General arguments [25] which identify the physical mechanism

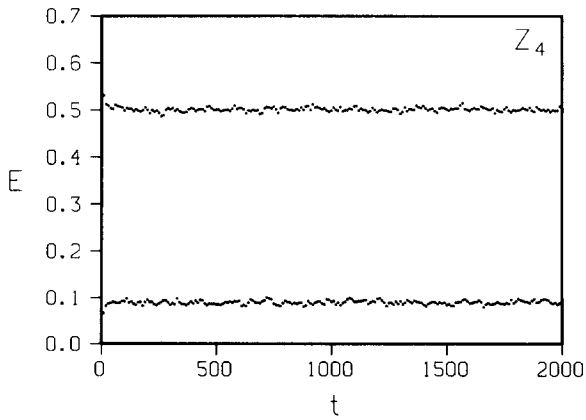

Fig. 7. Evolution of the Z_4 system from random and ordered configurations at the transition temperature.

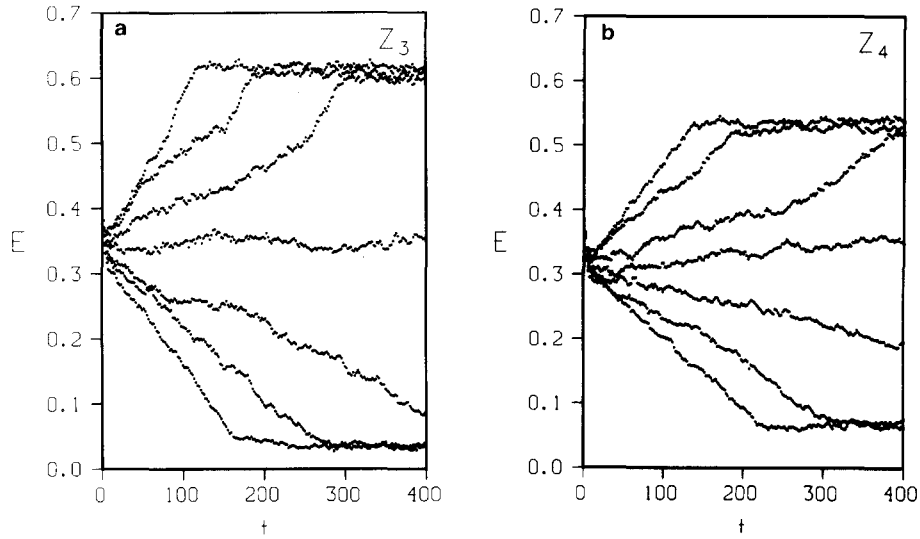

Fig. 8. Mixed phase runs for (a) Z_3 and (b) Z_4 systems. The values of β run from 0.64 to 0.70 in (a) and from 0.85 to 0.91 in (b), both in steps of 0.01.

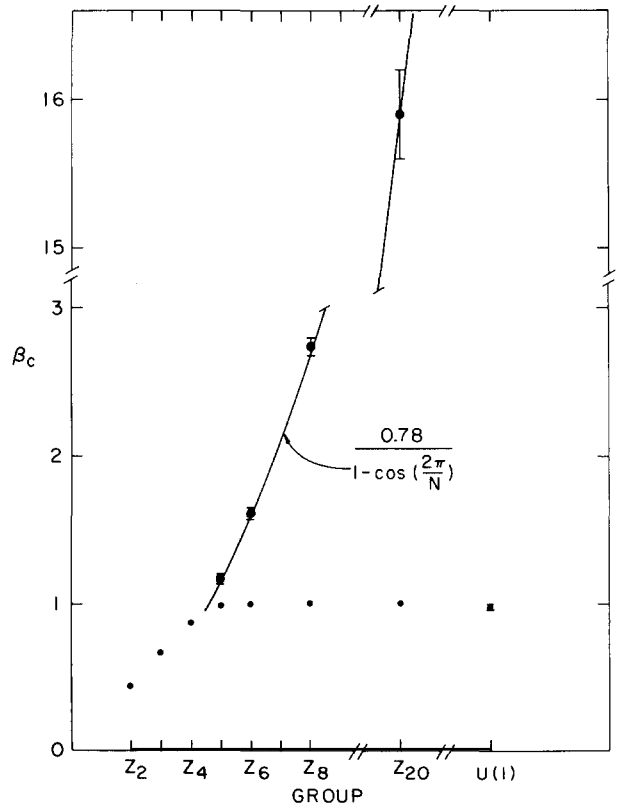

Fig. 9. The inverse transition temperatures for Z_N lattice gauge theory as a function of N.

responsible for these continuous transitions, based on an analysis of topological excitations present in the middle phase, imply that, for large enough N, the strong-coupling critical point in these models should converge to a value which is essentially independent of N. This is consistent with the MC analysis presented above. Since the point of approximate self-duality of these models occurs at an inverse coupling which grows linearly with N, the fact that one transition is essentially fixed at $\beta \approx 1$ leads one to expect that the second critical point should occur at a coupling g^2 which vanishes like $1/N^2$ as N goes to infinity. Indeed, since the energy difference (per plaquette) between the ground state and the first excited state vanishes with N as $1-\cos(2\pi/N) \approx O(N^{-2})$, it is natural to expect the second critical point to scale similarly. Agreement between the numerical results and the above theoretical expectations is clearly seen in fig. 9. Determination of the scaling coefficient $\alpha \approx 0.78$ from theoretical considerations remains a very difficult task.

Using a periodic Gaussian approximation to the Wilson action for the $Z(N)$ models, the phase structure described above was being conjectured by several groups [25] at the time this numerical analysis was being carried out. Success for theoretical analysis and the numerical simulation is clear from the welcome agreement between these two approaches.

The nature of the three phases in the $Z(N)$ models is well understood. The strong coupling phase is characterized by an area-law decay for the Wilson loops and leads to the confinement of elementary excitations. In both the intermediate as well as the weak coupling phases, correlations have a slower fall-off. However, unlike the weak coupling phase, the intermediate phase is dominated by massless, spin-wave excitations which correspond to the physical photon field in the continuum limit of the $N \to \infty$ model. In fig. 10 the average plaquette for the Z(20) model is compared with the spin-wave approximation value of $1/(4\beta)$. The rather good agreement between the numerical results and the spin-wave prediction in the intermediate phase is apparent.

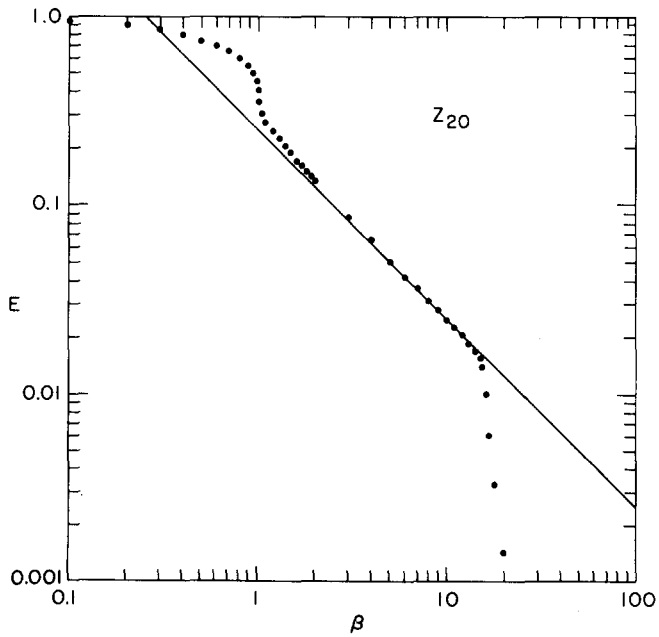

Fig. 10. The internal energy of the Z_{20} model as a function of inverse temperature. The solid line is the lowest order spin wave prediction for the U(1) model.

The phase structure of the U(1) model, as obtained from a direct simulation of the continuous group, is shown in fig. 11. The single transition point seen at $\beta \approx 1$ separates the confining phase from a QED-like phase containing the quantized photon field in the continuum limit. The existence of a continuous phase transition in the lattice formulation of the U(1) theory, as indicated by the above results as well as by the subsequent rigorous work of Guth [26], gives very strong support to the belief that the Wilson–Polyakov lattice formulation of gauge theory provides a correct regularization technique for defining a quantum field theory. Indeed, had this formulation led to unphysical results for this prototype gauge theory, its use in the analysis of the less well understood non-Abelian models would clearly be suspect.

Using finite-size scaling techniques, a detailed analysis of the U(1) transition has been carried out by Lautrup and Nauenberg [27]. Later, various renormalization group techniques were applied to this model by Bhanot [28] and by Hamber [29]. The results of these analyses provide strong evidence for a second-order critical point. In this connection, it is worth mentioning that the possible existence of an essential singularity in the correlation length was part of the current lore when this transition was discovered. The main reason for this belief was that the U(1) theory, being intimately related to the planar $(X-Y)$ spin model in two dimensions through the Migdal–Kadanoff recursion relations, might share this property with the spin system [30]. Although we now have good evidence that the transition is not of infinite order, the work of Bhanot indicates that the weak-coupling phase of the O(2) model does share with the spin system the property of being a line of renormalization-group fixed points.

Before passing on to discuss the non-Abelian groups, we will anticipate the analysis described in greater detail in section 5 concerning topological excitations in these theories. As is the case with the planar model and other spin systems, a possible description of the Abelian gauge models is in terms of variables which represent their topological excitations. In an interesting analysis, DeGrand and Toussaint [17, 31] identified a physical mechanism responsible for the U(1) transition as being the condensation of such topological excitations (monopoles in this case) at the critical point, in a manner analogous to the way in which the condensation of vortices is responsible for the phase transition in the planar model.

A consequence of the study of these theories in terms of such topological variables (which correspond to the elementary variables in the dual theory) is that, away from the freezing transition observed for finite N, the $Z(N)$ models in the intermediate phase are essentially indistinguishable from the U(1) model. The computational advantages of this fact are obvious. Although the arguments leading to the above assertions cannot be simply applied to the non-Abelian models, it is believed that, at least with the Wilson action, models corresponding to discrete subgroups of a non-Abelian group can also

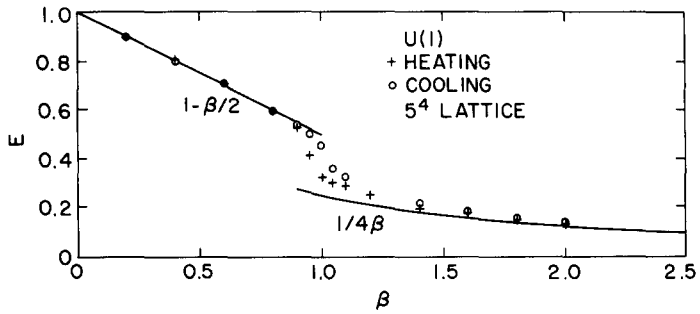

Fig. 11. A thermal cycle on the U(1) model.

mimic the continuous group for some range of values of the coupling. As we discuss in the following subsection, for the extensively studied case of SU(2) and its discrete subgroups, the evidence in favor of this belief is rather good.

The critical properties of spin systems depend crucially upon the dimensionality of the lattice where the model is defined. In view of the deep statistical analogies which exist between gauge models and spin systems, one expects the existence of critical dimensions for gauge theories. In particular, we have presented evidence that the U(1) model in four dimensions has a continuum limit describing free massless photons, in accordance with physical expectations. The question is whether $d = 4$ is the critical dimension for gauge theories in the same way that $d = 2$ is for spin systems. This has been investigated for both the Abelian as well as the non-Abelian cases. The expectation is that the $d = 3$ U(1) model cannot avoid the confinement of photons, whereas the expected confining property of non-Abelian models should be lost when $d > 4$. This picture is now known to be rigorously true in the Abelian case, as we briefly discuss here. The situation with the non-Abelian models will be analyzed in the next subsection.

An analysis of the $d = 3$ $Z(N)$ models, entirely analogous to the one presented above for $d = 4$, has been carried out [32]. The main finding is that these models undergo a single continuous transition for all N, with a critical coupling which scales with the action gap and therefore vanishes like N^2 in the U(1) limit. In accordance with these results, renormalization-group analyses [29, 33] indicate that the $d = 3$ U(1) model is disordered for all finite couplings. A direct simulation of the U(1) model in $d = 3$ and $d = 5$ gives further evidence of the critical nature of $d = 4$. It is observed that, while the three-dimensional model does not seem to undergo any transitions, the second-order critical point of the four-dimensional model hardens into a clear first-order transition [32] when $d = 5$. Finally, in a very recent investigation, a rigorous proof confirming these numerical findings has been achieved by Gopfert and Mack [34].

4.2. Non-Abelian models

In this subsection we will describe the phase structure of the physically relevant non-Abelian systems corresponding to the SU(2) and SU(3) gauge groups. The methods used in this analysis are entirely analogous to those used in the study of the Abelian groups, so the discussion will be brief.

Most of the advantages and limitations encountered in the Monte Carlo analysis of the U(1) model using its discrete $Z(N)$ subgroups apply in this case as well [35, 36]. In particular, from a computational point of view, the ability to store several spin variables in a single computer word allows for the simulation of larger lattices [37]. Although this is not a major advantage in the study of the phase structure of the models, it will be crucial in the analysis of nonlocal observables, as will be discussed in section 5. As we have discussed in section 3, the fact that the group operation is more complicated here than in the Abelian case makes the parallel processing of several spins through a logical implementation of the group algebra generally impractical. However, as long as the group is not too large, the product of two group elements can be performed by retrieving the result from a multiplication table stored in memory, a procedure which takes much less time than carrying out the matrix multiplications explicitly. If the order of the group is very large, the group operation can be reproduced by first factoring the group elements into products of the elements of a subgroup H times a representative of the cosets of H. A few tables which specify how these elements are commuted and multiplied can then be stored in memory.

An obvious difficulty with non-Abelian groups, which is absent in the U(1) case, stems from the fact that, whereas the sequence of $Z(N)$ subgroups of U(1) is infinite and its limit is dense in U(1), non-Abelian groups have only a finite number of truly non-Abelian discrete subgroups, if we exclude trivial generalizations of their Abelian subgroups. Thus, for example, the dihedral groups $D(N)$, obtained by combining rotations of $2\pi/N$ around a fixed axis with rotations of π around axes orthogonal to it, reveal little of the non-Abelian nature of the three-dimensional rotation group. As was the case with the $Z(N)$ groups, it is clear that at sufficiently weak couplings the physics of the discrete non-Abelian subgroups will differ from that of the Lie group under study. Therefore, in order to profit from the use of discrete subgroups, it is crucial that the Lie group in question should have a sufficiently dense subgroup so that the interesting physical region one wishes to probe occurs at couplings where the continuous group is still well approximated by the discrete group. Indeed, whereas the approximation to the SU(2) model by discrete subgroups is excellent, the interesting physical region where the crossover between strong and weak coupling takes place for the SU(3) theory is outside the range of couplings for which the approximation obtained from the largest discrete subgroup is still good (at least with the Wilson form of the action) [38]. Recent work [39] has shown that it may be possible to overcome this limitation by considering sets of group elements which do not themselves form a subgroup. Using the exact action, derived from tables as noted above, for the product of elements around the plaquettes, one obtains a useful scheme for rapid computation with such an approximation to SU(3).

The relevant subgroups $\bar{G}$ of SU(2) can be reduced to subgroups G of O(3) by factoring out the center Z(2). The subgroups of O(3) are the symmetry groups of the polyhedra. Excluding Abelian and dihedral cases, the finite subgroups of O(3) are:

(i) the 12 element symmetry group of the tetrahedron, denoted by T;

(ii) the 24 element symmetry group of the cube and the octahedron, denoted by O;

(iii) the 60 element symmetry group of the icosahedron and the dodecahedron, denoted by Y;

together with their subgroups. Corresponding to these, SU(2) has the following subgroups:

(i) $\bar{T}$ (24 elements),

(ii) $\bar{O}$ (48 elements),

(iii) $\bar{Y}$ (120 elements),

where $\bar{G}/Z(2) = G$.

For the above subgroups, any two different neighbors of the identity, that is, any two elements of the form $g = \cos\theta + i \sin\theta\, \boldsymbol{\sigma} \cdot \boldsymbol{n}$ corresponding to the smallest non-vanishing value of θ, call it θ_m, and such that they are not mutual inverses, generate the whole group. Moreover, any such g generates a maximal cyclic group. If this group is $Z(N)$, then $\theta_m = 2\pi/N$ and the action gap of the model is the same as in the Abelian system with gauge group $Z(N)$. Thus, $\bar{T}$ has 8 neighbors of the identity and its maximal Abelian subgroup is Z(6), $\bar{O}$ has 6 neighbors of the identity with maximal Abelian subgroup Z(8) and $\bar{Y}$ has 12 neighbors of the identity with maximal Abelian subgroup Z(10).

In figs. 12–14 we display [35] the results of thermal cycles for the models with gauge groups Q (the eight element quaternion subgroup of O with maximal Abelian subgroup Z(4)), $\bar{T}$ and $\bar{O}$. A clean hysteresis loop, indicating the existence of a single order–disorder transition, is clear in all cases. The critical coupling is seen to move toward $g = 0$ as the order of the group increases with no sign of other critical points. This situation, pointedly different from the observed behavior of the $Z(N)$ systems, supports the notion that the SU(2) model should have no transitions for finite coupling. A particularly striking difference between Abelian and non-Abelian cases can be seen between the thermal cycle of the $\bar{O}$ model in fig. 14 and that of the Z(8) model in fig. 5. The action gap of these models is the same, but, whereas the Z(8) model shows the appearance of a spin-wave phase behind the transition which

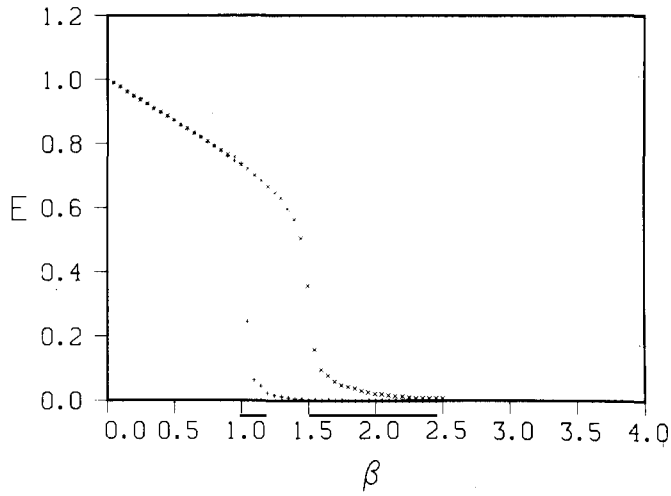

Fig. 12. A thermal cycle with the quaternian group $Q = \{\pm 1, \pm i\sigma\}$.

scales with the gap, no such phase is seen in the $\bar{O}$ system. A comparison of the average plaquette in the $\bar{O}$ model with the corresponding quantity obtained from a direct simulation of the SU(2) system is also shown in fig. 14. An excellent agreement is seen almost up to the phase transition.

Using mixed-phase simulations, the transitions in these three models have been determined to be first-order and the critical points are estimated to be

$$\beta_c = 1.23 \pm 0.02, \qquad G = Q \tag{4.4}$$

$$\beta_c = 2.175 \pm 0.025, \qquad G = \bar{T} \tag{4.5}$$

$$\beta_c = 3.21 \pm 0.01, \qquad G = \bar{O}. \tag{4.6}$$

The results of these simulations are shown in fig. 15.

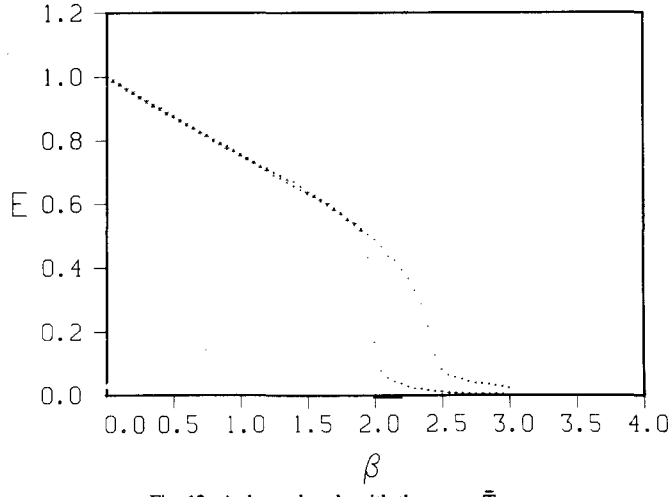

Fig. 13. A thermal cycle with the group $\bar{T}$.

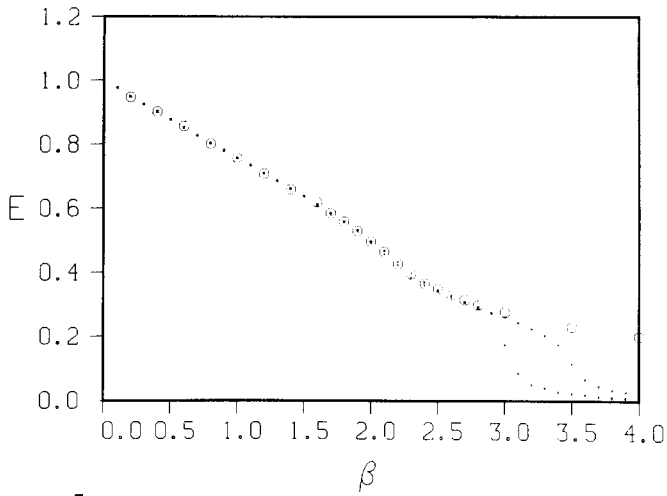

Fig. 14. A thermal cycle with the group $\bar{O}$. The crosses represent cooling, plusses, heating and the circles are the internal energy for the SU(2) model.

The largest subgroup, $\bar{Y}$, shows [36,37] a single, first-order phase transition at $\beta_c \approx 5.9$. The simulation of this model was done on a very large lattice of 16 sites in each direction [37]. As noted before, the advantages of being able to simulate systems on larger lattices becomes apparent when the measurement of extended, non-local operators is needed. In the next section, where we discuss the observables, the high statistics results for SU(2) were obtained on this system. A more subtle advantage of using this large lattice, also discussed in further detail in the next section, comes from the fact that the high (physical) temperature deconfining transition observed in the SU(2) model occurs at a value of β which increases with the size of the lattice according to the relation $a(\beta_c) = (1/T_c)d$, where a is the lattice spacing, T_c is the physical deconfining temperature and d is the lattice size.

A precise determination of the average plaquette for the group $\bar{Y}$ is shown in fig. 16 as a function of the inverse coupling. The statistical errors are smaller than the size of the points in the graph. The solid lines shown correspond to various Padé approximants to a strong-coupling series, evaluated to order J^{20} by Wilson [40], where J is given by

$$J(\beta) = \frac{\mathrm{d}}{\mathrm{d}\beta} \log\left(\int \mathrm{d}U \, \mathrm{e}^{\beta \, \mathrm{Tr} \, U/2} \right). \tag{4.7}$$

A very good agreement between data and series results is seen to occur up to $\beta \approx 2$, after which the series results depart sharply from the MC data.

Direct simulation of the SU(2) model shows no signs of a phase transition at finite coupling. For further support of confinement at all couplings, in the next section we will show that the behavior of observables is consistent with renormalization-group predictions assuming a vanishing critical bare coupling. Here we shall end our discussion of the numerical analysis of the phase structure of the SU(2) model by mentioning that, because of the same motivation which led us to study the U(1) model in three and five dimensions, a study of the SU(2) model in five dimensions has been carried out [41]. In striking contrast with the four-dimensional system, the results of this analysis reveal the existence of a first-order phase transition at an inverse coupling $\beta_c = 1.642 \pm 0.015$, thus giving further evidence to the critical nature of four dimensions for gauge theories.

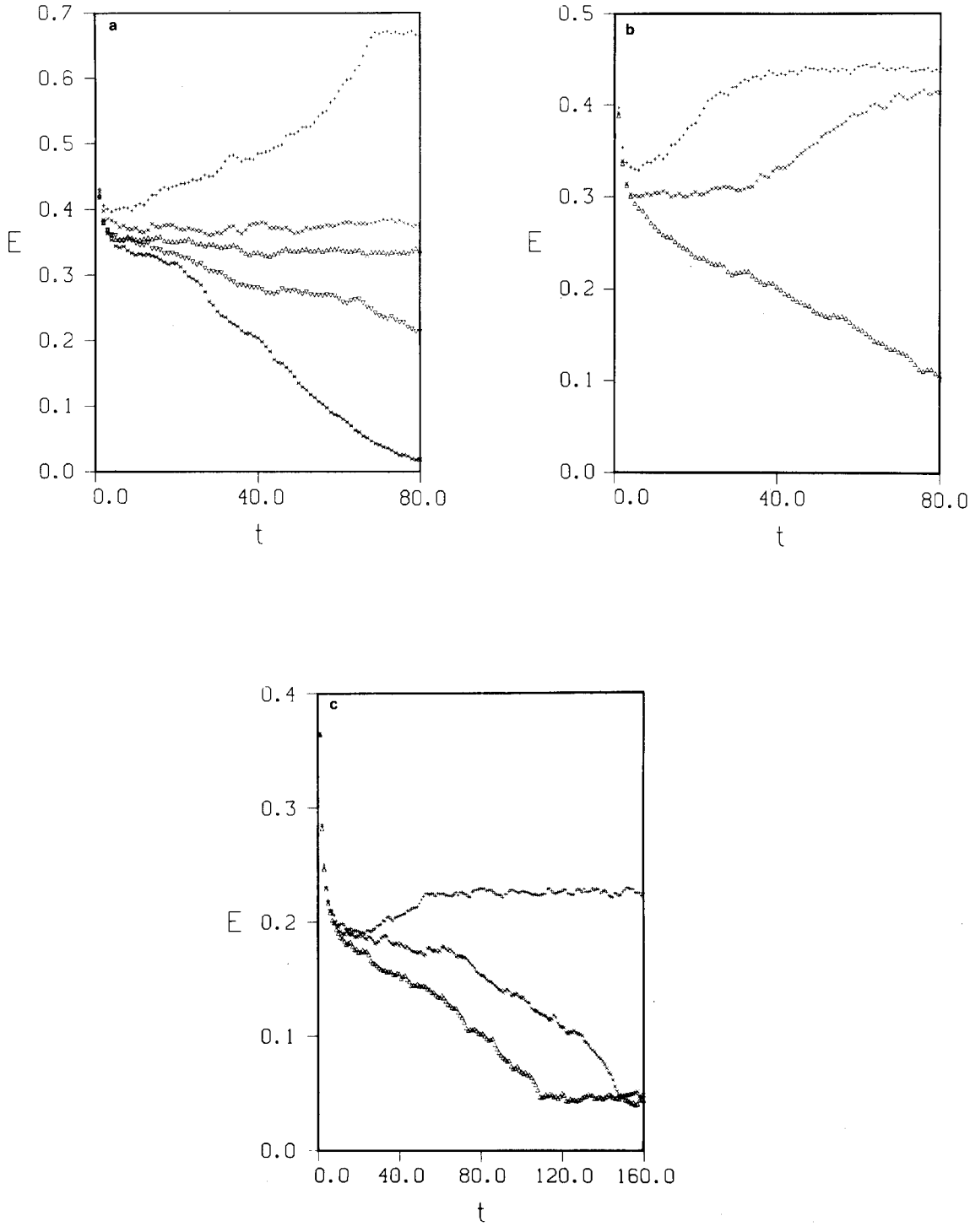

Fig. 15. Mixed phase runs with (a) Q at $\beta = 1.2$, 1.23, 1.25, 1.27 and 1.3 (from the top down), (b) $\bar{T}$ with $\beta = 2.1$, 2.15 and 2.2, (c) $\bar{O}$ with $\beta = 3.2$, 3.22 and 3.24.

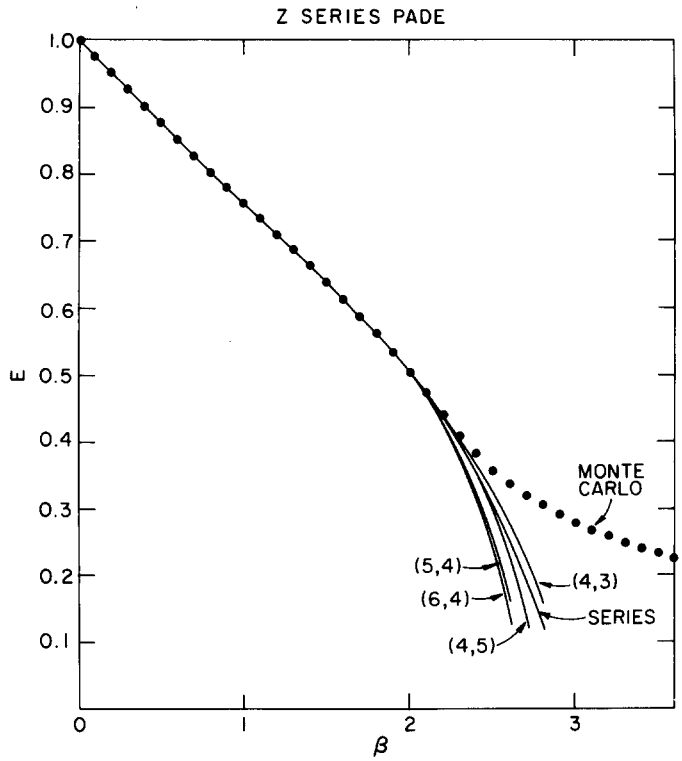

Fig. 16. The average plaquette for the group $\bar{Y}$ as a function of inverse coupling. The solid lines correspond to various Padé approximants to the strong coupling series.

We close this subsection with a discussion of the phase structure of the SU(3) model, the relevant gauge group for the strong interactions. There is little reason to suspect that SU(3) would have a deconfining transition if such effect is absent in the SU(2) model, and indeed, a direct simulation of this system [42] shows no sign of a phase transition in the explored range of couplings.

A simulation of the SU(3) system through a study of its discrete subgroups would be extremely useful given the complexity of the group operations involved in a simulation of the continuous group. Unfortunately, the interesting physical region for this model occurs at an inverse coupling $\beta \approx 6$, as will be discussed in section 5, whereas the largest discrete subgroup of SU(3) has [38] a (first-order) transition at $\beta_c = 3.6$. Therefore, the continuum limit of the SU(3) theory cannot be usefully approximated with any of its discrete subgroups, at least with the Wilson form for the action. We briefly present the results of the analysis of these models not only for completeness, but also because it is known that the region of couplings for which the strong coupling region turns into the asymptotic freedom region, the so-called crossover point, depends strongly on the specific form of the action employed. Therefore, it is possible that an action other than the Wilson form may still permit the use of discrete subgroups in this case as well.

Apart from its dihedral subgroups, SU(3) with the center Z(3) factored out has crystal-like subgroups which can be thought of as the generalizations of the polyhedral subgroups of O(3) to the eight-dimensional sphere [43]. We describe here an analysis of the groups containing 108, 216, 648 and 1080 elements, which we shall denote by S(N), N being the number of elements. In fig. 17 we show the results of a thermal cycle for the S(1080) model together with a strong-coupling series up through order β^5.

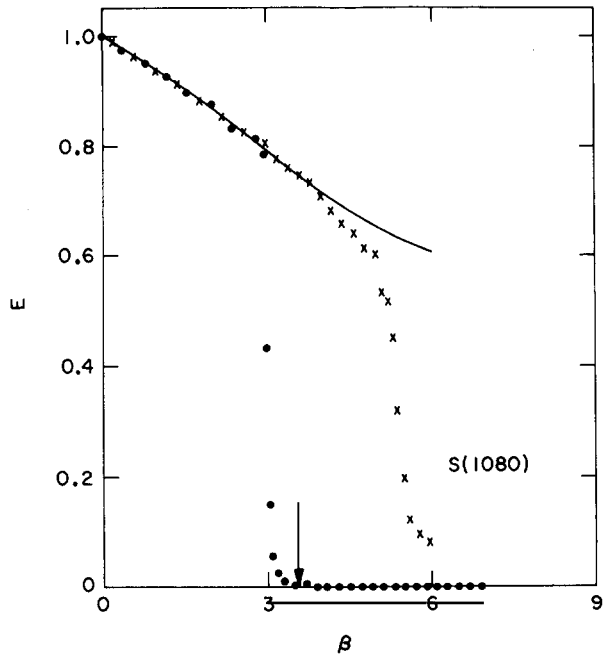

Fig. 17. A thermal cycle with the S(1080) subgroup of SU(3) as the gauge group.

Mixed-phase simulations for this model indicate a first-order transition at $\beta_c = 3.58 \pm 0.02$. Both kinds of simulations have been performed with the other models as well, with the results that a first-order transition is present at $\beta_c(108) = 2.5 \pm 0.2$, $\beta_c(216) = 3.2 \pm 0.1$ and $\beta_c(648) = 3.43 \pm 0.02$. The reason β_c remains relatively small despite the large number of elements is that the action gap, which sets the scale for the critical coupling, is never small and the increase in entropy which would tend to increase β_c is never sufficient to offset this effect.

We close this subsection by mentioning that great progress has been made through very recent work of Tomboulis [44] in the attempt at finding an analytic proof of the absence of a deconfining transition in these models. Hopefully, this proof can be completed in all rigor in the near future.

4.3. Phase structure of models with generalized actions

The imposition of a cut-off on a field theory is a highly non-unique procedure. Even in the framework of a lattice theory, variations are interesting to study with Monte Carlo simulation. Such analyses provide important consistency tests on the extraction of continuum numbers and indeed bear directly on the question of uniqueness of the continuum limit.

A simple alternative to the Wilson model is to place a vector field A_μ on the lattice sites and define an action by replacing derivatives in the continuum Yang–Mills Lagrangian with nearest neighbor differences. This formulation differs from conventional lattice gauge theory in two fundamental respects; first, exact local gauge symmetry is broken, and, second, the integral over gauges is no longer compact. The latter feature forces the imposition of gauge fixing at the outset. Patrasciou, Seiler and Stametescu [45] have performed preliminary simulations with this model. They have as yet not seen the area law in large loops, but this is probably due to a renormalization of the bare charge making the linear potential observable only at extremely strong coupling.

Remaining closer in spirit to the Wilson formulation, Edgar [46] considered replacing the plaquette with the 2×1 Wilson loop as the fundamental term in the action. Simulations with this "fenêtre" action show a clear first-order transition. One important conclusion is that the mere presence or absence of a phase transition is not a universal property of the gauge group. Indeed, when the lattice spacing is not small, variations of the action can introduce new physics as lattice artifacts.

Drawing still closer to the Wilson theory, one can keep the action as a sum over class functions of the group elements associated with the plaquettes, but change the form of that function. Manton [47] presented a particularly simple alternative, taking for the action on a plaquette

$$S_P(U) = \beta d^2(U, I), \tag{4.8}$$

where d is the minimal distance in the group manifold between the element U and the identity. This takes advantage of the fact that there exists a unique (up to an overall normalization) invariant metric in a Lie group manifold. In the case of SU(2) the distance is simply

$$d(U_1, U_2) \propto \arccos(\tfrac{1}{2}\mathrm{Tr}(U_1 U_2^{-1})). \tag{4.9}$$

The Manton action is convenient for analytic work in the weak coupling limit but is singular for those elements with maximum distance from the identity (-1 for SU(2)). This singularity results in a transfer matrix which is not positive definite [48].

Another generalization, similar in spirit but different in detail from that of Manton, is the "heat kernel" or generalized Villain action [49]. The Boltzmann weight or exponentiated action

$$\exp\{-S_P(U)\} \tag{4.10}$$

should peak strongly near the identity for weak coupling but should become uniform over the group for a simple strong coupling limit. This is reminiscent of the expectation of the evolution of the temperature distribution in a piece of material shaped like the group manifold and initially possessing a delta function temperature spike at the identity. As time evolves towards infinity, the hot peak will spread and eventually become uniform over the group. This can be made mathematically precise using a group theoretical generalization of the Laplacian to formulate a heat equation. The exponentiated action is then identified with the solution of this equation, where the coupling constant corresponds to the time after the initial singular distribution of heat. This action has the technical advantage over the Manton form of being smooth over the entire group manifold and of giving rise to a positive definite transfer matrix. Both the Manton and heat kernel action have been subjected to Monte Carlo analysis [50] and show no phase transition at finite β.

An interesting change in the phase structure of the SU(2) theory results from simply replacing the trace of a plaquette with the corresponding trace in the adjoint representation [51]. This amounts to working with the group SO(3). In fig. 18 we show a thermal cycle on this model with a 5^4 lattice [51]. Fig. 19 shows the evolution of this system from random and ordered starts at our estimate of the transition temperature. As far as the classical limit is concerned, SO(3) and SU(2) theories are identical. They only differ in their global properties which come into play when quantum fluctuations bring plaquette operators far from the identity. As with the fenêtre action, the new transition occurs when the lattice spacing is large and lattice artifacts should be expected.

One possible explanation of this SO(3) transition is in terms of Z_2 monopole excitations [53]. These

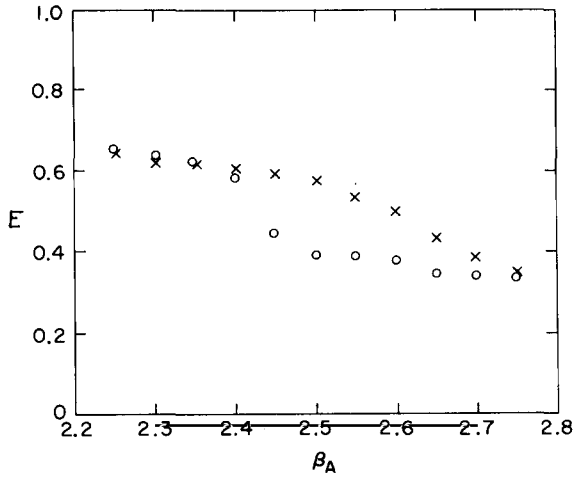

Fig. 18. A thermal cycle with the gauge group SO(3).

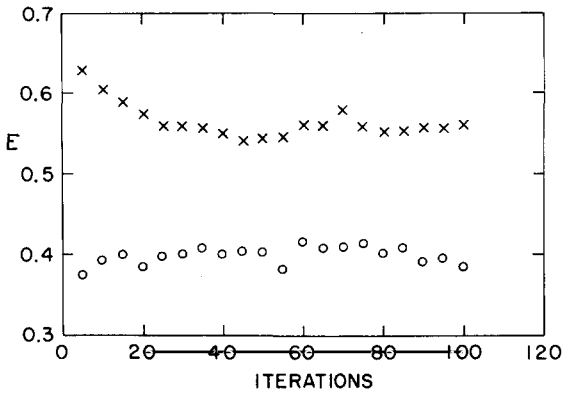

Fig. 19. Evolution of the average plaquette for SO(3) from random and ordered starts at $\beta = 2.5$.

arise because the adjoint representation of SU(2) does not see the Z_2 center of the latter group. A plaquette variable near -1 has the same energy as one near $+1$. This can be used to define a Dirac string as a sequence of plaquettes near -1. Several closely related schemes for making this precise have been presented [54, 55]. We will present that of Halliday and Schwimmer, which entails a slight modification of the theory. To make the action insensitive to the group center, introduce a new set of variables $\{\sigma_P\}$, each from the group $Z_2 = \{\pm 1\}$, located on the lattice plaquettes. We study the partition function

$$Z = \sum_{\{\sigma P\}} \int dU \exp\left\{\beta \sum_P \sigma_P \operatorname{Tr} U_P\right\}. \tag{4.11}$$

As the action is linear in σ_P, that sum can be done to give

$$Z = \int dU \exp\left\{\beta \sum_P S_P(U_P)\right\}, \tag{4.12}$$

where

$$S_P(U_P) = \ln(2\cosh(\beta \operatorname{Tr} U_P)). \tag{4.13}$$

This is an even function of Tr U_P and thus does not see the group center. Halliday and Schwimmer studied this variation of the SO(3) theory and found that it also has a first-order phase transition.

The quantity σ_P is essentially a Dirac string variable: $\sigma_P = +1$ weights U_P towards the identity and $\sigma_P = -1$ weights towards -1. A natural definition of a monopole is to count the number of negative strong variables entering any given three-dimensional cube and to say that a monopole is in that cube if this number is odd. In four dimensions these monopoles trace out world lines and the strings sweep out world sheets. Halliday and Schwimmer measured the density of these monopole world lines and found a

sharp increase at the transition temperature. Note that the path of a Dirac string can be changed by absorbing factors of -1 in the link variables. The string is not physically observable but its endpoints are.

The monopoles are easily suppressed with the addition of a mass term. Thus we can consider the partition function

$$Z = \sum_{\{\sigma_P\}} \int dU \exp\Big(\beta \sum_P \sigma_P \operatorname{Tr} U + \lambda \sum_c \prod_{P \in c} \sigma_P\Big), \tag{4.14}$$

where the new sum in the exponent is over all three-dimensional cubes in the lattice. The presence of a monopole in any of these cubes is now penalized by a factor $e^{-2\lambda}$. As λ becomes large, the product of the string variables over the surface of any cube must go to unity. When this is the case, an elementary exercise shows that there exists a set of Z_2 variables on the links such that any σ_P is the product of these around the given plaquette. In this event, all Z_2 factors can be absorbed in the SU(2) measure and the theory goes over into the usual SU(2) model which has no phase transition. Another interesting limit is $\beta = 0$. In eq. (4.14) this gives a rather complicated looking Z_2 system. However, a duality transformation turns it into the usual four-dimensional Ising model which has a single second order phase transition. Halliday and Schwimmer provided Monte Carlo evidence that as λ is increased the SO(3) transition moves to smaller β and eventually becomes the Ising transition. The value of λ at which the transition changes from first to second order is unknown.

An alternative method for continuing between SU(2) and SO(3) begins with both representations in the action. Thus for the plaquette action to be inserted in eq. (4.12) we take

$$S_P(U) = \tfrac{1}{2}\beta \operatorname{Tr}(U) + \tfrac{1}{3}\beta_A \operatorname{Tr}_A(U). \tag{4.15}$$

Here Tr_A denotes the trace of U in the adjoint or spin one representation and the factors are inserted for normalization convenience. For $\beta_A = 0$ this becomes the oridinary SU(2) model; on the other hand, $\beta = 0$ gives the SO(3) theory. A third interesting limit is reached as β_A goes to infinity, in which case all plaquettes are forced to lie in the center of the gauge group. Up to a gauge transformation, all links are themselves driven to the center. Thus for SU(2) the model becomes a Z_2 gauge theory with coupling β. At the outset, therefore, we know this model has at least two first-order transition lines entering its phase diagram.

Monte Carlo simulations have explored the evolution of these transitions into the two-coupling plane [52]. The resulting phase diagram is shown in fig. 20. Note that the Z(2) and SO(3) transitions are stable and meet at a triple point located at

$$(\beta, \beta_A) = (1.57 \pm 0.05, 0.78 \pm 0.05). \tag{4.16}$$

From this triple point extends a first-order line which points towards the Wilson axis but terminates at a critical point before reaching it. This line points directly at the position of the peak in the specific heat of the ordinary SU(2) model. Thus the peak may be thought of as a remnant of this transition, a shadow of its critical endpoint.

As the parameter β_A increases relative to β, the extremum of the action at $U = -I$ changes from a maximum to a minimum. This occurs along the line

$$\beta_A = 3\beta/8. \tag{4.17}$$

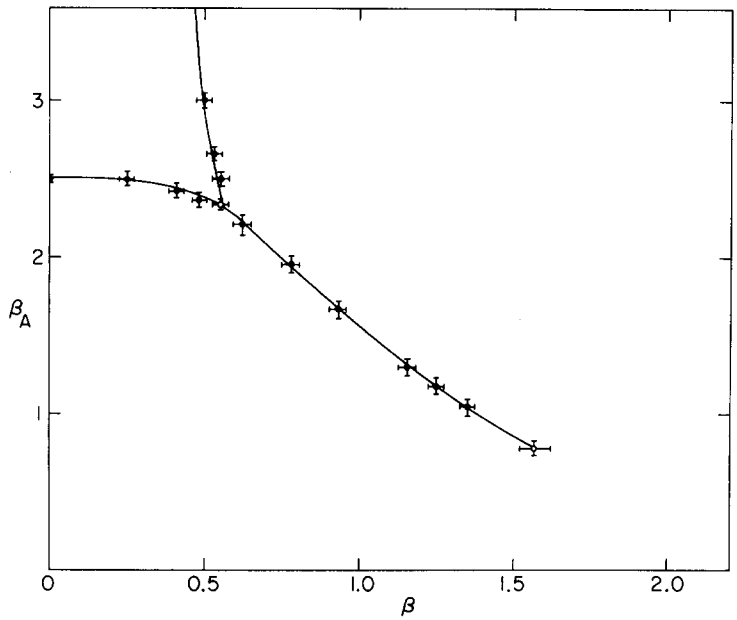

Fig. 20. The phase diagram for SU(2) lattice gauge theory with both fundamental and adjoint couplings.

Finally, along the β_A axis the two minima are degenerate. Note that the critical endpoint lies slightly above the line in eq. (4.17). Bhanot has studied a similar two coupling SU(3) theory and finds a critical endpoint again near the appearance of new minima of the plaquette action at group elements in the group center [56]. As the N of SU(N) increases beyond four, those elements of the group center near the identity become minima of the action even for the ordinary Wilson action. This observation correlates well with the Monte Carlo results that the Wilson SU(4), SU(5) and SU(6) theories all display first order phase transitions [57]. Presumably a negative β_A will permit continuation around these transitions, which would therefore not be deconfining.

5. Observables of a pure quantum gauge theory

The Monte Carlo method, beyond allowing one to obtain information on the phase structure of a lattice quantum gauge theory, permits the actual determination of several observables of physical interest. The quantum expectation value of an observable O, which would be given exactly by eq. (2.23), is approximated by the average value of O taken over several configurations in the MC sequence, after a certain number of initial configurations have been discarded to allow for the onset of statistical equilibrium (see eq. (3.1)). Of course, in the applications to quantum gauge field theories, one must remember that the lattice version of the model constitutes a regularization. So, whatever observable one determines, one must make sure that the number can be legitimately extrapolated to the continuum limit.

Although any field theory can in principle be formulated on the lattice and simulated by the Monte Carlo algorithm, the major interest of the method lies in its application to quantum chromodynamics, the gauge theory of strong interactions, because of the many features of this theory which are not accessible to ordinary perturbative analysis. Thus, the most valuable MC results on physical observables have

been obtained precisely for the theory of strong interactions, where the gauge group is SU(3), the group of color transformations. As a matter of fact, whereas several MC computations have been done with the full SU(3) gauge system, very frequently SU(2) has been taken as an approximation to the color group. The hope is that the non-Abelian nature of SU(2) already accounts for most of the properties of the correct theory and that the passage between the SU(2) and the SU(3) gauge groups involves only minor extrapolations. Of course from the technical point of view, using SU(2) rather than SU(3) as a gauge group implies a great reduction in the computer time needed for a simulation, a saving which can be made even greater if SU(2) is approximated by its discrete subgroup $\bar{Y}$ (for the values of β which are of practical interest, the SU(2)-model and the $\bar{Y}$-model are essentially indistinguishable).

Particularly relevant quantities which have been determined by MC simulations are the string tension σ, i.e., the value of the constant attractive force felt by two static sources carrying fundamental color (quarks) at large separation; the deconfining temperature T_c, i.e. the temperature above which, because of thermal fluctuations, the excitations of the gauge field (in the adjoint representation) can effectively screen sources in the fundamental representation; the mass gap, m_g, or mass of the glueball, i.e. the mass of the lowest lying state in the spectrum of the pure quantized gauge theory. Moreover, properties of the potential at short separation have been determined by MC computations, finding agreement with the analysis of perturbative QCD, and some interesting observables with topological significance have been evaluated. We shall consider the MC determination of these various quantities in separate subsections. For reasons of space we will not describe in this review computations of observables, such as the string tension in the confining phase of QED, which do not have an immediate bearing for the gauge theory of strong interactions.

5.1. The string tension

The measurement of the string tension is achieved by considering the expectation value of transport operators defined along suitable closed paths. Let γ be a closed path and U_γ the corresponding transport operator (see section 2.1). We form a gauge invariant quantity W_γ, called the Wilson loop factor, by considering a suitable class function of U_γ: typically U_γ will be represented by matrices in the fundamental representation and W_γ will be given by

$$W_\gamma = \frac{1}{N} \operatorname{Tr} U_\gamma \tag{5.1}$$

if the group is SU(N); the expectation value of W_γ will then furnish information on the propagation of sources in the fundamental representation.

With the normalization given by eq. (5.1), W_γ will take value 1 if the gauge variables U_{ji} along the path equal the identity or a pure gauge form $U_{ji} = g_j g_i^{-1}$. A completely random averaging over even a single link variable in U_γ will instead produce $\langle W_\gamma \rangle = 0$. We expect therefore $\langle W_\gamma \rangle$ to take smaller and smaller values as the correlation between gauge variables along the path decreases. In particular, $\langle W_j \rangle$ will decrease toward zero when the size of the loop γ becomes larger, because more link variables will enter in the averaging and because those farther away will become less and less correlated. Crucial information is contained in the specifics of the rate of decay of $\langle W_\gamma \rangle$. To appreciate this it is useful to develop a more physical picture for the meaning of the Wilson loop factor.

The insertion of W_γ in the integral over configurations of $\exp\{-S_G\}$ corresponds to adding to the action of the system a perturbation due to the propagation of a source along the path γ. This is

particularly evident in the formal continuum limit: W_γ reduces then to the trace of a (path ordered) exponential where A_μ is coupled to a current loop. It is convenient to take for γ a rectangle extending for m and n lattice sites along two directions, which, for definiteness, we shall take to be the x and t directions. We shall denote by $W_{m,n}$ the corresponding W_γ. The physical dimensions of the rectangle are given by $x = ma$, $t = na$, a being the lattice spacing. Introducing a complete set of energy eigenstates ϕ, defined in presence of the sources, $\langle W_{m,n}\rangle$ (which equals the ratio of the partition functions in presence and absence of the current loop) can be expressed as follows

$$\langle W_{m,n}\rangle = \sum_\phi |\langle\phi|0\rangle|^2 \exp\{-E_\phi t\}\,, \tag{5.2}$$

where $\langle\phi|0\rangle$ represents the amplitude for the transition between the ordinary vacuum state and a state with two static sources at separation x, induced by the part of the transport operator defined along the x side of the rectangle, and where $\exp\{-E_\phi t\}$ represents the correct factor for the propagation of a state with energy E_ϕ along a duration t of Euclidean time. The energy of the state will of course be a function of the separation of the sources: $E_\phi = E_\phi(x)$. For sufficiently large time t the term with lowest E_ϕ will dominate and we conclude

$$\langle W_{m,n}\rangle \underset{t\to\infty}{\longrightarrow} c\, \mathrm{e}^{-E(x)t}\,, \tag{5.3}$$

where now $E(x)$ stands for the ground state energy in presence of static sources with separation x. Thus, on general grounds, we expect that a measurement of $\langle W_{m,n}\rangle$ on the lattice will produce a result

$$\langle W_{m,n}\rangle \underset{n\to\infty}{\longrightarrow} c\, \mathrm{e}^{-\varepsilon(g,\,m)n}\,, \tag{5.4}$$

ε being a dimensionless function of the bare coupling constant g, and the separation in lattice units. Comparison with eq. (5.3) gives

$$E(x) = a^{-1}\,\varepsilon(g,\, x/a)\,. \tag{5.5}$$

$E(x)$ cannot however be immediately extrapolated to the continuum limit because the self-energy of the sources is still included in the expression.

A quantity of particular interest is the possible linear term in the asymptotic behavior of E for large x:

$$E(x) \underset{x\to\infty}{\longrightarrow} \sigma x\,. \tag{5.6}$$

The coefficient σ of this linear term is called the string tension and represents a constant attractive force between the sources at large separation. In the lattice measurements such a linear term is revealed by a behavior

$$\varepsilon(g,\, m) \underset{m\to\infty}{\longrightarrow} K(g)\, m\,. \tag{5.7}$$

We then have

$$\sigma = K(g)/a^2 . \tag{5.8}$$

Contrary to $E(x)$, which requires a subtraction, σ is a renormalization group invariant, i.e., one expects the continuum limit for σ to be obtained simply by letting g approach the scaling critical value g_c ($g_c = 0$, in the case of a non-Abelian system) and simultaneously taking the lattice spacing a to zero according to the functional dependence expressed by eqs. (2.27 and 2.30).

Clearly, for rectangular paths of increasing size, and in general for any loop of increasing size, a non-vanishing string tension manifests itself with an area law decay of $\langle W_\gamma \rangle$,

$$\langle W_\gamma \rangle \propto \mathrm{e}^{-K(g)A} , \tag{5.9}$$

where A is the area, in lattice units, of the minimal surface enclosed by the loop. For the above rectangular path $A = mn$. Given the implication of a non-vanishing string tension for the problem of quark confinement, a MC determination of σ is of obvious importance. This was done first in ref. [21] for an SU(2) theory, through the consideration of square loops of increasing size. A fit to the measured values for $\langle W_{m,n} \rangle$ in the form

$$\langle W_{m,n} \rangle \approx \exp(-Km^2 - bm - c) \tag{5.10}$$

allowed extraction of $K(g)$. The analysis, beyond showing that $K(g)$ was not vanishing, also revealed that when $\beta = 4/g^2$ became of the order of 2, the functional form of K underwent a rather rapid crossover from a behavior (for $\beta < 2$) well fit in terms of a strong coupling expansion, to a behavior (for $\beta > 2$) consistent with the scaling form

$$K(g) = \sigma a^2(g) = \frac{\sigma}{\Lambda^2}\left(\frac{24\pi^2}{11g^2}\right)^{102/121} \exp\{-(24\pi^2/11g^2)\} \tag{5.11}$$

predicted by the renormalization group.

The determination of K from a study of square loops only is beset by ambiguities: factors other than those included in eq. (5.10) may appear in the size dependence; finite size effects may distort the results (as the square loop comes close to the size of the periodic lattice, correlations between the variables along the loop and those on the images induced by periodicity tend to make $\langle W_{m,n} \rangle$ grow again and mask the fall-off). It was suggested in ref. [35] and ref. [42] that a better determination of K might be achieved considering ratios of Wilson factors for loops which are similar in shape and differ only by one unit of area. The expression

$$K_{\mathrm{eff}}(g, m) = -\ln \frac{\langle W_{m,m} \rangle \langle W_{m-1,m-1} \rangle}{\langle W_{m,m-1} \rangle^2} \tag{5.12}$$

appears to be particularly convenient, as one can show that various dependences on the size (perimeter terms, logarithmic terms) cancel out of the ratio, at least in a perturbative analysis [58]. K has been dubbed K_{eff} in eq. (5.12), because in principle one would want to proceed to the limit $m \to \infty$, but statistical fluctuations inherent in the MC method limit the maximum size of the loop one can consider

to 5 or 6 lattice spacings ($\langle W_{m,n}\rangle$ becomes too small for larger sizes to be distinguished from the fluctuations). Thus one measures an effective, m-dependent, string tension and tries to obtain information on the asymptotic limit [35, 37, 42, 59]. Such measurements are displayed in fig. 21 for SU(2) [42] and fig. 22 for SU(3) [60]. One notices in fig. 21 that, for fixed m, K_{eff} as a function of $\beta = 4/g^2$ follows first quite closely the strong coupling prediction, then departs from it at $\beta \approx 2$ and appears to follow for a while the scaling behavior of eq. (5.11). The larger m is, the longer the domain becomes for which the scaling behavior is followed. This is of course to be expected, as well as the eventual departure from the scaling curve: when β becomes large enough that the physical size of the loop becomes smaller than the confinement scale, then perturbative behavior $K_{\text{eff}}(\beta, m) \propto \text{const} \times \beta^{-1}$ should set in.

Still, in the envelope of the curves $K_{\text{eff}}(\beta, m)$ one recognizes a curve $K(\beta)$ with the expected scaling behavior. Fitting the functional dependence of eq. (5.11) to the envelope, one obtains

$$\begin{aligned} \sigma &= (5.9 \pm 1.8) \times 10^3 \, \Lambda^2 \qquad \text{SU(2)} \\ \sigma &= (2.8 \pm 0.9) \times 10^4 \, \Lambda^2 \qquad \text{SU(3)}. \end{aligned} \tag{5.13}$$

In ref. [37] the $\bar{Y}$ subgroup of SU(2) was used as an approximation to the continuous group in the

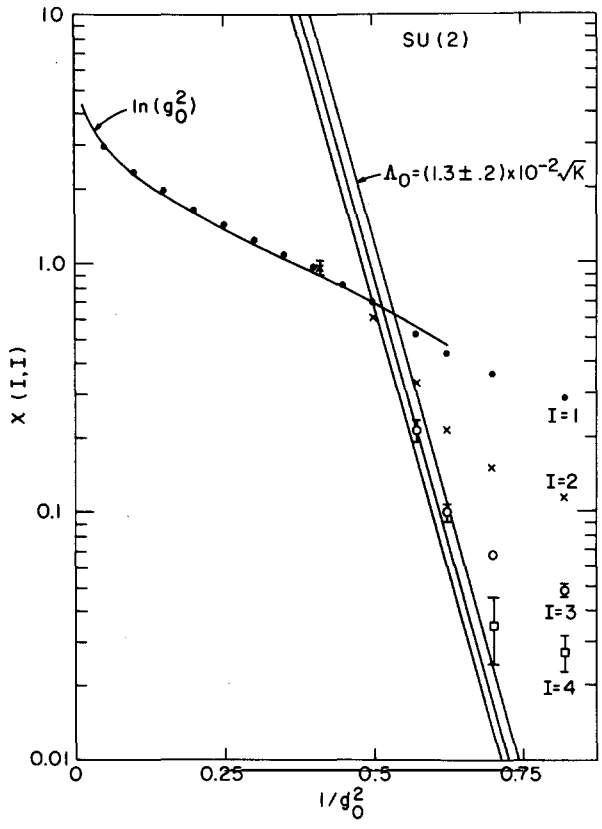

Fig. 21. Extracting the string tension for SU(2) lattice gauge theory. The quantity $X(I, I)$ refers to $K_{\text{eff}}(g, 1)$ of the text.

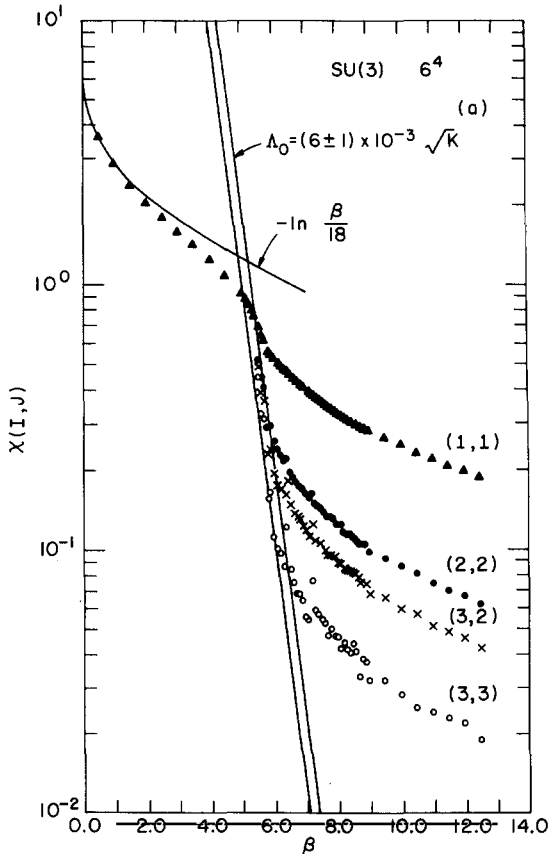

Fig. 22. Extracting the string tension for SU(3) lattice gauge theory.

definition of the lattice gauge model. The approximation is well justified by the fact that the crossover to the scaling region occurs at $\beta \approx 2$, whereas the transition to the ordered phase, due to the discreteness of the group, does not occur until $\beta \simeq 6$. Thus the SU(2)-model and the $\bar{Y}$-model give practically indistinguishable results for the observables up to values of β which place the system well inside the scaling domain. The computational advantages of dealing with a finite group are remarkable. In ref. [37] for instance, it was relatively easy to simulate a system extending for 16 sites in each dimension, thus containing 262144 link variables. A fast program for simulating the $\bar{Y}$ model has been published in ref. [18].

The result of eq. (5.13) does not really constitute a determination of the string tension, rather, assuming the string tension as basic observable to set the scale of all physical quantities, it fixes the value of the lattice scale parameter Λ. The computation of any subsequent observable will now give a result expressible entirely in terms of σ, with no reference to the bare coupling constant. No freedom of adjusting parameters is thus left in the theory and all observables are uniquely determined. The trade-off between the coupling parameter of the regularized lattice theory and the only, rather trivial, freedom of selecting one observable in the continuum limit to set the standard for dimensional quantities has been given the marvellous name of dimensional transmutation [61].

The values of physical observables may be expressed straightforwardly in terms of σ if they are computed within the same scheme of regularization (namely, the lattice gauge theory with Wilson's action). Otherwise the scales introduced in the definition of the various renormalization procedures must be related. In computations of perturbative QCD theorists use different methods of renormalization (the lattice regularization would indeed be a quite awkward one) and the results may for instance be expressed in terms of a convenient parameter called Λ_{mom} [62]. With an elaborate computation the scales Λ and Λ_{mom} (in the Feynman gauge) have been related, ref. [63], and one finds

$$\begin{aligned} \Lambda &= 0.0174\, \Lambda_{\text{mom}} \qquad \text{for SU(2)}, \\ \Lambda &= 0.0120\, \Lambda_{\text{mom}} \qquad \text{for SU(3)}. \end{aligned} \tag{5.14}$$

The values

$$\begin{aligned} \Lambda_{\text{mom}} &= (0.75 \pm 0.12)\, \sigma^{1/2} \qquad \text{SU(2)}, \\ \Lambda_{\text{mom}} &= (0.5 \pm 0.1)\, \sigma^{1/2} \qquad \text{SU(3)} \end{aligned} \tag{5.15}$$

that one would infer from eq. (5.13) are not in disagreement with values estimated in various applications of perturbative QCD (for instance, to scaling violations in deep inelastic scattering, Drell–Yan process, etc.). A direct comparison, however, requires some caution because the perturbative analysis itself is not free of ambiguities and also the calculation above neglects light quark loops.

It is nevertheless possible to compare results obtained with different renormalization prescriptions entirely within the framework of MC simulations. This has been done in ref. [50] where the string tension was measured using alternative actions to Wilson's in the definition of the lattice gauge system. This possibility was mentioned in the previous section. Precisely, expressing always the action as

$$S = \sum f(\phi_{\text{P}}, \beta), \tag{5.16}$$

where ϕ_P is defined by

$$U_P = \cos\phi_P + i\sigma \cdot n \sin\phi_P \tag{5.17}$$

(SU(2) gauge theory), Wilson's action corresponds to

$$f \equiv f_W(\phi_P, \beta) = \beta(1 - \cos\phi_P), \tag{5.18}$$

whereas the form of the plaquette action f_M proposed by Manton [47]

$$f_M(\phi_P, \beta) = \tfrac{1}{2}\beta\phi_P^2, \qquad -\pi < \phi \leq \pi \tag{5.19}$$

and the so-called heat-kernel action [49]

$$\exp\{-f_{HK}(\phi_P, \beta)\} = \Big(\sum_{n=-\infty}^{\infty} \frac{\phi_P + 2\pi n}{\sin\phi_P} \exp\{-\tfrac{1}{2}\beta(\phi_P + 2\pi n)^2\}\Big)\Big(\sum_{n=-\infty}^{\infty} (1 - 4\beta n^2\pi^2)\exp\{-2\beta n^2\pi^2\}\Big)^{-1} \tag{5.20}$$

have been considered in ref. [50]. Manton's action is a simple quadratic expression in ϕ_P, assuming that ϕ_P is defined so as to lie in the range $-\pi < \phi_P \leq \pi$. It is singular near $U = -I$. The heat-kernel action is defined so as to make the measure factor itself equal to the matrix element of the operator $e^{-\Delta/\beta}$, where Δ is the Laplacian defined over the SU(2) group manifold. The heat-kernel action generalizes to an arbitrary group the measure proposed by Villain [64] for the U(1) system or $x-y$ model, i.e., a periodic sum of Gaussians.

Use of a different action in the lattice theory corresponds to a different renormalization prescription and we shall denote by Λ_W (formerly simple Λ), Λ_M and Λ_{HK} the scales for the systems defined with Wilson's, Manton's and the heat-kernel action respectively. The MC computations done in ref. [50] have shown that the string tension scales, after the crossover region, in Manton's and in the heat-kernel systems as well (see fig. 23). Indeed the pattern of the $K_{eff}(m, \beta)$ curves is quite similar to the one already found with Wilson's action. For the ratios between string tension and scales one obtains however

$$\Lambda_M = (0.0616 \pm 0.0020)\sqrt{\sigma}, \tag{5.21}$$

$$\Lambda_{HK} = (0.0206 \pm 0.0011)\sqrt{\sigma}. \tag{5.22}$$

This must be compared with $\Lambda_W = (0.013 \pm 0.002)\sqrt{\sigma}$ obtained in ref. [42]. The ratios between these various scales may be computed theoretically and one finds [50]

$$\Lambda_M/\Lambda_W|_{th} = 3.07, \tag{5.23}$$

$$\Lambda_{HK}/\Lambda_W|_{th} = 1.25. \tag{5.24}$$

From the numerical computations one finds instead

$$\Lambda_M/\Lambda_W|_{MC} = 4.74, \tag{5.25}$$

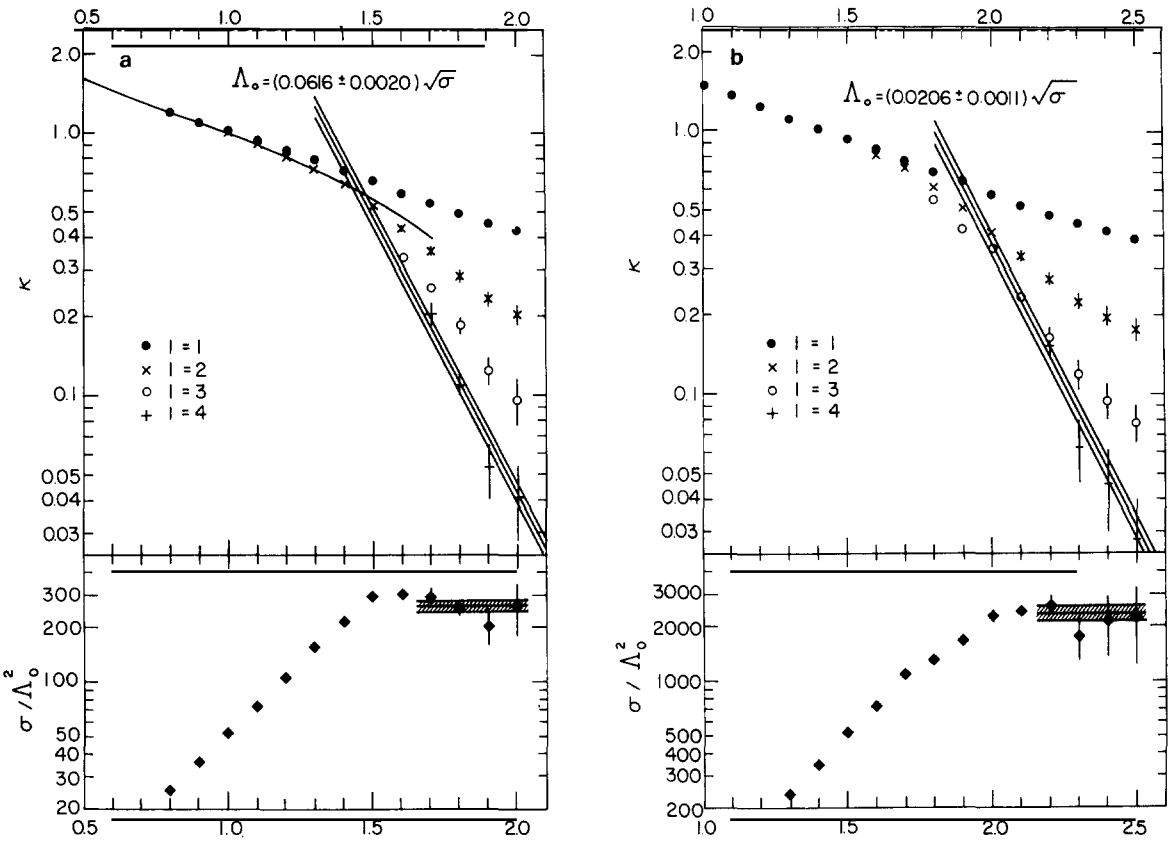

Fig. 23. Extracting the string tension for (a) Manton's action and (b) the heat-kernel action for SU(2). The variable K refers to K_{eff} in the text.

$$\Lambda_{\text{HK}}/\Lambda_{\text{W}}|_{\text{MC}} = 1.58\,. \tag{5.26}$$

The discrepancy may be explained remembering that the theoretical ratios are calculated with a one loop perturbative computation, at the end of which the limit $g \to 0$ is taken (and the results are exact, no truncation of an expansion is involved); the numerical estimates instead are made at finite values of the bare coupling constant. The scaling result is

$$K = \frac{C_{\text{i}}}{\Lambda_{\text{i}}^2}\left(\frac{24\pi^2}{11g^2}\right)^{102/121} \exp\left\{-\frac{24\pi^2}{11g^2}\right\}(1 + C_{\text{i}}^{(1)}g^2 + C_{\text{i}}^{(2)}g^4 \ldots) \tag{5.27}$$

where i refers to the scheme of regularization. The higher-order terms could in principle be computed, or estimated numerically, but in practice are neglected. As we work with g^2 of order unity, these terms could easily account for the discrepancy. Thus one should regard with some caution MC results estimated soon after the onset of scaling. The power corrections to scaling, however, are universal, in $d = 4$ as is the case here, within a definite scheme of regularization and therefore the direct comparison of observables evaluated within the same lattice model should be less sensitive to finite coupling effects.

5.2. Deconfinement temperature

The Monte Carlo technique may be used to study properties of quantized fields at finite temperature T. The investigation proceeds through a reformulation of the formula for the partition function,

$$Z = \mathrm{Tr}\, \mathrm{e}^{-H/T} \tag{5.28}$$

(we use units with the Boltzmann's constant k equal to 1) in terms of a functional integral

$$Z = \int\limits_{\phi(x,\,1/T)=\phi(x,\,0)} \mathrm{d}\phi \exp\left\{-\frac{1}{T}\int\limits_0^{1/T} \mathrm{d}t \int \mathrm{d}^3x\, \mathscr{L}[\phi]\right\}. \tag{5.29}$$

The r.h.s. of eq. (5.29) is of course only a formal expression, to which a precise mathematical definition must be given; but once again, this is precisely what is achieved by the lattice regularization. From eq. (5.29) we infer that finite temperature effects are taken into account by considering a lattice which extends to infinity in the three space-like directions, but only for a finite number n_t of lattice sites in the temporal direction. Periodic boundary conditions in time must be imposed on the dynamical variables and the temperature is related to n_t and lattice spacing a by

$$T = \frac{1}{n_t a}. \tag{5.30}$$

We are ultimately interested in the limit of a going to zero and n_t increasing so as to keep T constant.

In actual Monte Carlo simulations one works with a lattice which is finite also in the space-like directions, extending for n_s lattice spacings, and typically with periodic boundary conditions. In principle n_s should be much larger than n_t, although in practice this ideal condition is never realized and one must be careful about finite space effects. In this subsection we shall assume that the system and all pertinent mathematical expressions are defined on an $n_s^3 \times n_t$ lattice.

The free energy F_0 of the discretized system is given by

$$F_0 = -T \ln Z_0, \tag{5.31}$$

where

$$Z_0 = \sum_{\{U_{ji}\}} \exp\{-S(\{U_{ji}\})\} \tag{5.32}$$

(the summation symbol stands for a multiple integration over the group manifold if the group is continuous). One of the most interesting quantities to consider is the shift in free energy ΔF induced by a static source. The propagation of a static source in time is represented in the continuum formulation by the insertion of

$$\mathrm{Tr}\, P \exp\left\{\mathrm{i}g \int\limits_0^{1/T} A_0\, \mathrm{d}t\right\}$$

in eq. (5.32) with the factor $\exp(-S)$. This term is the trace of the transport operator along a path in the time-like direction, closed by virtue of the periodic boundary conditions. We shall denote the corresponding transport operator on the lattice by U_x:

$$U_x = U_{i_1 i_{n_t}} \cdots U_{i_3 i_2} U_{i_2 i_1}, \tag{5.33}$$

where $i_1, i_2, \ldots i_{n_t}$ indicate a sequence of lattice sites in the temporal direction at fixed space lattice coordinate x. A corresponding Wilson loop factor is defined

$$W_x = \frac{1}{N} \operatorname{Tr} U_x \tag{5.34}$$

(the normalization is for the group SU(N) and a source in the fundamental representation, but the normalization of W_x is irrelevant for the considerations which follow). The free energy in presence of the static source is then given by

$$F = -T \ln Z, \tag{5.35}$$

where

$$Z = \sum_{\{U_{ji}\}} W_x \exp\{-S(\{U_{ji}\})\}. \tag{5.36}$$

It follows that the variation of free energy can be expressed in terms of the average value of W_x,

$$\Delta F = -T \ln(Z/Z_0) = -T \ln\langle W_x \rangle, \tag{5.37}$$

a quantity particularly adapted for a Monte Carlo numerical evaluation.

Before presenting results on ΔF let us comment briefly on the physical expectations. If confinement occurs, the free energy of a single source should be infinite and therefore one ought to find

$$\langle W_x \rangle = \mathrm{e}^{-\Delta F/T} = 0. \tag{5.38}$$

Notice that an infinite ΔF cannot result from an ultraviolet divergence (which should be subtracted) in the regularized lattice version of the theory: if ΔF comes out infinite, it is an infrared effect and a genuine signal of confinement. It is interesting that SU(N) and also U(1) systems possess a symmetry which would insure $\langle W_x \rangle = 0$ for a source in the fundamental representation, if realized at the level of expectation values. The symmetry operation consists in multiplying all the link variables U_{ji} associated with links in the temporal direction and a fixed time coordinate by a constant element $C_n = \mathrm{e}^{2\pi \mathrm{i} n/N}$ from the center of the group. Since any plaquette contains either none or a pair of these links with opposite orientations, and because C_n commutes with all elements of the group, the plaquette transport operators U and the action are not affected by the transformation. This is therefore a symmetry of the system. (As a matter of fact the value of any transport operator for a closed loop entirely contained within $t = 0$ and $t = 1/T$ will also be unchanged.) But the paths along which U_x is defined are closed by virtue of the periodic boundary conditions, which give to the system the topology of a torus, and contain

a single one of the links affected by the transformation. The values of all U_x therefore change

$$U_x \to e^{2\pi i n/N} U_x \tag{5.39}$$

and so change the loop factors

$$W_x \to e^{2\pi i n/N} W_x . \tag{5.40}$$

If the symmetry is realized at the level of quantum averages, then

$$\langle W_x \rangle = e^{2\pi i n/N} \langle W_x \rangle \tag{5.41}$$

and $\langle W_x \rangle = 0$ follows.

The symmetry expressed by eqs. (5.39–41) may however be dynamically broken, resulting in finite expectation values for $\langle W_x \rangle$ and ΔF. The meaning of this symmetry violation is that the excitations of the gauge field induced by thermal fluctuations, although in the adjoint representation, effectively screen the quantum numbers of the source in the fundamental representation (Debye screening); the infrared effects are suppressed and the source becomes deconfined.

In ref. [65] theoretical arguments were given for a deconfinement of quarks, due to Debye screening, when the temperature becomes sufficiently high. Finite temperature effects in an SU(2) gauge system were first considered by means of Monte Carlo simulations in the work of refs. [66, 67]. The numerical results clearly showed that at low temperature $\langle W_x \rangle = 0$, but that $\langle W_x \rangle$ became nonzero when T exceeded some critical temperature T_c. Notice that the temperature of the lattice system may be increased either by lowering n_t (remember $T = 1/n_t a$) or by making the lattice spacing a smaller. The latter, by virtue of the functional relation between coupling parameter β and a needed to achieve a continuum limit, corresponds to increasing β. If deconfinement is a physical effect, it must occur at fixed T_c, at least for sufficiently small lattice spacing. It was confirmed in ref. [67] that, when n_t was made larger, the value of β at which $\langle W_x \rangle$ became non-vanishing also increased. Moreover the relation

$$n_t \, a(\beta_{cr}(n_t)) = \text{const} , \tag{5.42}$$

with $a(\beta)$ given by the renormalization group formula eq. (2.30), appeared beautifully verified. The deconfinement temperature was thus estimated as

$$T_c \approx (0.35 \pm 0.35) \times \sqrt{\sigma} , \tag{5.43}$$

σ being the string tension. A computation of T_c in the SU(3) system was done in ref. [68] with the result, $T_c \approx \Lambda^{\text{mom}} \approx 200\,\text{MeV}$.

Considering the expectation value of the product of several loop factors W_{x_1}, W_{x_2}, ... at different space locations one can evaluate the free energy of a system of several sources. This was done in refs. [66, 67] for two SU(2) sources in the fundamental representation separated along a lattice axis, and, also in the SU(2) theory, for arbitrary separation in ref. [69]. The Monte Carlo results clearly show that the potential between the sources is confining for $T < T_c$, with a string tension which becomes progressively smaller as the temperature increases, and Debye-screened for $T > T_c$. A graph illustrating the behavior of the force between the sources as a function of separation and temperature is displayed in fig. 24.

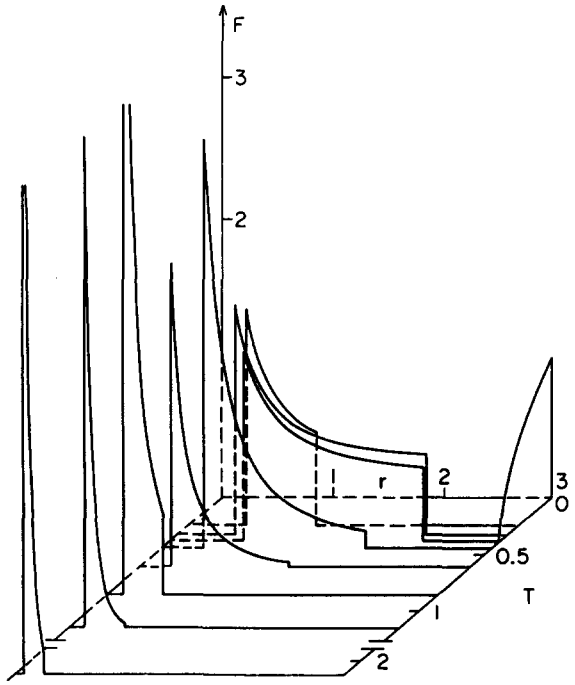

Fig. 24. The force between fundamental SU(2) sources as a function of separation and temperature.

Beyond considering the thermal properties of a system of static sources, Monte Carlo computations can be used also to investigate directly the properties of the finite temperature, quantized gauge field (gluon gas). These could be derived from a knowledge of Z_0, the partition function of the system itself. But Z_0 always appears as normalizing factor in the quantum averages and cannot be computed directly in MC simulations. Rather, one must consider suitable derivatives of Z_0 with respect to the physical parameters: on the one hand, these derivatives can be related to statistical averages, such as the average of the plaquette action, on the other hand they have an interpretation in terms of physical quantities, such as pressure and internal energy. These ideas have been pursued in a series of investigations by Engels et al. [70], and several interesting properties of the gluon gas have been determined. In particular, the occurrence of the deconfining phase transitions has been observed in the thermodynamic quantities. These finite temperature effects also provide information on the glueball spectrum [70, 71].

5.3. The mass gap

A pure gauge theory, like any quantum mechanical system, will be characterized by a spectrum of eigenvalues for the energy operator. With Lorentz covariance, this translates into a mass spectrum. On the lattice rather than energy eigenvalues, one should properly speak of eigenvalues of the transfer matrix T, i.e., the operator which generates translations by one lattice spacing. In the continuum limit, however, one may identify T with e^{-Ha} (where H is the Hamiltonian and the exponential is real decreasing because of the rotation to imaginary time) and reconstruct the eigenvalues of energy from those of T.

In a confined theory where no long range forces are present one expects the absence of zero mass

states. The mass spectrum should therefore begin with the first state above the vacuum having a positive definite mass eigenvalue m_g: this is called the mass gap of the theory. It represents the mass of a well defined particle-like excitation of the pure gauge system. In the application to quantum chromodynamics, this state is often referred to as a glueball, a term which is applied also to similar states of higher mass. In the absence of quarks, at least the lowest lying glueball must be stable. The coupling to quarks complicates the picture and glueballs may be experimentally detected only as resonant states outside of the main quark model sequence.

In any event, given a non-Abelian system, it is of obvious importance to determine the value of the mass gap. Monte Carlo computations of m_g have been done for SU(2) and SU(3) systems.

The numerical analysis proceeds through a study of the time dependence of the connected correlation function

$$G(t) = \langle O(t)\, O(0)\rangle - \langle O\rangle^2 , \tag{5.44}$$

where O is some suitable operator and 0, t represent time coordinates on the lattice (i.e., t is some multiple of a). O must have a non-vanishing matrix element between the vacuum and the sought after state. In the lattice theory the simplest choice for O is the trace of the transporter around the plaquette, the same quantity which appears in the definition of the action. Such a choice makes O dependent on a lattice spatial coordinate and on the orientation of the plaquette P which we denote by the subscript or:

$$O_{\mathrm{or}}(\boldsymbol{x}, t) = \frac{1}{N}\,\mathrm{Tr}\; U_{\mathrm{P}} . \tag{5.45}$$

The plaquette–plaquette correlation function

$$G_{\mathrm{or,or'}}(\boldsymbol{x}, t; \boldsymbol{x}', 0) = \langle O_{\mathrm{or}}(\boldsymbol{x}, t)\, O_{\mathrm{or'}}(\boldsymbol{x}', 0)\rangle - \langle O\rangle^2 \tag{5.46}$$

can be expanded into a series by insertion of a complete set of eigenstates $|n\rangle$ of energy and momentum

$$G_{\mathrm{or,or'}}(\boldsymbol{x}, t; \boldsymbol{x}', 0) = \sum_{n\neq 0} \langle 0|O_{\mathrm{or}}|n\rangle \langle n|O_{\mathrm{or'}}|0\rangle \exp(-E_n t - \mathrm{i}\boldsymbol{P}_n \cdot (\boldsymbol{x} - \boldsymbol{x}')) . \tag{5.47}$$

Early MC studies considered precisely this quantity with $\boldsymbol{x} = \boldsymbol{x}' = 0$ and or = or' corresponding to parallel plaquettes facing each other. The sum takes the form

$$\sum_{n\neq 0} |\langle n|O|0\rangle|^2\, \mathrm{e}^{-E_n t} .$$

For t sufficiently large the rate of decrease is dominated by the term with lowest E_n, which in principle allows a determination of m_g. In practice, the correlation length turns out to be rather small, of the order of one lattice unit, throughout the β domains where the MC simulation is possible. $G(t)$ falls off very fast and for $t = 3$ or 4 lattice spacings it becomes at most of the order of the statistical fluctuations. At such short separations the behavior of G is still strongly influenced by power-like terms, induced by the summation over momenta, and these mask the exponential fall-off. For all these reasons a direct study of plaquette–plaquette correlations can produce only rather rough upper estimates on the value of m_g.

A more refined analysis, suggested in the strong coupling analysis of Münster [12], proceeds through a summation over all space positions x and orientations of the plaquettes. This removes from the sum states with nonzero momentum or higher spins, and leaves only states for which $E_n = m_n$. We therefore define

$$O'(t) = \sum_{x,\mathrm{or}} O_{\mathrm{or}}(x, t) \tag{5.48}$$

and

$$G'(t) = \langle O'(t)\, O(0)\rangle - \langle 0\rangle^2 . \tag{5.49}$$

One expects

$$G'(t) = \sum_{n\neq 0} |\langle n|O'\rangle|^2 \exp(-m_n t) \tag{5.50}$$

and

$$G'(t) \propto \exp(-m_g t) \tag{5.51}$$

for t sufficiently large.

In a Monte Carlo simulation $G'(t)$ is measured for t of the order of a few lattice spacings at most. Let $t = na$ and define effective masses in lattice units

$$\mu_{\mathrm{eff}}(n, \beta) = -\frac{1}{n} \ln \frac{G'(na)}{G'(0)} \tag{5.52}$$

(the alternative definition

$$\mu'_{\mathrm{eff}}(n, \beta) = -\ln \frac{G'(na)}{G'((n-1)a)}$$

may also be used: μ' converges faster to the asymptotic value but is affected by larger errors). The true mass gap at finite β is given by

$$m_g = \lim_{n\to\infty} \mu_{\mathrm{eff}}(n, \beta)\, a^{-1} . \tag{5.53}$$

As one approaches the continuum limit $\beta\to\infty$, $a(\beta)\to 0$, one expects to observe a scaling behavior

$$\mu_{\mathrm{eff}}(\infty, \beta) \xrightarrow[\beta\to\infty]{} C\, a(\beta) , \tag{5.54}$$

which allows in turn a determination of the physical m_g:

$$m_g = C\Lambda\,. \tag{5.55}$$

The discussion already presented for the measurement of the string tension can now be repeated to argue that the numerical computation will give an indication of the scaling behavior as an envelope for the curves $\mu_{\text{eff}}(n, \beta)$. As a matter of fact, the situation is somewhat worse than for the string tension because the perturbative, large β behavior is $\mu_{\text{eff}}(n, \beta) \to \text{const}$ (rather than $O(1/\beta)$ as for the string tension). These constants, which can be evaluated in a spin-wave expansion, are rather large for small n and approach zero only slowly for $n \to \infty$. The behavior of μ_{eff} in the SU(2) theory, as determined from a MC study done on a $4^3 \times 16$ lattice [72] is illustrated in fig. 25. The dashed curve represents the leading term in the strong coupling expansion. The solid lines illustrate the scaling behavior corresponding to

$$m_g = 2.4 \pm 0.6\sqrt{\sigma}\,. \tag{5.56}$$

A further refinement of the numerical study is achieved considering for O a linear combination of operators corresponding to Wilson factors around different shapes of loops:

$$O''(t) = \sum_{x,\text{or}} \sum_{i} \alpha_i W_{\gamma i}(x, t)\,. \tag{5.57}$$

The idea is that, if it were possible to define an operator $O''(t)$ which has matrix elements only between the vacuum and the lowest quantum mechanical excitation, then the behavior

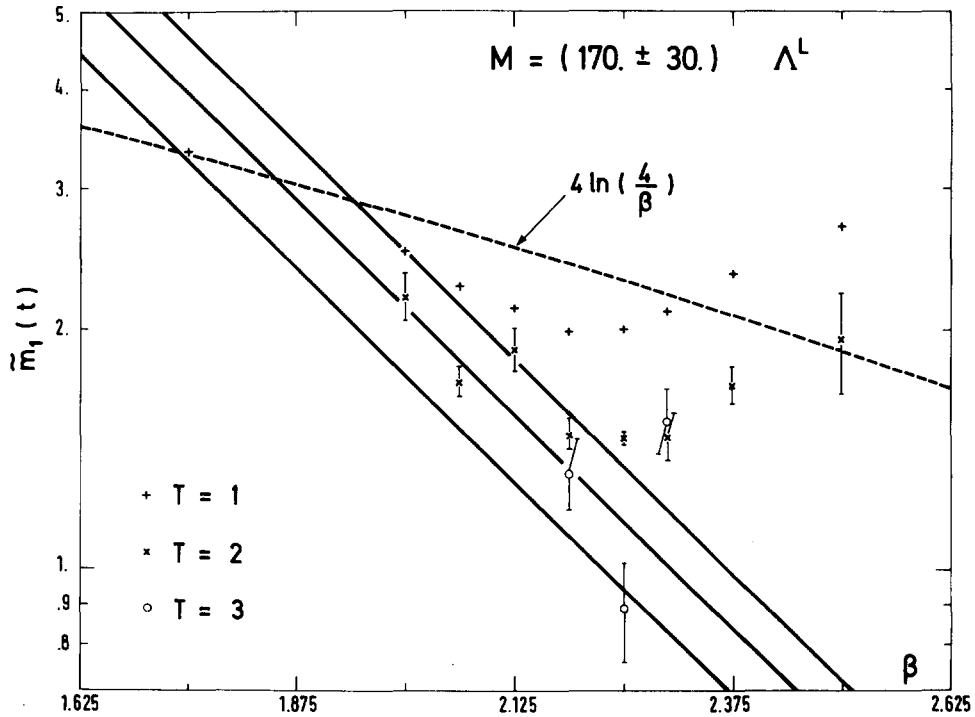

Fig. 25. The SU(2) mass gap in lattice units as obtained from the plaquette–plaquette correlation at separation of 1, 2 and 3 lattice sites.

$$G''(t) \equiv \langle O''(t)\, O''(0)\rangle - \langle O''\rangle^2 = |\langle 1|O|0\rangle|^2 \exp(-m_g t) \tag{5.58}$$

would be true at all separations, not only asymptotically, and one might express m_g as

$$-\frac{1}{a}\ln\frac{G''(1)}{G''(0)}.$$

While it is impossible to find such an operator exactly, one may change the parameters α_i so as to come as close to it as possible. In other words, in analogy with a variational determination of the eigenstates of the Hamiltonian, one obtains better upper bounds to m_g by considering variationally improved effective masses

$$\mu''_{\text{eff}}(n, \beta) = \min_{\alpha_i}\left(-\frac{1}{n}\ln\frac{G''(na)}{G''(0)}\right). \tag{5.59}$$

This procedure has been followed in refs. [72–76]. One finds that the variational technique indeed gives much better lower bounds on m_g at a definite separation in time. The inclusion of more operators in the analysis, however, especially if they are coupled mainly to higher excitations, increases the amount of statistical fluctuations and it becomes more difficult to increase the separation. From fig. 26, taken again from the work of ref. [72], one sees that the variational computation with t limited to $2a$ gives comparable results to the analysis based on the single plaquette operator, where G could be measured at separation $t = 3a$.

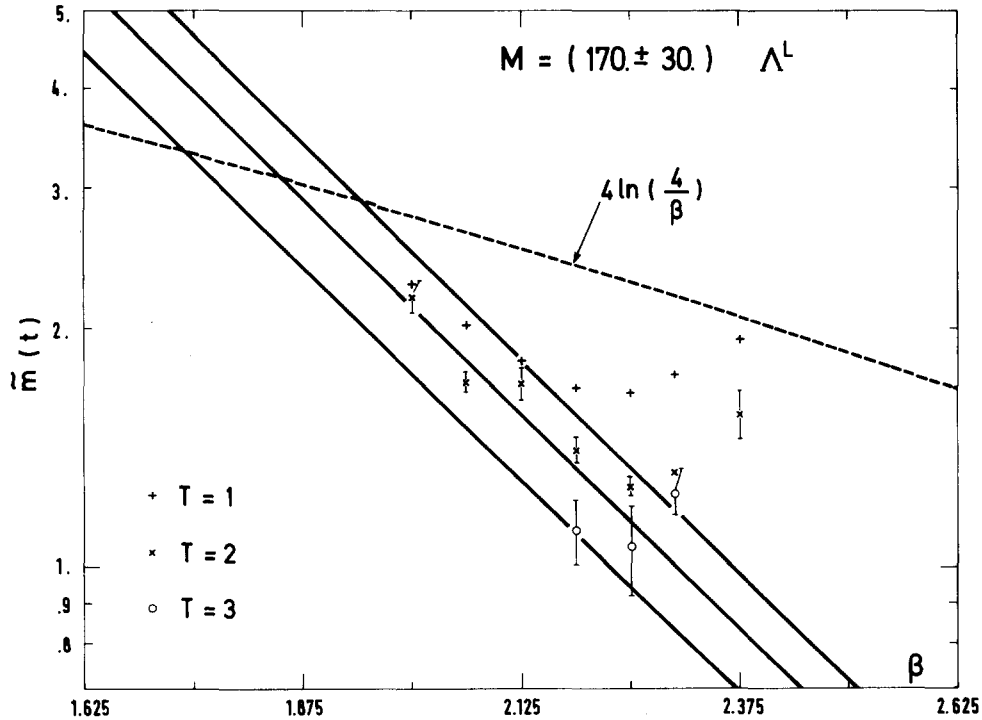

Fig. 26. The SU(2) mass gap as obtained from the variational techniques.

Together with the estimate $m_g = (2.4 \pm 0.6)\sqrt{\sigma}$ of ref. [72] the following results have been obtained for the SU(2) theory: $m_g = (2.9 \pm 0.4)\sqrt{\sigma}$, ref. [73], and $m_g = (2.5 \pm 0.3)\sqrt{\sigma}$, ref. [74]. In refs. [75 and 76] computations for the SU(3) system were presented, with the estimates $m_g = (2.6 \pm 0.3)\sqrt{\sigma}$ and $m_g = (1.8 \pm 0.1)\sqrt{\sigma}$, respectively.

By adding suitable weights in the sum over orientations one can project out states transforming according to a non-trivial representation of the lattice rotation groups. These representations can in turn be expanded into sums of representations of the O(3) rotation group, which will typically start with angular momentum greater than zero. Following this procedure a few authors have attempted a MC evaluation of the masses of higher spin glueballs. The results tend to be rather large with respect to the estimate of the mass of the 0^{++} state, which may be due to substantial contributions from higher excited states. We refer to the original literature [76] for a detailed account of the results.

Further information on the glueball spectrum can be obtained from finite size effects [71] or from consideration of alternative boundary conditions [77]. The internal energy on a finite lattice differs from that on an infinite lattice by corrections exponential in the masses of all possible glueballs. These effects are very sensitive to the number of states, and detailed measurements indicate a rich low energy spectrum [71].

5.4. Potential and recovery of rotational symmetry

Monte Carlo computations can be used to measure the behavior of the potential $V(\boldsymbol{r})$ between two static sources at small separation. Although this is a domain where, because of asymptotic freedom, the perturbative analysis is applicable, the Monte Carlo results can be used to confirm the validity of the method.

In ref. [37] the potential (or, more properly, the free energy) between two SU(2) sources in the fundamental representation was determined from the correlation function $\langle W_{\boldsymbol{x}} W_{\boldsymbol{0}} \rangle$ (see subsection 5.2) at the rather high value $\beta = 4.5$. This corresponds to a lattice spacing $a = 0.002(\sqrt{\sigma})^{-1}$. The analysis was made approximating SU(2) with its icosahedral subgroup and working on a 16^4 lattice. The results for $V(\boldsymbol{r})$ are shown in fig. 27: the Coulombic behavior is apparent. (Notice that even if one may argue that the values for a and n_t place the system in the deconfined region, although $n_s \gg n_t$ would be required for a clear-cut interpretation, the range of distances over which Debye screening should become manifest exceeds by far the maximum separation considered in the measurement.)

The results illustrated in fig. 27 do little more than confirm the compatibility of the MC simulation with a perturbative spin-wave analysis for sufficiently large β. Working at smaller values of β one can achieve more. Indeed, as the separation between sources grows larger (reducing β increases the lattice spacing), one expects the potential to be for a while still of the Coulombic form, but with a running coupling constant

$$V(\boldsymbol{r}) \propto g^2(r)/r. \tag{5.60}$$

A measurement of $V(\boldsymbol{r})$ will then give information on the scale Λ_{coul} present.

A rather detailed study of the potential $V(\boldsymbol{r})$ between two SU(2) fundamental sources has been presented in ref. [78]. $V(\boldsymbol{r})$ (or rather, once again, the corresponding free energy) was obtained from the measurement of the correlation $\langle W_{\boldsymbol{x}} W_0 \rangle$ for all possible on-axis and off-axis separations $\boldsymbol{x}$ leading to a statistically significant result. Lattices extending for $8^3 \times n_t$, $n_t = 4$, 6 and 8, and $16^3 \times 6$ sites, at values of β spanning the whole crossover region were considered. An accurate determination of the potential from the analysis of Wilson loops in the SU(2) theory has also been recently presented in ref. [79].

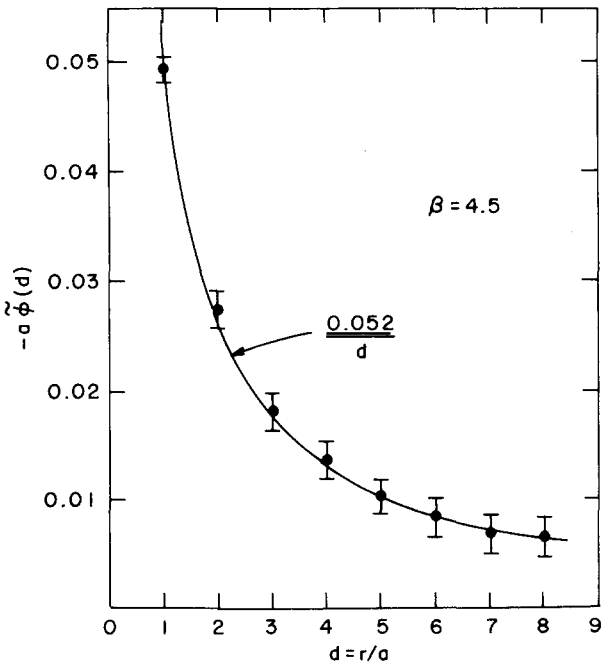

Fig. 27. The SU(2) interquark potential as a function of separation in lattice units.

An interesting study of the rotational properties of the potential in the U(1) model was presented in ref. [31]. The main goal of the analysis of ref. [78] was to study these properties of the SU(2) lattice potential, but, as a by-product, information of the thermal properties of the system and on the short distance behavior of the potential was obtained. In the confining region the curves obtained for the force between sources (see fig. 24) appear consistent with a fit

$$F(r) = \frac{9\pi}{22}\left[\left\{r^2 \ln\left(1 + \frac{1}{\Lambda_{\text{coul}}{}^2 r^2}\right)\right\}^{-1} - \Lambda_{\text{coul}}{}^2\right] + \sigma(T) \tag{5.61}$$

with $\Lambda_{\text{coul}} \approx 0.3\sqrt{\sigma}$. This formula incorporates a constant, but temperature dependent, string tension at large separation and a Coulombic behavior with running coupling constant at small distances [80]. The value found for the scale is compatible with previous MC and perturbative results [81–82].

Returning to the rotational properties of the potential, the results obtained for $V(\boldsymbol{r})$, which is defined of course only at the lattice sites, were interpolated throughout the lattice in the following way. Several lines of nearby, aligned lattice sites were considered (the lines did not have to pass through the origin) and the values assumed there by $V(\boldsymbol{r})$ were fit according to a formula

$$V(\boldsymbol{r}) = a + b/r + C(\boldsymbol{r}) .$$

Equating this expression to a fixed value V_0 allows then to determine the point (in between lattice sites) where the interpolated potential would assume a fixed constant value. The equipotential points thus found for several different values of V_0 and for $\beta = 2$ (on a $8^3 \times 4$ lattice) and $\beta = 2.25$ (on a $16^3 \times 6$ lattice) are reproduced in figs. 28 and 29 respectively. The lines joining the points are fits to the

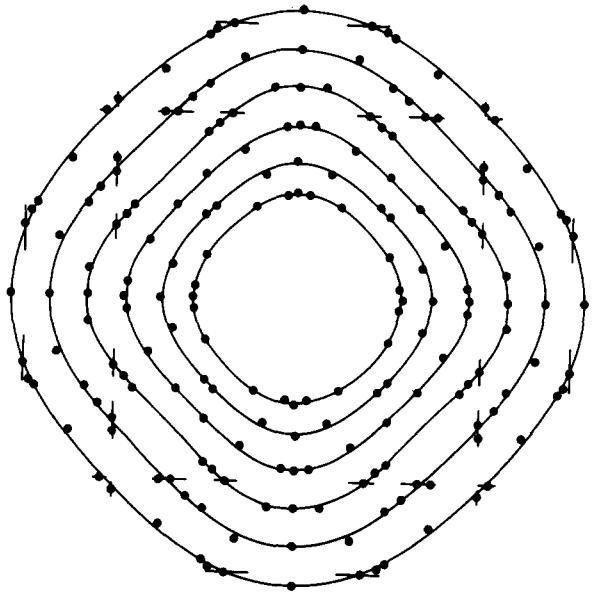

Fig. 28. Equipotential surfaces for fundamental sources in SU(2) lattice gauge theory at $\beta = 2.0$, just before the crossover.

equipotential surfaces of the form $r = r(\phi) = r_0(1 + \Delta \cos 4\phi)$. Notice that, with Wilson's action, the crossover from the strong coupling regime to the scaling regime occurs rather abruptly between $\beta \approx 2.0$ and $\beta \approx 2.25$. The results of ref. [78] show that the crossover is also accompanied by a restoration of rotational symmetry, as one would expect on physical grounds.

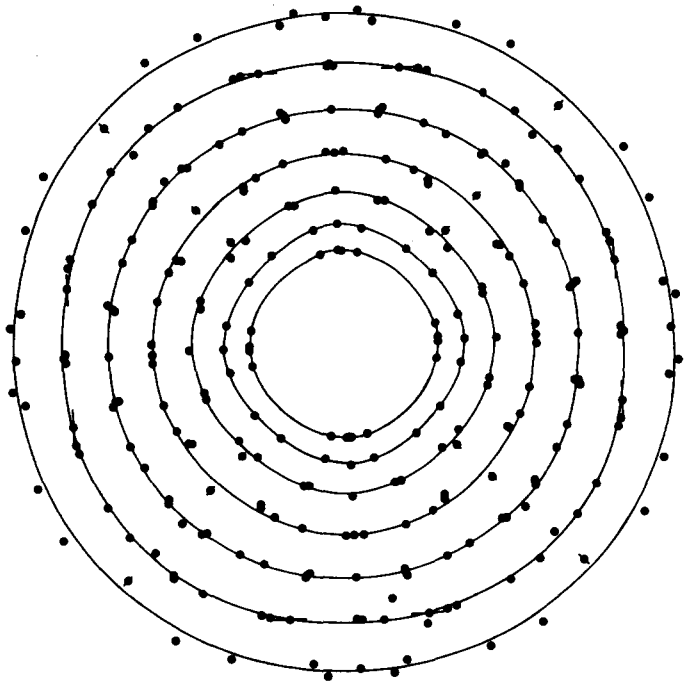

Fig. 29. Equipotential surfaces at $\beta = 2.25$, just after the crossover.

5.5. Observables with topological significance

It has long been recognized in the study of spin systems that excitations of a topological nature play a crucial role in determining the critical properties of such theories. These are local excitations of the lattice fields with properties determined by global constraints alone.

There are two basically different kinds of topological excitations of interest in the study of gauge theories on a lattice. The first kind concerns excitations which are involved in the critical and crossover properties of the lattice model itself and are not present in the continuum limit, whereas the second kind concerns excitations which are relevant for the continuum properties of the theory. Thus, as mentioned in section 4.3, in an SU(2) lattice gauge theory the condensation of Z_2 monopoles and strings can be invoked as the underlying dynamical mechanism responsible for the rapid crossover from strong to weak coupling observed in this model [53–55]. Such objects, though, are not present in the continuum theory because $\pi_1(\mathrm{SU}(2)) = 0$. Likewise, confinement in the strong-coupling phase of the four-dimensional U(1) model can be understood [83] as arising from the condensation of magnetic monopoles, which can only exist for finite lattice spacing. On the other hand, the continuum SU(2) pure gauge model does have instantons as topological excitations and it has been argued [84] that their presence may lead to a solution of the $U_A(1)$ problem in QCD.

The existence and properties of both types of topological objects can be studied by Monte Carlo methods. In this subsection we review some of the results which have emerged from these analyses.

The first Monte Carlo analysis of the topology of gauge fields was done for the U(1) model by DeGrand and Toussaint [17]. Dirac monopoles inside a volume V can be detected by counting the net number of Dirac strings which cross the closed surface S bounding V. The effect of a string crossing a plaquette is to contribute an integer multiple of 2π to the plaquette angle. By defining the physical fluctuations in θ_P to lie between $-\pi$ and π, this provides an algorithm for deciding whether a given plaquette has a string passing through it. If one looks at unit three-dimensional cubes one can thus decide whether a given cube contains a monopole. In four dimensions the topological excitations correspond to continuous strings of monopole current, i.e. monopole world lines. Two observables were measured to test the effect of these strings on the critical properties of the theory. By measuring the total length of the monopole world lines appearing per configuration one can determine the average density of monopole loops at fixed coupling. The results [17] show a dramatic change in the behavior of this function as the coupling is varied through the critical point [15, 41, 27, 28] at $\beta_c \approx 1$. In the strong-coupling phase the density of strings is large and slowly varying; it drops sharply at β_c, and, as the coupling is lowered past β_c, the density falls exponentially with β (as expected from an analysis of the Villain version of the theory [83]). This behavior is a clear indication that the topological excitations play a role in driving the system through its phase transition. To understand better what this role is, one can study the magnetic susceptibility of the system. A practical way of doing this is to place the system in an external magnetic field and observe the response of the monopoles by measuring the total field deep inside the system. A time-independent external magnetic field which points in the z-direction can be introduced by fixing, in each time slice, all the plaquettes in the xy face of the lattice at $z = 0$ to some value. However, for the flux to be anything other than an integer multiple of 2π, the boundary conditions in the z-direction must be twisted by adding to the links in the x-direction an amount such that the sum of the angles on this face equals the flux passing through it (modulo 2π). If the susceptibility is infinite, magnetic fields are screened because of the presence of unbound monopoles. A finite susceptibility corresponds to a finite renormalization of electric and magnetic charges.

A finite system with twisted boundary conditions can be thought of as a slice in the middle of an

infinite system in an external field. The total flux through the system lies between $-\pi$ and π. (These are just the twisted boundary conditions introduced by 't Hooft [16].) The results of these simulations are striking [17]. When $\beta < \beta_c \approx 1$ the average flux vanishes, implying the confinement of electric charge by the magnetic condensate. As β is increased past β_c, however, the reduced flux rapidly rises to a constant value, implying a finite value for the magnetic susceptibility. Because this picture directly indicates that the system can support long range magnetic fields when $\beta > \beta_c$, the above results lend strong evidence to the existence of a Coulomb phase and, therefore, of a massless photon in the continuum limit of lattice QED.

A mechanism which is formally analogous to the one given above has been invoked to describe the phase transitions predicted for the SO(N) lattice models and seen in Monte Carlo simulations [51–55]. Furthermore, Z(2) monopoles and strings can be defined for SU(2) lattice configurations, and a mechanism of condensation of these objects has been proposed to explain the SU(2) crossover as well [54]. These papers also discuss extension to the Z(N) monopoles and their possible role in the dynamics of SU(N) theories. Here we only mention that the Monte Carlo procedures needed to study these objects are of the same nature as those described above for the U(1) case. Twisted boundary conditions are also of value in the non-Abelian models [84, 85].

As a last example of a topological observable, we will discuss the case of instantons in the SU(2) theory. Monte Carlo results here are on a less firm footing than those discussed above. Part of the reasons for this are technical in nature but there are also problems of principle in measuring the topological charge of the continuum theory from a local lattice operator with the appropriate continuum limit. All the lattice operators which have been used suffer from the problem of having perturbative contributions which must be subtracted from the data before a comparison with a scaling law can be made. Further, because for the lattice definitions used in Monte Carlo analyses operators of arbitrarily high dimension contribute to the weak-coupling expansion of the charge, this subtraction is not in general possible. Nevertheless, under certain assumptions, this procedure has been tried [86] for several definitions of the lattice topological charge density. Self-consistent results which are not in complete contradiction with phenomenological estimates and which provide a plausible solution to the $U_A(1)$ problem in QCD have been obtained.

The main problem of principle which is involved in the construction of an adequate lattice definition of the topological charge is the fact that any lattice gauge field can be continuously deformed to the identity. Therefore, for finite lattice spacing, the SU(N) models have no topological structure. A possible way out of this has been recently proposed by Lüscher [87], who observed that, since one is really only interested in a region near the continuum limit where the bare coupling constant is small, it is possible to restrict the fields over which the functional integral is defined to a set with small action density. Imposing this constraint introduces a degree of space-time continuity on the fields and allows one to prove that these small action fields carry an integer topological charge. An explicit form for this charge has been given [87]. Unlike other definitions, this charge has no perturbative tail. Unfortunately, because of its complexity, no numerical work has yet been done with this quantity.

6. Coupled spin-gauge systems

Realistic models for particle interactions would contain dynamical matter fields beyond the gauge field themselves. The matter fields could represent fermionic degrees of freedom (such as those of the quarks in quantum chromodynamics) or bosonic degrees of freedom (such as those of Higgs particles)

and are naturally associated with the sites of the lattice. In this section we shall consider bosonic matter fields.

Let us denote by ϕ_i the matter field associated with the lattice site with the index i. Of course, more than one type of bosonic field could enter in the definition of the theory, but we shall not consider this possibility here: all the arguments we present for a single matter field can be easily generalized to the case where several are present. ϕ_i will transform according to some representation of the gauge group with indices which we shall usually leave implicit. Thus the notations

$$\phi_i \to \tilde{\phi}_i = g_i \phi_i \tag{6.1}$$

and

$$\bar{\phi}_i \phi_i , \tag{6.2}$$

defining the gauge transformation of ϕ and the scalar product, will stand for the more explicit formulae

$$\phi_i^{\alpha} \to \tilde{\phi}_i^{\alpha} = (g_i)^{\alpha}{}_{\beta} \phi_i^{\beta} \tag{6.3}$$

and

$$\phi_i^{*\alpha} \phi_{i\alpha} , \tag{6.4}$$

where $(g_i)^{\alpha}{}_{\beta}$ are the matrix elements of g_i in the representation under which ϕ_i transforms.

Crucial ingredients of the continuum action are the derivatives $\partial_\mu \phi_i$. On the lattice these will be replaced by finite differences $(\phi_j - \phi_i)/a$ where i and j denote neighboring lattice sites. However, a straightforward difference between the values of ϕ at neighboring sites has no gauge-invariant meaning. Rather, one should form the covariant finite differences

$$(\Delta\phi)_j = (\phi_j - U_{ji}\phi_i)/a , \tag{6.5}$$

where ϕ_i is transported from site i to site j by the link variable U_{ji} before the difference is taken. Under a gauge transformation $(\Delta\phi)_j$ transforms covariantly:

$$(\Delta\phi)_j \to (g_j\phi_j - g_j U_{ji} g_i^{-1}(g_i\phi_i))/a = g_j(\phi_j - U_{ji}\phi_i)/a = g_j(\Delta\phi)_j . \tag{6.6}$$

From the modulus squared of $(\Delta\phi)_j$, i.e. the gauge invariant quantity $(\bar{\Delta}\bar{\phi})_j\ (\Delta\phi)_j$, summing over all lattice sites and all orientations of the links, one can construct a kinetic term for the matter field in the action.

In the lattice regularization of a theory it is often convenient to impose a constraint on the modulus of the bosonic fields ϕ_i. This turns the system into a σ-like model. While imposing a constraint on $|\phi|$ would spoil the renormalizability of the continuum theory, such a constraint is acceptable in the lattice version and is not expected to rule out the possibility of a well-defined continuum limit. Indeed, in the process of renormalization ($a \to 0$), the quantum field of the continuum limit $\phi_{\mathrm{Ren}}(x)$ should not be identified with the fields ϕ_i at definite lattice points but rather with averages of ϕ_i over extended domains of the lattice; thus, even though the modulus of the renormalized ϕ_i may be constrained, no constraint limits the possible values of the continuum field.

If the modulus of the matter fields ϕ_i is constrained, then the kinetic term in the action reduces to the form

$$S_{\mathrm{MF}} = \beta_{\mathrm{M}} \sum_{\{ij\}} \{\bar{\phi}_j U_{ji} \phi_i + \mathrm{c.c.}\} \tag{6.7}$$

where the sum is extended over all pairs of neighboring sites, i.e., over all links of the lattice. β_{M} is a suitable coupling parameter for the matter field. We shall refer to the expression

$$E_L = \{\bar{\phi}_j U_{ji} \phi_i + \mathrm{c.c.}\}$$

as the (internal) energy of the matter field associated with the link $L = ij$ and to $S_L = \beta_{\mathrm{M}} E_L$ as the action associated with L. A rescaling of (ϕ_i) can be absorbed into a redefinition of β_{M} and we shall therefore assume

$$\bar{\phi}_i \phi_i = 1 . \tag{6.8}$$

Sometimes the manifold defined by eq. (6.8) coincides with the manifold of the gauge group itself: then the dynamical variables of the theory consist of group elements associated with both links and sites of the lattice.

This class of models possesses a rich structure. Several authors have discussed the resulting phase diagrams [5, 10, 88]. When the site spins are in the fundamental representation of the gauge group, the ordered spin phase describing the Higgs mechanism is analytically connected to the disordered confinement phase of the pure gauge field. This remarkable result shows the complex nature of the confinement mechanism when scalar fields are present. If the spins are in a higher representation of the gauge group, the confinement and Higgs phases can be distinct.

Several Monte Carlo studies [89–94] have been made on these systems with gauge groups Z_N, U(1) and SU(2). We describe first the Z_N system, which possesses gauge variables U_i on the links in addition to spin variables s_i on the sites. The s_i are elements of the group Z_M where we require that the quotient

$$l = N/M \tag{6.9}$$

be an integer so that Z_M is a subgroup of Z_N. The dynamics of these variables are determined by the action

$$S = \beta_{\mathrm{M}} \sum_{(i,j)} E_L(i,j) + \beta \sum_{\mathrm{P}} E_{\mathrm{P}} .$$

The first sum is over all nearest neighbor pairs of sites (i, j) and each such pair contributes

$$S_L(i,j) = \beta_{\mathrm{M}} E_L = (1 - \mathrm{Re}[s_i U_{ij}^l s_j]) \tag{6.10}$$

where the power l is defined in eq. (6.9). The second sum is over all elementary squares and represents the action used for the pure gauge theory,

$$S_{\mathrm{P}} = \beta E_{\mathrm{P}} = \beta(1 - \mathrm{Re}(U_{ij} U_{jk} U_{kl} U_{li})) \tag{6.11}$$

where i, j, k and l circulate around the plaquette.

The theory is defined by the path integral

$$Z = \sum_{s_i, U_{ij}} e^{-S} \tag{6.12}$$

where the sum is over all configurations of the site and link variables. For the U(1) system both s_i and U_{ij} are taken from the group U(1) and the model depends on the integer l appearing in eq. (6.10). The simplest gauge invariant correlation functions to study are the average link and average plaquette energies, defined by

$$L = \langle E_L(i,j) \rangle = -\frac{1}{4N_S} \frac{\partial}{\partial \beta_M} \ln Z(\beta, \beta_M), \tag{6.13}$$

$$E = \langle E_P \rangle = -\frac{1}{6N_S} \frac{\partial}{\partial \beta} \ln F(\beta, \beta_M), \tag{6.14}$$

where N_S is the number of lattice sites.

This system has four simple limits, $\beta_M \to 0, \infty$ and $\beta \to 0, \infty$. For $\beta_M = 0$ the site spins randomize and the model reduces to the pure gauge theory. For $\beta_M \to \infty$ the average link energy L must vanish. Using the gauge invariance of the system, the spins can all be set to unity; consequently, vanishing L implies

$$U_{ij}^l = 1. \tag{6.15}$$

Thus the theory reduces to pure Z_l gauge theory in this limit. If $l = 1$, i.e. if the spins are in the fundamental representation of the gauge group, the theory becomes trivial and both L and E vanish. When $\beta \to 0$ the link variables decouple and the theory can be solved to give

$$L(\beta = 0, \beta_M) = -\frac{\partial}{\partial \beta_M} \ln \Big[\sum_{U \in Z_N} \exp\{-\beta_M (1 - \mathrm{Re}(U^l))\} \Big], \tag{6.16}$$

$$E(\beta = 0, \beta_M) = 1 - (1 - L)^4 \delta_{l,1}. \tag{6.17}$$

Finally we come to the limit $\beta \to \infty$. Here all plaquettes must go to the identity. The gauge fields are then gauge equivalent to total order and the model reduces to a pure Z_M spin system (M state "clock" model) with nearest neighbor couplings. The Z_2 system is then the Ising model.

We expect these models to have transition lines entering their phase diagrams from the pure gauge transitions at $\beta_M = 0$ or ∞ as well as from any transition exhibited by the spin system at $\beta = \infty$. The latter transition line is called the Higgs line because it arises from an ordering of the spin or "Higgs" fields. When the parameter l is unity, no phase transitions are expected along the lines $\beta = 0$ or $\beta_M = \infty$. These lines connect the confinement regime of the pure gauge theory with the ordered on "Higgs" phase of the pure spin system. In ref. [88] it was shown that this smooth continuation between the regimes can be extended into the phase diagram. This is the result mentioned earlier that the distinction between the Higgs mechanism and confinement is obscure when the Higgs fields are in the fundamental representation.

In figs. 30 and 31 we show Monte Carlo results from ref. [89] for contours of constant L and E in the

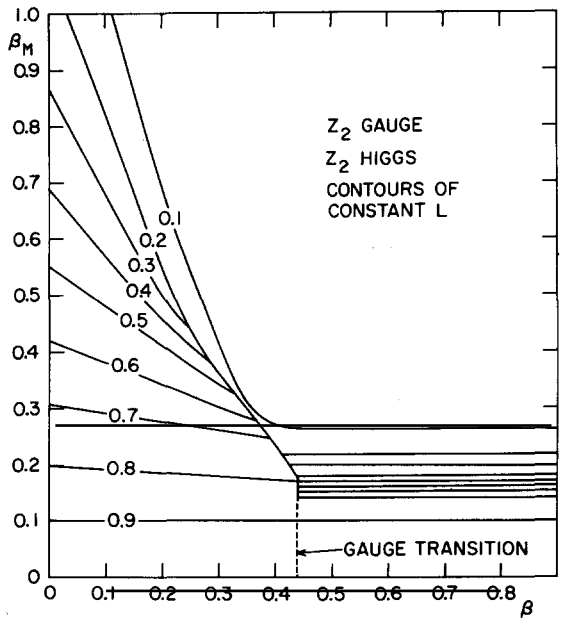

Fig. 30. Contours of constant L in the coupled Z_2 gauge-Higgs system.

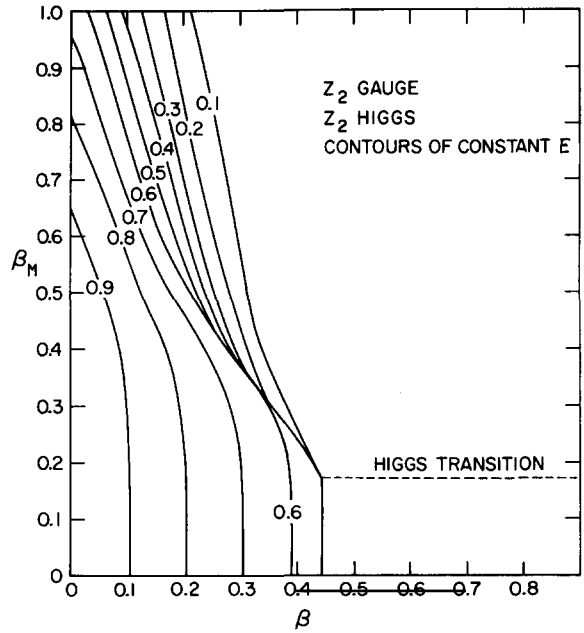

Fig. 31. Contours of constant E in the coupled Z_2 system.

four-dimensional system with gauge group Z_2 and Higgs field also in Z_2. These results were obtained using the heat bath technique on both the links and spin variables on a 5^4 lattice. The trajectory of the gauge transition through the diagram is apparent as a "cliff" in the values of E and L. The Higgs transition appears as a steep "hill" in the value of L. This hill disappears beneath the cliff at a triple point. Beyond this triple point a first-order line continues into the diagram until it unfolds at a critical point. Beyond that critical point the system appears smooth, as predicted. These features of the phase diagram for this system are shown in fig. 32. This analysis has been extended [90] to negative β to give the phase diagram in fig. 33. The diagram is symmetric under $\beta_M \to -\beta_M$.

Ref. [90] also presents results of a Monte Carlo study of the three-dimensional version of this model. The phase diagram obtained is similar in structure except that the gauge and Higgs transition are both second-order and dual to each other. Beyond the triple point the transition is first-order, similar to that seen in four dimensions.

In figs. 34 and 35 we show phase diagrams from ref. [89] for the Z_6 gauge system coupled respectively to Z_6 and Z_3 Higgs fields. The Z_6 Higgs case is similar to that for the Z_2 system except there are now two second-order gauge transitions rather than a single first-order one. Correspondingly there are two triple points. When the Higgs field is in Z_3, the value of l is 2 and at $\beta_M = \infty$ there is a residual Z_2 gauge theory. The first-order transition of this theory smoothly joins the first-order line coming from the low β triple point connecting the gauge and Higgs transitions. Thus in this model the Higgs and confinement phases are distinct, as they must be by the arguments in ref. [88]. Recent studies [91] of the $d = 4$ U(1) model essentially reproduce the Z_6 results with the large β gauge transition moved to $\beta = \infty$.

The U(1) coupled system in three dimensions was studied in ref. [92] as an example of a system where the pure gauge theory has only a confining phase. When $l = 2$ the spin transition and the gauge transition of the residual Z_2 theory are connected by a single critical line. When $l = 1$ the results were somewhat ambiguous, but, supported by small β series analyses, the authors of ref. [92] suggested a

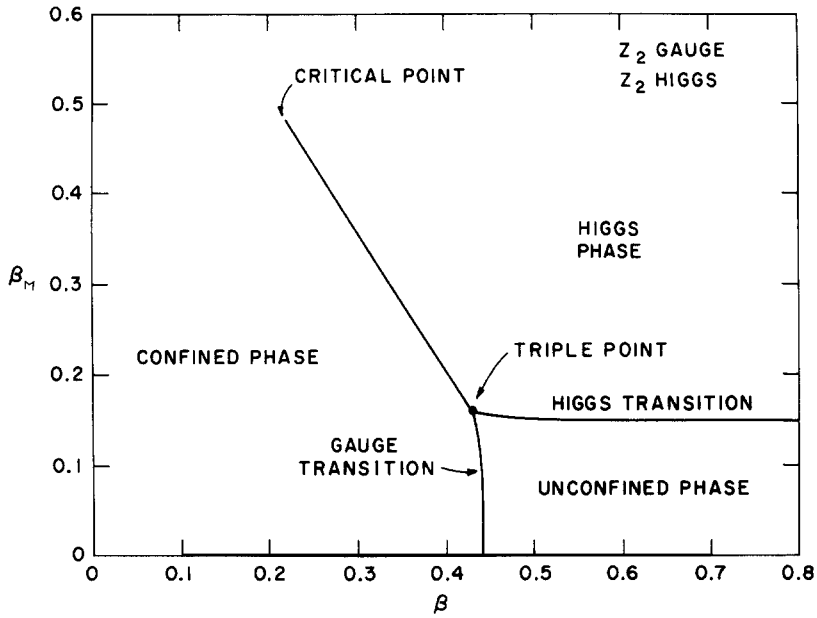

Fig. 32. The phase diagram for the coupled Z_2 system.

single transition line entering the diagram from the spin transition at $\beta = \infty$ and ending at a critical point.

The gauge-Higgs field system based on the non-Abelian group SU(2) has been studied in refs. [93, 94]. The most interesting situations are those where the Higgs field ϕ transforms under the (a) fundamental, (b) adjoint representation of SU(2). In case (a) the Higgs manifold, with the constraint $\bar{\phi}\phi = 1$, is the three-dimensional sphere S^3, i.e., is isomorphic to the group manifold itself. Indeed one

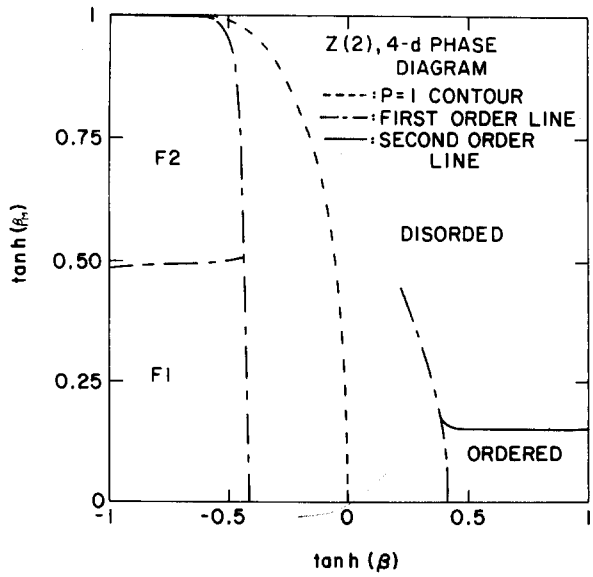

Fig. 33. The Z_2 phase diagram including negative β.

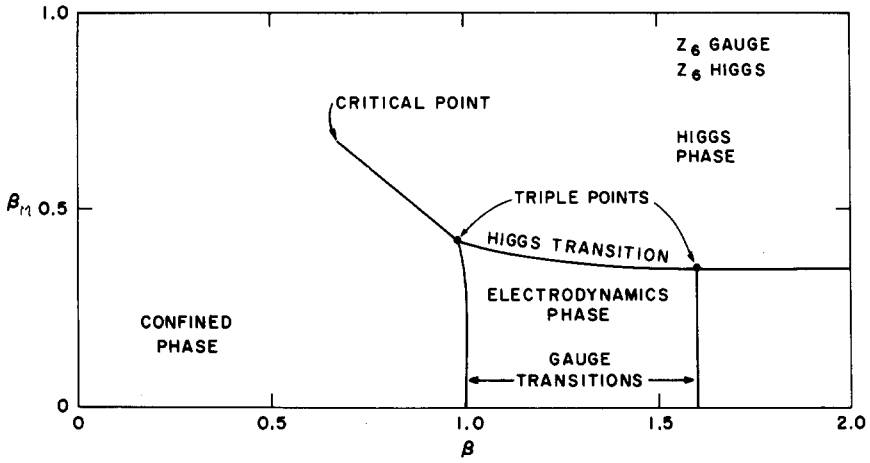

Fig. 34. The coupled Z_6 gauge-matter phase diagram.

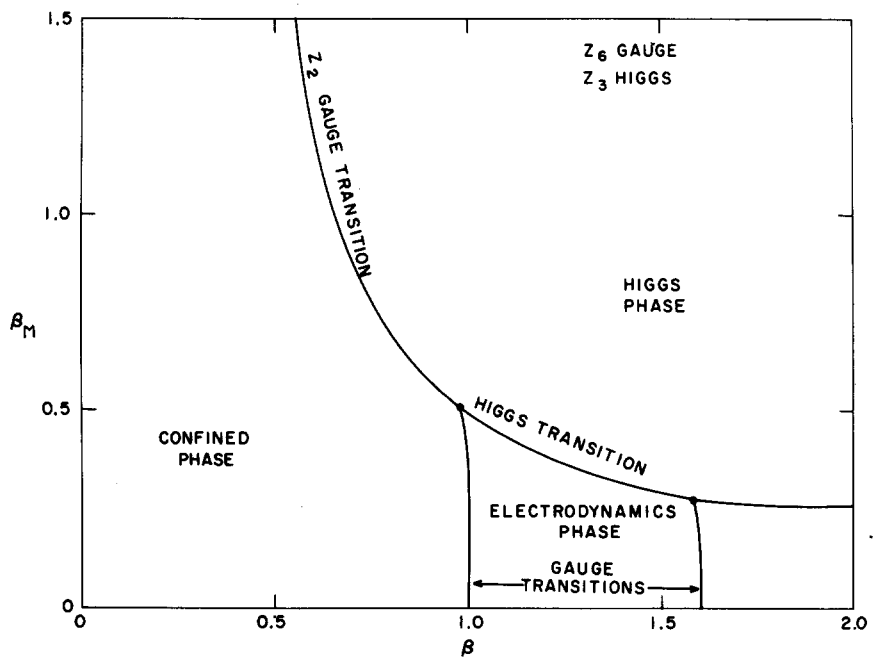

Fig. 35. Phase diagram for Z_6 gauge field coupled to Z_3 spins. Note the surviving Z_2 gauge theory as $\beta_M \to \infty$.

may set up a one-to-one correspondence between complex field elements $\phi \equiv \phi_\alpha$ ($\alpha = 1, 2$) and group elements $V_{\alpha\beta}$ ($\alpha, \beta = 1, 2$) by defining

$$V \equiv \begin{pmatrix} \phi_1 & -\bar{\phi}_2 \\ \phi_2 & \bar{\phi}_1 \end{pmatrix}.$$

In case (b) the Higgs manifold is isomorphic to the quotient space $SU(2)/U(1) = S^2$ and the field elements can be put in a one-to-one correspondence with the elements of any non-trivial class of SU(2).

One can, for instance, define $V(\phi) = \cos\mu + i\sigma \cdot \phi \sin\mu$, where ϕ is the Higgs field and μ is a fixed angle, different from 0 or π. These isomorphisms have been exploited in ref. [93] to approximate both the gauge field and the Higgs field by finite sets (thus reducing the required computer time). This work used the 120-element icosohedral subgroup $\bar{Y}$ of SU(2) to represent the group variables and the Higgs variables in the fundamental representation, and used the 12 elements of the class $\bar{Y}/Z_{10}$ to represent the Higgs variable in the adjoint representation. Monte Carlo simulations have been done to determine the behavior of $\langle E_P \rangle$ and $\langle E_L \rangle$ in thermal cycles at fixed β or β_M. The results are illustrated in figs. 36 and 37. Hysteresis loops or increased statistical fluctuations are signals of possible phase transitions. From the Monte Carlo simulations the authors of ref. [93] inferred the phase diagrams shown in figs. 38 and 39. Both graphs exhibit a line originating at $\beta \approx 6$, which represents a spurious phase transition induced by the discretization of the gauge manifold. The other lines are expected to approximate well the transitions in the continuous systems. In both cases, as $\beta \to \infty$ and the systems reduce to systems of coupled spins, these lines tend to the transition point β_M of the corresponding pure spin models. With ϕ in the adjoint representation a U(1) gauge symmetry still survives in the Higgs phase. Correspondingly the line of phase transitions persists to $\beta_M = \infty$, with β approaching the critical value of the U(1) model. (As a matter of fact, with the discretized manifolds the gauge symmetry becomes Z_{10} for $\beta_M = \infty$ and the two lines of phase transitions approach indeed the two critical points of the Z_{10} Abelian model, see section 4.1.)

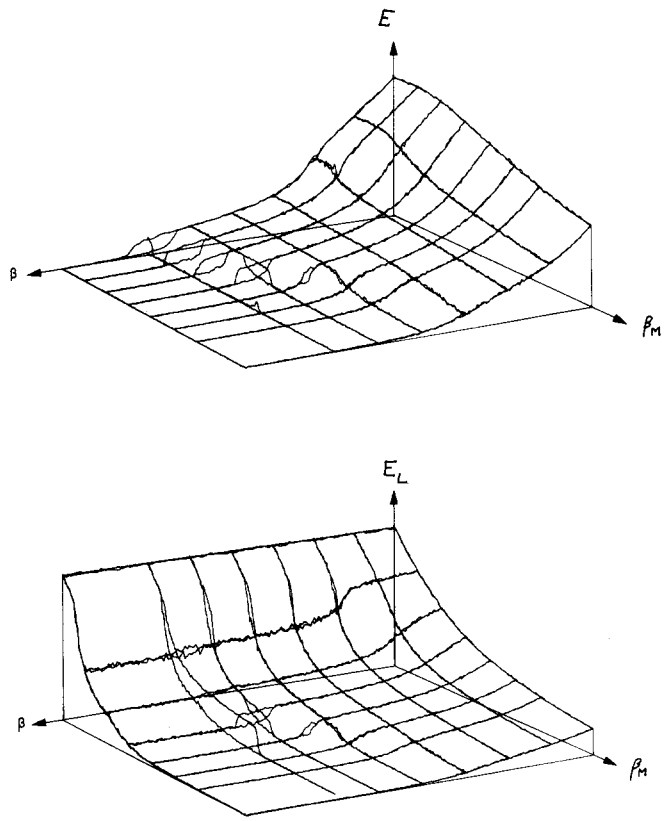

Fig. 36. Hysteresis cycles for the SU(2) system coupled to Higgs fields in the fundamental representation.

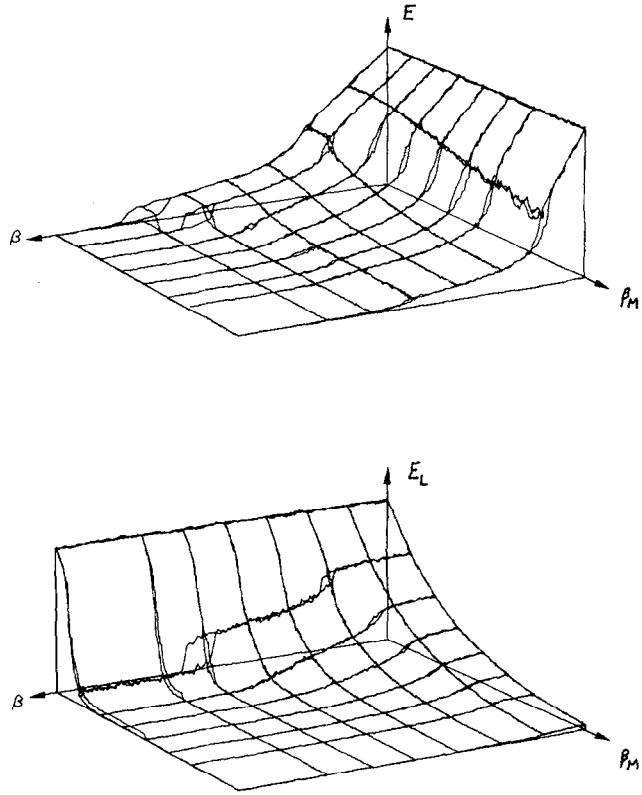

Fig. 37. Hysteresis cycles for the SU(2) system with adjoint Higgs fields.

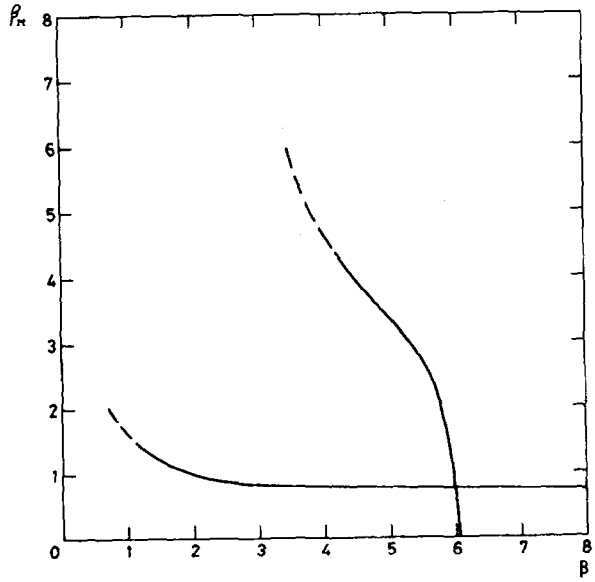

Fig. 38. The phase diagram inferred from fig. 36.

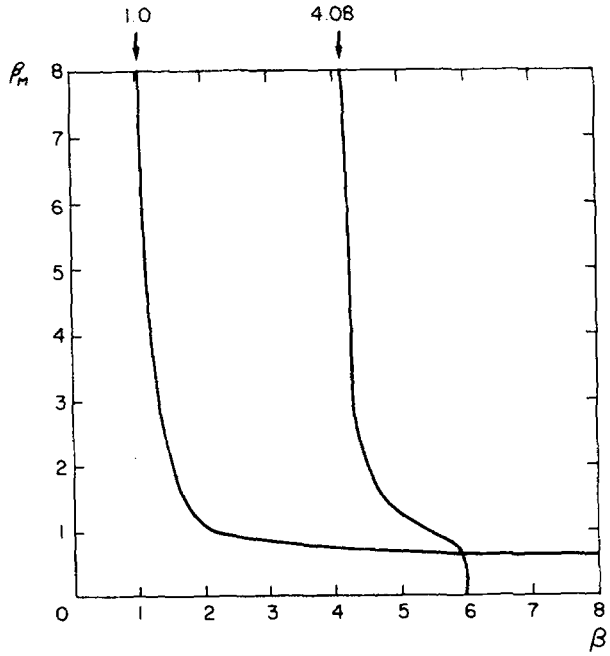

Fig. 39. The phase diagram inferred from fig. 37.

With the Higgs field in the fundamental representation, notwithstanding the critical lines, all points in the β, β_M plane can be joined by paths without singularities, and thus the system really possesses a single phase; this corresponds to the concept of duality between the confining and Higgs realizations of the symmetry. Although in this model no order parameter discriminating the two realizations exists, one still wonders whether they will still be distinguishable in some physical way. In ref. [93] the correlation between matter fields ϕ_i and ϕ_j at the opposite vertices of the hypercubes of the lattice was studied, by measuring the scalar products

$$X = N_\gamma^{-1} \bar{\phi}_j \Big(\sum_\gamma U_\gamma \Big) \phi_i \,. \tag{6.18}$$

In this equation $\Sigma_\gamma U_\gamma$ represents the sum of all possible transport operators from i to j along the sides of the hypercube and N_γ the total number of such paths. The distributions of average values of X found at $\beta = 5.2$ and $\beta_M \approx 0.6, 0.7, 0.8, 0.9$ are shown in fig. 40. One sees that the orientations of ϕ_i and ϕ_j are always correlated. When β_M is lower than the value $\beta_M \approx 0.75$, at which the transition occurs, the fluctuations and average value of X are of the same order; however, as β_M increases beyond the transition value, the average of X becomes much larger than the fluctuations. This is precisely what one would expect to justify the semiclassical approximation around a Higgs vacuum obtained in a suitable gauge by setting $\langle \phi \rangle \neq 0$.

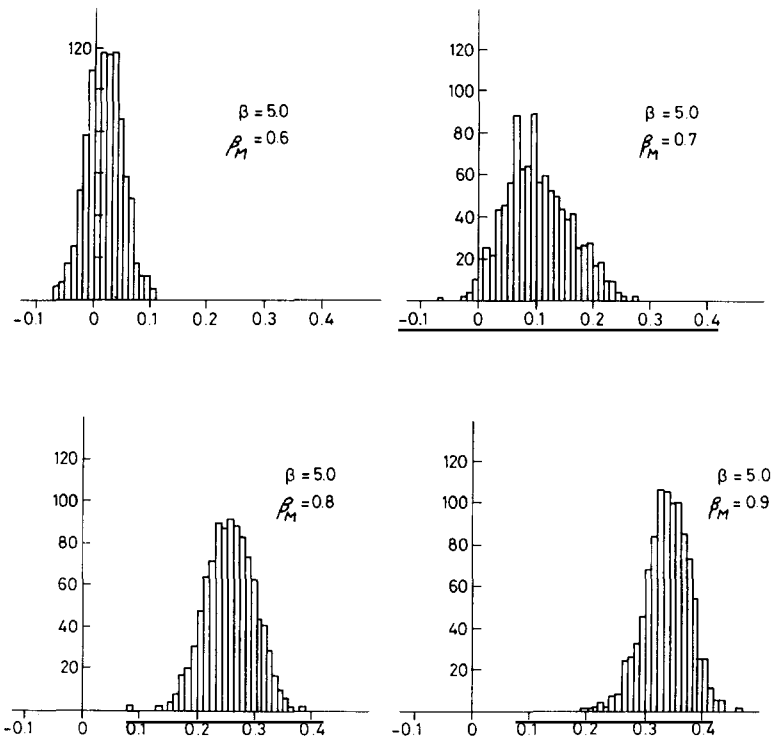

Fig. 40. The correlations X between Higgs fields at the oppostie corners of unit lattice hypercubes.

7. Systems with fermionic fields

Realistic models for particle interactions include fermionic fields and it is therefore of paramount importance to simulate systems with fermionic degrees of freedom. For reasons which we shall elucidate shortly, these simulations are computationally very demanding and no way has yet been found to perform Monte Carlo calculations for four-dimensional fermionic systems as efficiently as they can be done with only bosonic fields. The topic we are considering in this section constitutes a field where research is currently particularly active: an exhaustive review of what has been done up to now would add too many pages to this already long report. A later time, when the results will have become more definite, may be more appropriate for such a review. Thus, we shall give here only an outline of the major difficulties encountered, the techniques proposed to overcome them and the most relevant results.

The very definition of a fermionic system on a lattice involves conceptual problems. One must define a lattice equivalent of Dirac's action

$$S_{\mathrm{F,continuum}} = \bar{\psi}(D+m)\psi, \tag{7.1}$$

where D denotes Dirac's operator

$$D = \gamma^{\mu}(\partial_{\mu} + \mathrm{i}gA_{\mu}). \tag{7.2}$$

Difficulties arise in the lattice transcription of the first-order derivatives. As with bosonic matter fields, fermionic fields are usually associated with lattice sites and a natural substitute for $\partial_{\mu}\psi$, which preserves the antihermiticity properties of D, is the central difference

$$\frac{\psi(x+\hat{\mu}) - \psi(x-\hat{\mu})}{2a},$$

where x represents a generic lattice site, a is the lattice spacing and $\hat{\mu}$ is the displacement vector by one site in the μ direction. This leads to what we shall call the naive lattice action

$$S_{\mathrm{F}} = \frac{1}{2a}\sum_{x,\mu}(\bar{\psi}_x\gamma^{\mu}U_{x,x+\hat{\mu}}\psi_{x+\hat{\mu}} - \bar{\psi}_{x+\mu}\gamma^{\mu}U_{x+\hat{\mu},x}\psi_x) + m\sum_x \bar{\psi}_x\psi_x, \tag{7.3}$$

where the gauge link variables have been inserted to make the coupling among nearest neighbors covariant. The use of the central difference effectively makes the size of the unit cell equal to $2a$, twice the lattice spacing. If one considers the free theory, with $U = I$, and solves for the spectrum, one finds that the lowest energy states, those expected to dominate in the continuum limit, are obtained not only in correspondence with the obvious modes of small lattice momenta $k_{\mu} \approx 0$, but also in correspondence to modes where any of the components of k_{μ} is shifted by π/a. In these modes a long range, smooth variation of ψ is modulated by factors which alternate in sign from site to site. Thus, in a D-dimensional lattice one finds 2^D modes which survive in the continuum limit: the naive theory exhibits an unwanted 2^D degeneracy in the number of fermions as the cut-off is removed ($a \to 0$). This agrees with the notion that the unit cell is of size $2a$ and contains therefore 2^D degrees of freedom.

The action of eq. (7.3) is of course not the only possible fermionic lattice action and one would think

that a more sophisticated transcription of Dirac's operator on the lattice could eliminate the problem of unwanted multiplicities. This is correct, but with reservations. It can be indeed shown [95] on the basis of topological arguments or of arguments relative to the Adler–Bell–Jackiw anomaly that one cannot define a lattice action having all the formal properties of the continuum fermionic action. In particular, one must either give up the existence of a continuous chiral symmetry transformation when $m = 0$ or accept a degree of multiplicity which insures a cancellation of the anomaly in the currents associated with the surviving chiral symmetries. We shall not elaborate on this matter any further, but for future use, shall only mention that the most widely used fermionic lattice actions are those introduced by Wilson [96]:

$$S_F^W = \frac{K}{2a} \sum_{x,\mu} [\bar{\psi}_x(\gamma^\mu + 1)\, U_{x,x+\hat{\mu}} \psi_{x+\hat{\mu}} - \bar{\psi}_{x+\hat{\mu}}(\gamma^\mu - 1)\, U_{x+\hat{\mu},x} \psi_x] + \sum_x \bar{\psi}_x \psi_x \tag{7.4}$$

and one which represents a generalization to the Euclidean lattice [97] of an action introduced by Kogut and Susskind in a Hamiltonian context [98]:

$$S_F^S = \sum_{x,\mu} S_{x,y}(\bar{\psi}_x U_{x,x+\hat{\mu}} \psi_{x+\hat{\mu}} - \bar{\psi}_{x+\hat{\mu}} U_{x+\hat{\mu},x} \psi_x) + m \sum_x \bar{\psi}_x \psi_x\,, \tag{7.5}$$

with

$$S_{x,\mu} = 1 \text{ for } \mu = 1,\ (-1)^{x_1} \text{ for } \mu = 2,\ (-1)^{x_2+x_2} \text{ for } \mu = 3,\ (-1)^{x_1+x_2+x_3} \text{ for } \mu = 4\,.$$

Here ψ is a one component spinor; the four Dirac spinor components reside on different sites, as will be discussed below.

In Wilson's formulation additional terms, which effectively give to the $2^D - 1$ unwanted modes masses of the order of $1/a$, are inserted in the kinetic part of the action. In eq. (7.4) the mass parameter which would multiply the $\Sigma\, \bar{\psi}\psi$ term has been traded off for a parameter K (the hopping parameter) in front of the kinetic term. In the free case, it can be shown that the mass of the lowest mode behaves as

$$m = \frac{1}{K} - \frac{1}{K_{cr}} \approx \frac{K_{cr} - K}{K_{cr}^2}\,, \tag{7.6}$$

where K approaches the value $K_{cr} = 1/8$. The departure of K from a certain "critical" value measures the bare mass also in the interacting theory, but K_{cr} is renormalized by the interaction. In the strong coupling limit K_{cr} takes values $\approx 1/4$; for generic values of β, K_{cr} must be determined numerically. The extra terms in S_F^W violate chiral invariance, and one expects that a chirally invariant system may be recovered only in a suitably taken continuum limit. Monte Carlo simulations have shown however, that as $K \to K_{cr}$ the mass $m(K)$ of the lowest pseudoscalar excitation in the theory approaches zero. This is taken as a signal that a vestige of chiral symmetry, realized dynamically through the occurrence of a Goldstone boson, is recovered in that limit. As a matter of fact, K_{cr} is determined precisely as the value of K for which $m(K)$ vanishes: this is not a circular argument, because it is not a priori obvious that any mass should go to zero as K is varied.

In the generalized Susskind formulation a single component of the wave function is assigned to each site of the lattice (hence the absence of γ matrices in eq. (7.5)). The factors with alternating signs effectively introduce an algebra of γ matrices in Fourier space. The action of eq. (7.5) reduces, but does

not eliminate, the degeneracy problem; the theory describes, in the continuum limit, four degenerate fermions. A chiral symmetry is however recovered for $m = 0$: the symmetry operation consists in global, but separate, phase rotations of the fermionic fields at odd and even sites of the lattice [99, 100]. In terms of the degenerate modes this is not a diagonal chiral transformation and no violation of the theorem on the anomaly occurs. In the rest of this section we shall denote by D (or $D(U)$) the lattice Dirac operators which can be inferred from eq. (7.4) or (7.5).

The vacuum expectation values of observables are given by

$$\langle O\rangle = Z^{-1}\int \prod_{\{ij\}} \mathrm{d}U_{ji} \prod_i \mathrm{d}\bar{\psi}_i \prod_i \mathrm{d}\psi_i\, O(U,\bar{\psi},\psi)\exp\{-2S_{\mathrm{G}}(U)-\bar{\psi}(D+m)\psi\}\,, \tag{7.7}$$

$$Z = \int \prod_{\{ij\}} \mathrm{d}U_{ji} \prod_i \mathrm{d}\bar{\psi}_i \prod_i \mathrm{d}\psi_i \exp\{-S_{\mathrm{G}}(U)-\bar{\psi}(D+m)\psi\}\,, \tag{7.8}$$

where the fermionic fields ψ and $\bar{\psi}$ are to be considered as independent anticommuting elements of a Grassmann algebra, integration being defined by $\int \mathrm{d}\psi = 0$, $\int \psi\,\mathrm{d}\psi = 1$. Because they anticommute, one cannot represent the values of the fermionic fields with numbers in the computer memory as done to encode the gauge field configurations. Only for 2-dimensional systems (1 space–1 time coordinate) it is possible to represent the sum over configurations as a sum over fermionic occupation numbers while maintaining a positive measure [101]. Then Monte Carlo simulations can then be performed upon upgrading sequentially the c-number bosonic fields and the fermionic occupation numbers; applications to this procedure to a variety of two-dimensional systems have been quite successful.

Another possibility, available whenever the action is quadratic in the fermionic fields, as in the case of the models of practical interest, consists in performing explicitly the integration over the fermionic variables. This leads to [102]

$$\langle O\rangle = Z^{-1}\int \prod_{\{ij\}} \mathrm{d}U_{ij}\,\langle O\rangle_U \exp\{-S_{\mathrm{G}}(U)\}\,\mathrm{Det}(D+m)\,, \tag{7.9}$$

$$Z = \int \prod_{\{ij\}} \mathrm{d}U_{ij} \exp\{-S_{\mathrm{G}}(U)\}\,\mathrm{Det}(D+m)\,, \tag{7.10}$$

where $\langle O\rangle_U$ represents the expectation value of the observable O in the background of the fixed gauge field configuration $\{U_{ji}\}$. For instance, if O is given by $\bar{\psi}_i\psi_j$, then we have

$$\langle\bar{\psi}_i\psi_j\rangle_U = \{D(U)+m\}^{-1}_{ji}\,. \tag{7.11}$$

In eqs. (7.9) and (7.10) the quantum expectation values are expressed as averages over all configurations of the gauge field alone but with a new measure

$$\exp\{-S_{\mathrm{eff}}(U)\}\,, \tag{7.12}$$

where

$$S_{\mathrm{eff}}(U) = S_{\mathrm{G}}(U) - \ln\mathrm{Det}\{D(U)+m\} = S_{\mathrm{G}}(U) - \mathrm{Tr}\ln\{D(U)+m\}\,. \tag{7.13}$$

In most cases of interest, symmetry properties of the Dirac equation guarantee the reality and positivity of $\mathrm{Det}\{D+m\}$ and therefore the Monte Carlo technique can be applied to the estimate of quantum averages, provided the variation of $S_{\mathrm{eff}}(U)$ in the proposed upgrading $U \to U'$ can be calculated in an efficient way.

This last requirement is not straightforward to meet. Indeed, whereas the actions encountered so far always had properties of locality, so that the change $U \to U'$ modified S only through the variation of a few terms involving nearby dynamical variables, the quantity $\mathrm{Tr}\ln\{D(U)+m\}$ is non-local and an exact computation of its variation at each upgrading step would make the Monte Carlo algorithm excessively slow. A substantial part of the recent research on Monte Carlo simulation for fermionic systems has gone precisely into finding efficient approximate methods for evaluating ΔS_{eff} [103–108]. The most promising techniques all make use of the fact that if $\{D(U)+m\}^{-1}$ is known, then the calculation of ΔS_{eff} becomes almost immediate. We illustrate the point assuming that $\delta U = U' - U$ is small, although the argument can be made more general. For small δU we expand

$$\delta\,\mathrm{Tr}\ln\{D(U)+m\} = \mathrm{Tr}\{(D(U)+m)^{-1}\,\delta D(U)\}\,. \tag{7.14}$$

$D(U)$ is a local operator, and therefore $\delta D(U)$ will have very few non-vanishing elements, only those, indeed, corresponding to the matter field variables ψ_i and $\bar{\psi}_i$ which are coupled by the U_{ji} being upgraded. Thus, if $(D(U)+m)^{-1}$ is known, the evaluation of ΔS_{eff} can proceed very rapidly. As a matter of fact, knowledge is required only of those elements of $(D(U)+m)^{-1}$ which are contracted with non-vanishing elements of $\delta D(U)$ in eq. (7.14). Notice that a very simple physical interpretation can be given to eq. (7.14). Its r.h.s. will always be of the form $\Sigma_{ij} J_{ij}\delta U_{ji}$, where J_{ij} is a suitable operator constructed out of $(D(U)+m)^{-1}_{ij}$ and of factors, such as γ matrices, appearing in $\delta D/\delta U_{ji}$. Then the variation of the effective action, for small changes of the gauge field, can be thought of as the contraction δU with the fermionic "current" J_{ij} induced by the background gauge field itself.

Three different methods to obtain approximate values for the required matrix elements of $(D(U)+m)^{-1}$ have been proposed. In ref. [103] it has been suggested that the fermionic current J_{ij} be in turn evaluated by a Monte Carlo procedure, carried over a set of "pseudofermionic" variables ϕ and $\bar{\phi}$, which are coupled to the gauge field exactly as the fermions ψ and $\bar{\psi}$, but are c-numbers rather than elements of a Grassmann algebra. The method becomes efficient if all required J_{ij} elements can be computed before proceeding to the upgrade of all U_{ij} variables. This can be justified if the variation of the gauge field configuration in the upgrading is small. The method of ref. [103] has been successfully used for a simulation of the Schwinger model [106] and its application to realistic four-dimensional systems is in progress.

In ref. [107] it was suggested that all matrix elements of $(D(U)+m)^{-1}$ be calculated (for instance by a relaxation procedure), at the beginning of the algorithm and that they be upgraded together with the U_{ij} variables using the linearized formula

$$\delta(D+m)^{-1} = -(D+m)^{-1}\,\delta D(U)\,(D+m)^{-1}\,. \tag{7.15}$$

The locality of $D(U)$ again makes the computation of the r.h.s. of this equation straightforward. The method requires small δU_{ji} and periodic computations of the exact elements of the inverse Dirac operator to eliminate the build up of errors. This algorithm requires the calculation and storage in memory of all elements of $(D(U)+m)^{-1}$.

In ref. [108] the proposal was made to evaluate the required elements of $(D(U)+m)^{-1}$ by a

stochastic procedure, originally due to von Neumann and Ulam. Finally, it should also be mentioned that, with Wilson's fermions, an approximation based on an expansion in power series of the parameter K (see eq. (7.4)), the so-called hopping parameter expansion, has also been used in connection with Monte Carlo simulations [109].

Leaving aside all attempts to include the effects of $\mathrm{Det}(D(U)+m)$ into the measure, it was noticed by the authors of ref. [106], by Hamber and Parisi [110], and by Weingarten [111], that many relevant dynamical effects could be incorporated in an approximation where only the pure gauge measure $\exp\{-S_G(U)\}$ is used in the calculation of quantum averages. In this approximation the expectation value of a product of fermion operators

$$G(x) = \langle(\bar{\psi}^{(1)}\psi^{(2)})(x)\,(\bar{\psi}^{(2)}\psi^{(1)})(0)\rangle \tag{7.16}$$

(fields of different flavors, $\psi^{(1)}$ and $\psi^{(2)}$, have been introduced to remove annihilation processes) would for instance be given by

$$G(x) = Z^{-1}\int \prod_{ij} \mathrm{d}U_{ji}\,\langle\bar{\psi}^{(1)}(x)\,\psi^{(1)}(0)\rangle_U\,\langle\psi^{(2)}(x)\,\bar{\psi}^{(2)}(0)\rangle_U\,\exp\{-S_G(U)\}\,, \tag{7.17}$$

where

$$Z = \int \prod_{ij} \mathrm{d}U_{ji}\,\exp\{-S_G(U)\}\,,$$

and

$$\langle\bar{\psi}^{(1)}(x)\,\psi^{(1)}(0)\rangle_U\,, \qquad \langle\psi^{(2)}(x)\,\bar{\psi}^{(2)}(0)\rangle_U$$

represent the expectation values of the corresponding operators in the presence of a fixed background field U. The interpretation of eq. (7.17) is that the Green's function $G(x)$ for the creation and subsequent annihilation of a fermion–antifermion pair is evaluated in a two-stage process: first, the propagation of the individual fermions in a fixed background field is calculated and the propagators combined together; then the result is averaged over all gauge field configurations with measure $\exp\{-S_G(U)\}$. In a perturbative expansion, the net result of these two steps would be to sum all graphs with two fermionic lines propagating from 0 to x and any number of interacting gauge field lines. What would still be missing are the diagrams with internal closed fermion loops (these would be introduced with the correct measure $\exp\{-S_{\mathrm{eff}}\}$ rather than simply $\exp\{-S_G\}$). Yet several arguments (relying on duality, on phenomenological rules, on large N expansions, etc.) suggest that many observables in the theory of strong interactions should be only weakly affected by internal fermionic loops. The approximation of replacing $\exp\{-S_{\mathrm{eff}}\}$ with $\exp\{-S_G\}$ (which, of course, bypasses all computational problems introduced by the non-locality of S_{eff}) appears then particularly suited for a Monte Carlo study of the dynamics of quarks and gluons. (The names "quenched approximation" [106] and "valence approximation" [111] have been used to characterize this neglect of $\mathrm{Det}(D(U)+m)$ in the measure.)

The quenched, or valence, approximation has been applied in refs. [111, 112 and 113] to the study of the spectrum of mesons in a simplified model using SU(2) as gauge group, and in refs. [110, 114–117] to the more realistic theory with the SU(3) gauge group. Both Wilson's and Susskind's formulations of the

lattice fermions have been investigated. Masses of the lowest lying states in the spectrum are estimated using the same procedure described in connection with the study of the glueball spectrum (see section 5.3), i.e., from the rate of decay in Euclidean time of suitable correlation functions. However, the method by which these correlation functions are calculated is different. As outlined above, one finds first the propagator of the fermions in a fixed background gauge field configuration. Usually this is done by relaxation methods. The results are much more accurate than in Monte Carlo determinations of the same quantities, and the decay of propagators and Green functions can be followed over several orders of magnitude. However, the computations are also very time consuming. Thus generally only a limited number of configurations is used in the final averaging step. Besides masses, other interesting quantities, such as the fermion condensate $\langle\bar{\psi}\psi\rangle$, can be evaluated.

The calculations described above may be affected by various sources of errors: the averaging over only few configurations may underestimate the importance of statistical fluctuations; computational constraints limit the calculations to lattices of rather small extent (several results have been obtained with lattices spanning 5 or 6 sites in each spatial direction), barely large enough to contain the hadrons, and finite size effects may be important. The convergence of the relaxation procedure becomes slower as m (bare fermion mass) approaches zero (in Susskind's formulation) or as $K \to K_{cr}$ (in Wilson's formulation), so substantial extrapolations in m or K are required. Keeping in mind all these possible sources of uncertainty, nevertheless the results of the calculations have been quite satisfactory. One finds that as $m \to 0$, or as K approaches a suitable critical value, the mass of the lowest pseudoscalar excitation (m_π) approaches zero as well, according to a relation

$$m_\pi^2 \approx \text{const} \times m \tag{7.18}$$

$$m_\pi^2 \approx \text{const} \times (K_{cr} - K)/K_{cr}^2 . \tag{7.19}$$

This agrees with the notion of dynamical breaking of chiral symmetry. Eq. (7.18) or (7.19) is then used to fix the bare quark mass (assuming a common mass for the lightest quarks, $m_u = m_d = m$), which is an external parameter of the theory. The values so determined translate into current algebra masses of about 6 or 7 MeV. Also, the numerical evidence is that the expectation value $\langle\bar{\psi}\psi\rangle$ remains finite as $m \to 0$, again in agreement with theoretical expectations. The pion decay constant f_π can be then estimated by current algebra (from $\langle\bar{\psi}\psi\rangle$, m and m_π) and values ranging from ~90 to ~150 MeV are found (exp $f_\pi \approx 93$ MeV).

The masses of the other quark model states appear more stable as m is varied and approach finite limits as $m \to 0$. The independently computed string tension can then be used to set the scale (sometimes instead a definite mass, such as m_ρ is used for the purpose, in which case the string tension is an output of the computation) and typical results give

$m_\rho = 800 \pm 100$ MeV (exp 776)

$m_\delta = 950 \pm 150$ MeV (exp 981)

$m_{A_1} = 1100 \pm 150$ MeV (exp ~1100)

$m_N = 1000 \pm 150$ MeV (exp 938)

$m_\Delta = 1300 \pm 150$ MeV (exp 1236)

for masses of particles such as the ρ, δ and A_1 mesons, of the proton and Δ baryonic resonance. These

numbers are not taken from any specific work among the quoted references, but, keeping in line with the rather general presentation offered in this section, represent a condensation, done freely by the authors, of the various results. In any case, substantial work is still in progress and an exhaustive review of current results could have at best only temporary validity.

To conclude this section, let us report that the quenched approximation has also been used for a successful calculation of baryonic magnetic moments in refs. [118, 119] and of a few other parameters of spectroscopic relevance. An investigation of finite temperature effects [120], moreover, has hinted that the chiral symmetry of the vacuum states becomes restored ($\langle\bar{\psi}\psi\rangle$ vanishes) at a temperature slightly above the deconfinement temperature.

8. Concluding remarks

The successes of the Monte Carlo method as applied to gauge theories have been truly remarkable. Not only have we gained insight into the quark confinement problem, but we are now beginning to calculate observables totally inaccessible to traditional perturbative approaches. These results are all the more satisfying in the light of the severe limitations of available lattice sizes. For believable physical results the lattice spacing must be smaller than relevant hadronic scales, and yet the overall lattice must be larger than the scale of physics under consideration. A lattice with only of order ten sites in any direction leaves little leeway in such an analysis. Furthermore the exponential dependence of the lattice spacing on inverse coupling, as predicted by asymptotic freedom, implies that at best only a narrow range of coupling can be useful for the extraction of realistic numbers.

The fact that interesting results have been obtained despite these limitations is undoubtedly related to the experimental observation of precocious scaling in inelastic scattering experiments with momentum transfers of order 2 GeV. Thus a 10^4 site lattice may potentially give useful information on physics at energy scales as low as a few hundred MeV, exactly where strong confinement forces come into play. In this context we should also remark on the successes of the theory when internal quark loops are neglected, as in the pure gauge theory calculations and the fermion work with the quenched approximation. That we can get away with such approximations is probably for the same reason that the simple quark model has had such a long and illustrious history. Had virtual loops been a major effect, it is unlikely that the multiplet structure of the eightfold way could have been so clear.

The future problem remains in the full system with interacting fermionic fields. Current techniques are extremely intensive in their consumption of computer cycles. Developments on both the theoretical and technological fronts are occurring at an astounding pace. We may optimistically hope that in a few years reliable calculations of hadronic properties will be commonplace.

References

[1] K. Wilson, Phys. Rev. D10 (1974) 2445; Phys. Reports 23 (1975) 331.
[2] F.J. Wegner, J. Math. Phys. 12 (1971) 2259.
[3] K. Binder, in: Phase Transitions and Critical Phenomena, eds. C. Domb and M.S. Green (Academic Press, N.Y., 1976) Vol. 5B.
[4] N.H. Christ, R. Friedberg and T.D. Lee, Nucl. Phys. B210[FS6] (1982) 310.
[5] K. Osterwalder and E. Seiler, Ann. Phys. 110 (1978) 440.
[6] H.D. Politzer, Phys. Rev. Lett. 30 (1973) 1346;
D. Gross and F. Wilczek, Phys. Rev. Lett. 30 (1973) 1343; Phys. Rev. D8 (1976) 3633.
[7] W.E. Caswell, Phys. Rev. Lett. 33 (1974) 244;
D.R.T. Jones, Nucl. Phys. B75 (1974) 531.
[8] J. Kogut and L. Susskind, Phys. Rev. D11 (1975) 395.

[9] M. Creutz, Phys. Rev. D15 (1977) 1128.
[10] R. Balian, J.M. Drouffe and C. Itzykson, Phys. Rev. D10 (1974) 3376; D11 (1975) 2098; D11 (1975) 2104.
[11] M. Creutz, J. Math. Phys. 19 (1978) 2043.
[12] G. Munster and P. Weisz, Phys. Lett. 96B (1980) 119;
G. Munster, Nucl. Phys. B190[FS3] (1981) 439; B200, 536(E): B205, 648(E).
[13] N. Metropolis, A.W. Rosenbluth, M.N. Rosenbluth, A.H. Teller and E. Teller, J. Chem. Phys. 21 (1953) 1087.
[14] C.-P. Yang, Proc. Symp. in Applied Mathematics, Vol. XV (Amer. Math. Soc., Providence RI, 1963) p. 351.
[15] M. Creutz, L. Jacobs and C. Rebbi, Phys. Rev. Lett. 42 (1979); Phys. Rev. D20 (1979) 1915.
[16] G. 't Hooft, Nucl. Phys. B153 (1979) 141.
[17] T. DeGrand and D. Toussaint, Phys. Rev. D22 (1980) 2478.
[18] G. Bhanot, C. Lang and C. Rebbi, Computer Phys. Commun. 25 (1982) 275.
[19] L. Jacobs and C. Rebbi, J. Comp. Phys. 41 (1981) 203.
[20] D. Barkai and K.J.M. Moriarty, Computer Phys. Commun. 25 (1982) 57.
[21] M. Creutz, Phys. Rev. D21 (1980) 2308.
[22] H.A. Kramers and G.H. Wannier, Phys. Rev. 60 (1941) 252.
[23] R. Savit, Rev. Mod. Phys. 52 (1980) 453.
[24] C.P. Korthals-Altes, Nucl. Phys. B142 (1978) 315;
T. Yoneya, Nucl. Phys. B144 (1978) 195.
[25] S. Elitzur, R. Pearson and J. Shigemitsu, Phys. Rev. D19 (1979) 3698;
D. Horn, M. Weinstein and S. Yankielowicz, Phys. Rev. D19 (1979) 3715;
A. Ukawa, P. Windey and A. Guth, Phys. Rev. D21 (1980) 1013.
[26] A.H. Guth, Phys. Rev. D21 (1980) 2291.
[27] B. Lautrup and M. Nauenberg, Phys. Lett. 95B (1980) 63.
[28] G. Bhanot, Phys. Rev. D24 (1981) 461.
[29] H. Hamber, Phys. Rev. D24 (1981) 941.
[30] L.P. Kadanoff, Rev. Mod. Phys. 49 (1977) 267.
[31] T. DeGrand and D. Toussaint, Phys. Rev. D24 (1981) 466.
[32] G. Bhanot and M. Creutz, Phys. Rev. D21 (1980) 2892.
[33] A.M. Polyakov, Phys. Lett. 59B (1975) 82; Nucl. Phys. B120 (1977) 429.
[34] M. Gopfert and G. Mack, Comm. Math. Phys. 82 (1982) 545.
[35] C. Rebbi, Phys. Rev. D21 (1980) 3350.
[36] D. Petcher and D. Weingarten, Phys. Rev. D22 (1980) 2465.
[37] G. Bhanot and C. Rebbi, Nucl. Phys. B180 (1981) 469.
[38] G. Bhanot and C. Rebbi, Phys. Rev. D24 (1981) 3319.
[39] P. Lisboa and C. Michael, Phys. Lett. 113B (1982) 303.
[40] K. Wilson, private communication.
[41] M. Creutz, Phys. Rev. Lett. 43 (1979) 553.
[42] M. Creutz, Phys. Rev. Lett. 45 (1980) 313.
[43] W.M. Fairbairn, T. Fulton and W.H. Klink, J. Math. Phys. 5 (1964) 1038.
[44] E. Tomboulis, Phys. Rev. D25 (1982) 606 and Princeton preprint (1982).
[45] A. Patrasciou, E. Seiler and I.O. Stametescu, Phys. Lett. 107B (1981) 364.
[46] R.C. Edgar, Nucl. Phys. B200[FS4] (1982) 345.
[47] N.S. Manton, Phys. Lett. 96B (1980) 328.
[48] N. Grosse and H. Kuhnelt, Nucl. Phys. B205 (1981) 273.
[49] J.M. Drouffe, Phys. Rev. D18, (1978) 1174;
P. Menotti and E. Onofri, Nucl. Phys. B190 (1981) 288.
[50] C.B. Lang, C. Rebbi, P. Salomonson and B.S. Skagerstam, Phys. Lett. 101B (1981) 173; Phys. Rev. D 26 (1982) 2028.
[51] J. Greensite and B. Lautrup, Phys. Rev. Lett. 47 (1981) 9;
E.G. Halliday and A. Schwimmer, Phys. Lett. 101B (1981) 327.
[52] G. Bhanot and M. Creutz, Phys. Rev. D24 (1981) 3212.
[53] E. Tomboulis, Phys. Rev. D23 (1981) 2371.
[54] G. Mack and V.B. Petkova, Ann. Phys. 123 (1979) 442;
R.C. Brower, D.A. Kessler and H. Levine, Phys. Rev. Lett. 47 (1981) 621; Nucl. Phys. B205 (1982) 77.
[55] I.G. Halliday and A. Schwimmer, Phys. Lett. 102B (1981) 327;
L. Caneschi, I.G. Halliday and A. Schwimmer, Nucl. Phys. B200 (1982) 409.
[56] G. Bhanot, Phys. Lett. 108B (1982) 337.
[57] M. Creutz, Phys. Rev. Lett. 46 (1981) 1441;
K.J.M. Moriarty, Phys. Lett. 106B (1981) 130;
M. Creutz and and K.J.M. Moriarty, Phys. Rev. D25 (1982) 1724.

[58] V.S. Dotsenko and S.N. Vergeles, Nucl. Phys. B169 (1980) 527.
[59] E. Pietarinen, Nucl. Phys. B190[FS3] (1981) 349.
[60] M. Creutz and K.J.M. Moriarty, Phys. Rev. D26 (1982) 2166.
[61] S. Coleman and E. Weinberg, Phys. Rev. D7 (1973) 1888.
[62] W. Celmaster and R.J. Gonsalves, Phys. Rev. D20 (1979) 1420.
[63] A. Hasenfratz and P. Hasenfratz, Phys. Lett. 93B (1980) 165;
R. Dashen and D. Gross, Phys. Rev. D23 (1981) 2340.
[64] J. Villain, J. Phys. (Paris) 36 (1975) 581.
[65] A.M. Polyakov, Phys. Lett. 72B (1978) 477;
L. Susskind, Phys. Rev. D20 (1979) 2610.
[66] L. McLerran and B. Svetitsky, Phys. Lett. 98B (1981) 195.
[67] J. Kuti, J.J. Polonyi and K. Szlachanyi, Phys. Lett. 98B (1981) 199.
[68] K. Kajantie, C. Montonen and E. Pietarinen, Zeit. Phys. C9 (1981) 253.
[69] C.B. Lang and C. Rebbi, Phys. Lett. 115B (1982) 137.
[70] J. Engels, F. Karsch, H. Satz and I. Montvay, Phys. Lett. 101B (1981) 89; 102B (1981) 332; Nucl. Phys. B205 (1982) 545.
[71] R. Brower, M. Creutz and M. Nauenberg, Nucl. Phys. (in press).
[72] B. Berg, A. Billoire and C. Rebbi, Ann. of Phys. 142 (1982) 185.
[73] M. Falcioni et al., Phys. Lett. 110B (1982) 295.
[74] K. Ishikawa, G. Schierholz and M. Teper, Phys. Lett. 110B (1982) 399.
[75] B. Berg and A. Billoire, Phys. Lett. 113B (1982) 65.
[76] K. Ishikawa, G. Schierholz and M. Teper, Phys. Lett. (in press);
B. Berg and A. Billoire, Phys. Lett. 114B (1982) 324.
[77] K.H. Mütter and K. Schilling, Phys. Lett. 117B (1982) 75.
[78] C.B. Lang and C. Rebbi, Phys. Lett. 115B (1982) 137.
[79] J. Stack, Phys. Rev. D27 (1983) 412.
[80] J.L. Richardson, Phys. Lett. 82B (1979) 272.
[81] M. Creutz, Proc. Johns Hopkins Workshop on Current Problems in Particle Theory, Vol. 4, Bonn 1980 (Johns Hopkins Univ., Baltimore, 1980) p. 85.
[82] A. Billoire, Phys. Lett. 104B (1981) 472.
[83] R. Savit, Phys. Rev. Lett. 39 (1977) 55;
T. Banks, R. Myerson and J. Kogut, Nucl. Phys. B129 (1977) 493.
[84] G. 't Hooft, Phys. Rev. Lett. 37 (1976) 8; Phys. Rev. D14 (1976) 3432.
[85] J. Groeneveld, J. Jurkiewicz and C.P. Korthals-Altes, Physica Scripta 23 (1981) 1022;
G. Mack and E. Pietrarinen, Phys. Lett. 94B (1980) 397; Nucl. Phys. B205 (1982) 141.
[86] P. Di Vecchia, K. Fabricius, G.C. Rossi and G. Veneziano, Phys. Lett. 108B (1982) 323; Nucl. Phys. B192 (1981) 392.
[87] M. Lüscher, preprint (1981).
[88] E. Fradkin and S. Shenker, Phys. Rev. D19 (1979) 3682.
[89] M. Creutz, Phys. Rev. D21 (1980) 1006.
[90] G. Bhanot and M. Creutz, Phys. Rev. B22 (1980) 3370.
[91] K.C. Bowler, G.X. Pawley, B.J. Pendleton, D.J. Wallace and G.W. Thomas, Phys. Lett. 104B (1981) 491;
D. Callaway and L. Carson, Phys. Rev. D25 (1982) 531.
[92] G. Bhanot and B.A. Freedman, Nucl. Phys. B190 (1981) 357.
[93] C.B. Lang, C. Rebbi and M. Virasoro, Phys. Lett. 104B (1981) 294.
[94] R. Brower, D. Kessler, T. Schalk, H. Levine and M. Nauenberg, Phys. Rev. D25 (1982) 3319.
[95] A. Chodos and J.B. Healy, Phys. Rev. D16 (1977) 387;
L. Karsten and J. Smit, Nucl. Phys. B183 (1981) 103;
W. Kerler, Phys. Rev. D23 (1981) 2384;
H. Nielsen and M. Ninomiya, Nucl. Phys. B195 (1981) 20; B193 (1981) 173.
[96] K. Wilson, in: New Phenomena in Subnuclear Physics, ed. A. Zichichi (Plenum Press, N.Y., 1977).
[97] N. Kawamoto and J. Smit, Nucl. Phys. B1982 (1981) 10;
J. Rabin, Nucl. Phys. B201 (1982) 315;
T. Banks, Y. Dothan and D. Horn, Tel Aviv Univ. preprint (1982);
P. Becker and H. Joos, Zeit. Phys. C15 (1982) 343.
[98] J. Kogut and L. Susskind, Phys. Rev. D11 (1975) 395;
T. Banks, S. Raby, L. Susskind, L. Kogut, D.R.T. Jones, P. Scharbach and D. Sinclair, Phys. Rev. D15 (1977) 1111.
[99] C. Rebbi, Brookhaven preprint, to appear in Proc. 19th Orbis Scientiae Meeting, 1982.
[100] H. Kluberg-Stern, A. Morel, O. Napoly and B. Peterson, Saclay preprint (1982).
[101] R. Blankenbeckler, J. Hirsch, D. Scalapino and R. Sugar, Phys. Rev. Lett. 47 (1982) 1628.
[102] P. Matthews and A. Salam, Nuovo Cim. 12 (1954) 563; Nuovo Cim. 2 (1955) 120.

[103] F. Fucito, E. Marinari, G. Parisi and C. Rebbi, Nucl. Phys. B180 (1981) 369.
[104] D. Weingarten and D. Petcher, Phys. Lett. 99B (1981) 333.
[105] H. Hamber, Phys. Rev. D24 (1981) 951.
[106] E. Marinari, G. Parisi and C. Rebbi, Nucl. Phys. B190 (1981) 266.
[107] D. Scalapino and R. Sugar, Phys. Rev. Lett. 46 (1981) 519.
[108] J. Kuti, Phys. Rev. Lett. 49 (1982) 183.
[109] A. Hasenfratz, P. Hasenfratz, Z. Kunszt and C.B. Lang, Phys. Lett. B110 (1982) 282.
[110] H. Hamber and G. Parisi, Phys. Rev. Lett. 47 (1982) 1792.
[111] D. Weingarten, Phys. Lett. 109B (1982) 57.
[112] E. Marinari, G. Parisi and C. Rebbi, Phys. Rev. Lett. 47 (1981) 1798.
[113] H. Hamber, E. Marinari, G. Parisi and C. Rebbi, Phys. Lett. 108B (1982) 314.
[114] H. Hamber and G. Parisi, Phys. Rev. D, to be published.
[115] D. Weingarten, IUHET preprint (1982).
[116] F. Fucito, G. Martinelli, C. Omero, G. Parisi, R. Petronzio and F. Rapuano, Nucl. Phys. B210 (1982) 407.
[117] C. Bernard, T. Draper and K. Olynyk, UCLA preprint (1982).
[118] G. Martinelli, G. Parisi, R. Petronzio and F. Rapuano, Phys. Lett. 116B (1982) 434.
[119] C. Bernard, T. Draper, K. Olynyk and M. Rushton, Phys. Rev. Lett. 49 (1982) 1076.
[120] J. Kogut, M. Stone, H. Wyld, J. Shigemitsu, S. Shenker and D. Sinclair, Phys. Rev. Lett. 48 (1982) 1140.